University of applied sciences Hamburg
Faculty Life Sciences
Pharmaceutical Biotechnology

Master thesis

Establishment of a biotechnological production process of a KlenTaq DNA polymerase with *Pichia pastoris* from cultivation to purification

Author:
Jakub Wirkus [redacted]
[redacted]

Submissions date:
1.2.2026

First appraiser: Prof. Dr. Gesine Cornelissen
Second appraiser: Prof. Dr. Christian Kaiser

Acknowledgements

I would like to thank everyone involved for their support and assistance with this work. Special thanks go to Prof. Dr. Cornelissen, who enabled me to carry out this work in the Laboratory for Bioprocess Automation and always provided me with content-related support.

My sincere thanks go to Dipl.-Ing. Ulrich Scheffler and Dipl.-Ing. Hans-Peter Bertelsen for their technical knowledge and support in the laboratory and for warmly welcoming me into the working group.

I would also like to thank Prof. Dr. Stefan Noll and Iris Ziehm from the Laboratory for Applied Microbiology for their support in the laboratory and their microbiological support.

I am thankful to Prof. Dr. Christian Kaiser and Dipl.-Ing. Petra Derr from the Laboratory for Bioprocess Engineering for their content-related and practical support.

Abstract

Recombinant production of thermostable DNA polymerases in *Picha pastoris* offers a promising alternative to classical *E. coli* based systems yet require reliable upstream and downstream integration. A previous thesis successfully expressed KlenTaq DNA polymerase in Erlenmeyer flasks. The objective of this work was therefore to establish a scalable bioprocess for KlenTaq production in a bioreactor, including cultivation, purification and evaluating enzymatic activity.

Initial experiments confirmed KlenTaq expression in Erlenmeyer flasks by SDS-PAGE, and PCR assay demonstrated clear enzymatic activity of the produced polymerase. When transferring the process to the bioreactor, KlenTaq was expressed but consistently showed no PCR activity, despite ultrafiltration and diafiltration. Systematic cultivation parameter adjustments were therefore implemented to replicate Erlenmeyer flask conditions, including medium composition, process management, pH value during cultivation and production temperature. None of these modifications restored the activity. Only after increasing the concentration factor during ultrafiltration and performing a more extensive buffer exchange during ultrafiltration could KlenTaq activity be recovered. This indicates that insufficient purification stringency led to inhibitory components or destabilizing buffer environments that masked activity.

Overall, this study establishes the first bioreactor-based process for KlenTaq DNA polymerase production in *P. pastoris.* The findings highlight the critical role of downstream processing, particularly concentration and buffer exchange, in retaining enzymatic activity and provide a foundation for further process optimization and scale up.

Declaration of oath

I hereby declare that I have completed this thesis independently without unauthorized help. All sources and materials used have been cited accordingly. Any passages based on other works have been identified as such.

Hamburg, _____ Signature: _____

Table of Contents

List of Figures

List of Tables

Abbreviations

AA	Amino acid
AOX	Alcohol oxidase
AU	Absorption units
bp	Base pair
BPA	Bioprocess automatization
BSA	Bovine serum albumin
DCU	Digital control unit
DHAS	Dihydroxyacetone synthase
DNA	Deoxyribonucleic acid
dNTPs	Deoxynucleotide triphosphates
DSP	Downstream processing
DV	Diafiltration volume
DW	Dry weight
HCDC	High cell density cultivation
IMAC	Immobilized metal affinity chromatography
IPTD	Isopropyl-β-D-thiogalactopyranoside
IR	Infrared
kDa	kilo Dalton
MCB	Master cell bank
Mut	Metnanol utilization
OD	Optical density
P. pastoris	*Picha pastoris*
PAGE	Polyacrylamide gel electrophoresis
PCR	Polymerase chain reaction
ppm	Parts-per-million
SDS	Sodium dodecyl sulfate
STRs	stirred-tank reactors
TFF	Tangential flow filtration
TRIS	Tris(hydroxymethyl)aminomethane
WCB	Working cell bank
wt	Wild type

Nomenclature

Notation	Description	Unit
c_{IK}	Concentration of compound I in subsystem K	g/L
m_{IK}	Mass of compound I in subsystem K	g
N_{St}	Stirrer speed	rpm
OD	Optical density measured at 600 nm	AU
pO_2	Dissolved oxygen saturation	%
μ	Cell specific growth rate	h^{-1}

1. Introduction

Biotechnology has become an essential interdisciplinary field in modern industry, with particular relevance in the production of enzymes, pharmaceuticals and biopharmaceutical products.[1] Microbial and cell-based production systems are widely applied due to their scalability, economic feasibility and ability to produce complex biomolecules. Depending on the target product, both prokaryotic systems such as *Escherichia coli* and eukaryotic hosts including yeasts and mammalian cells are employed, each offering distinct advantages and limitations with respect to protein folding, post-translational modifications and process robustness.

Among eukaryotic expression systems, yeasts represent a favorable compromise between simple cultivation and the ability to perform post-translational modifications. While *Saccharomyces cerevisiae* has a long tradition in biotechnology, *Pichia pastoris* has emerged over recent decades as a highly efficient host for heterologous protein production.[2] *P. pastoris* is characterized by its ability to grow to very high cell densities and by a tightly regulated methanol-inducible expression system based on the alcohol oxidase 1 (AOX1) promoter.[3] This enables strong and controllable induction of recombinant gene expression and allows protein titers in the gram-per-liter range to be achieved.

A major advantage of *P. pastoris* is its suitability for high cell density cultivation (HCDC), which is commonly implemented as a three-stage fermentation process consisting of a batch phase, a fed-batch phase and a methanol-induced production phase.[4] During the batch and fed-batch phases, biomass is accumulated, typically using glucose or glycerol as the carbon source, while the production phase is initiated by switching to methanol as substrate and inducer. This metabolic shift is accompanied by reduced growth rates and increased recombinant protein expression. However, HCDC processes are often limited by factors such as oxygen availability, proteolytic degradation and reduced cell viability, making careful process control and monitoring essential.[5]

In previous work conducted in the microbiology laboratory, a *P. pastoris* strain was successfully engineered to express KlenTaq DNA polymerase as a heterologous protein. KlenTaq polymerase is a truncated and thermostable variant of Taq polymerase and is widely used in PCR applications due to its robustness and high thermal stability. To date, production of this enzyme has only been carried out in Erlenmeyer flask cultivations, without a defined and controlled bioreactor process or a systematic downstream purification strategy.

The aim of this work is therefore the development of a process for the production, recovery and functional verification of KlenTaq DNA polymerase in a bioreactor system. This includes optimization of the upstream process comprising batch, fed-batch and methanol-induced production phases, the establishment of suitable downstream processing steps such as thermal purification, ultrafiltration and buffer exchange, and the evaluation of polymerase activity using PCR-based assays. Particular emphasis is placed on linking cultivation strategy, downstream processing and enzyme functionality in order to identify critical factors for the production of an active recombinant polymerase.

2. Theoretical Background

To understand the bioprocess developed in this work, theoretical aspects of the expression system, the target protein and the applied upstream and downstream strategies must be considered. This includes the methanol-inducible expression mechanism of *P. pastoris*, the biochemical properties of KlenTaq DNA polymerase, as well as the principles of biomass formation, substrate-limited fed-batch cultivation, methanol induction and protein recovery from the culture supernatant.

2.1 Expression system *Picha pastoris* BSY12MS_KlenTaq

Picha pastoris which is a methylotrophic yeast was first discovered in 1920 by Alexandre Guilliermond.[6] *P. pastoris* has characteristics that make it a valuable host for the production of biotechnological products. It is easy to genetically manipulate, grows rapidly and has the ability to synthesize core-glycosylated proteins or those with a "humanized" N-glycosylation pattern. [7] In addition, it is possible to dispense with the inducer isopropyl-β-D-thiogalactopyranoside (IPTG), as *P. pastoris* has a methanol metabolism that can be used to induce recombinant gene expression.

P. pastoris is known to produce enzymes which enable the metabolism of methanol as a substrate. The enzymes required for this are alcohol oxidases (AOX). Alcohol oxidases are encoded by two genes, AOX1 and AOX2, whose expression is induced by the presence of methanol. Both genes are localized in the peroxisome. Among these, AOX1 is the primary gene and is driven by a strong promoter. Transcription of AOX1 is upregulated in the presence of methanol and repressed when preferred carbon sources like glucose or glycerol are available.[3]

With this knowledge, three different phenotypes were engineered: Mut^S, in which the AOX1 gene is knocked out and thus significantly less AOX is available to the cell, resulting in slow methanol utilization. A Mut+ phenotype, where the AOX2 gene is knocked out, which is not the primary gene for AOX production, so that this phenotype has a similar methanol consumption behavior as the wild type. Mut- describes the phenotype in which both AOX genes are knocked out and therefore the cells are not able to metabolize methanol.[8]

2.2 Methylotrophy of *Picha pastoris*

As already described, *P. pastoris* is a yeast that is able to metabolize methanol. It is one of about a dozen yeast species that can utilize methanol as a substrate.[9] The first step of methanol metabolism is the oxidation of methanol to formaldehyde where hydrogen peroxide is formed by alcohol oxidase (AOX), as seen in Figure 1. Due to the formation of hydrogen peroxide, which is toxic, the first step takes place in the peroxisome which encapsulates the resulting hydrogen peroxide from the rest of the cell.[7] Hydrogen peroxide is subsequently broken down into water and oxygen by catalase. A part of the formaldehyde exits the peroxisome and is converted into NADH, an energy source, by formaldehyde dehydrogenase. The remaining formaldehyde enters a cyclic assimilation pathway, catalyzed by a third peroxisomal enzyme

dihydroxyacetone synthase (DHAS), to contribute to the synthesis of cellular components. Notably, AOX enzymes make up over 30 % of the total cellular protein in methanol-grown cells.[3]

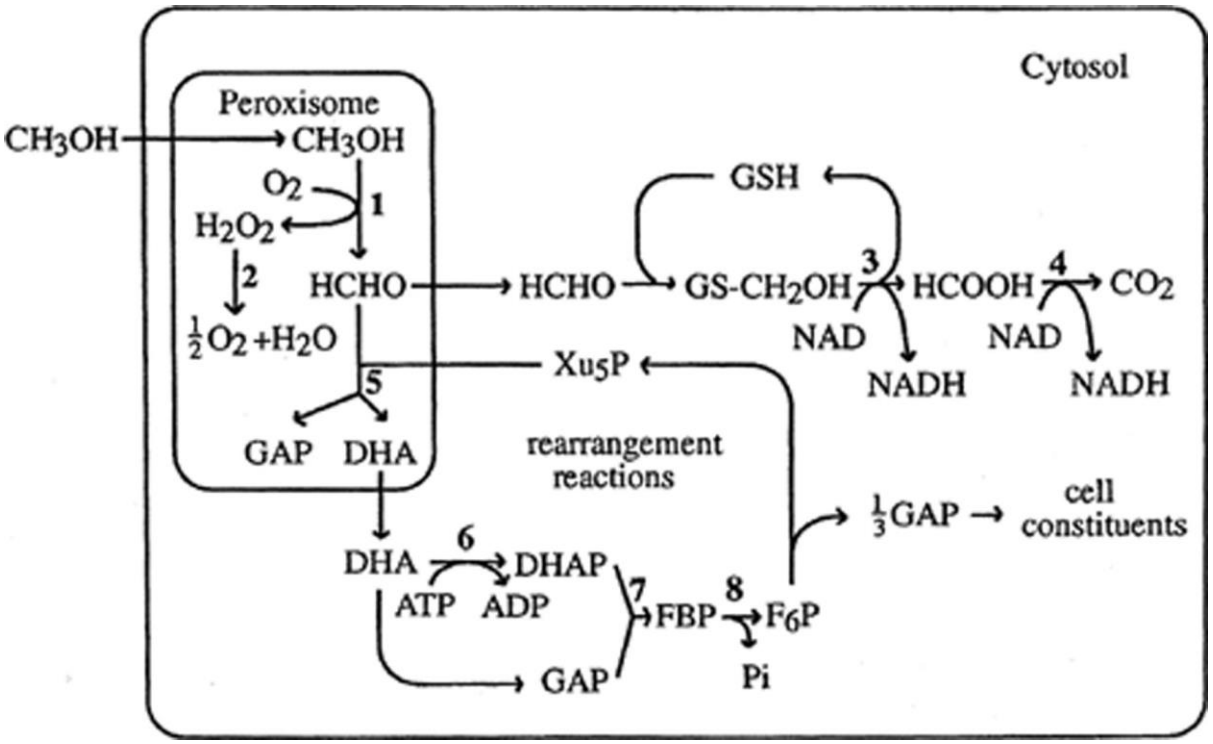

Figure 1: Methanol metabolism pathway. The first step of the pathway is AOX1 (1) which catalyzes the oxidation of methanol into formaldehyde and hydrogen peroxide. The catalase (2) then degrades hydrogen peroxide to oxygen and water. Part of the formaldehyde then leaves the peroxisome and is converted into the energy source NADH with the help of formaldehyde dehydrogenase (3,4). The remaining formaldehyde is assimilated via a cyclic pathway to form cell components.[3]

2.3 KlenTaq DNA Polymerase

DNA polymerases are enzymes that are used in PCR assays to replicate a specific DNA, they synthesize a new DNA strand by joining nucleotides together according to a DNA template. The DNA polymerase works in the 5'- 3' direction and requires a primer to attach to the DNA strand and start replication.

The KlenTaq DNA polymerase, which crystal structure can be seen in Figure 2, is a modified version of Taq DNA polymerase, which is derived from the bacterium *Thermus aquaticus*. To be more precise, KlenTaq DNA polymerase is the Klenow fragment of Taq DNA polymerase. The Klenow fragment is the larger fragment of the two protein fragments of DNA polymerase I from *E.coli*, which is produced during enzymatic cleavage with subtilin.[10] The Taq DNA polymerase is truncated at the N-terminal by 280 amino acids to obtain the KlenTaq DNA polymerase, therefore the Klenow term is also applied to the KlenTaq DNA polymerase. Due to the truncation at the N-terminal, KlenTaq DNA polymerase has no 3`-5` exonuclease activity, meaning that no proofreading takes place. Furthermore, the relative mutation rate of KlenTaq DNA polymerase is half as low compared to the full-length DNA polymerase.[11]

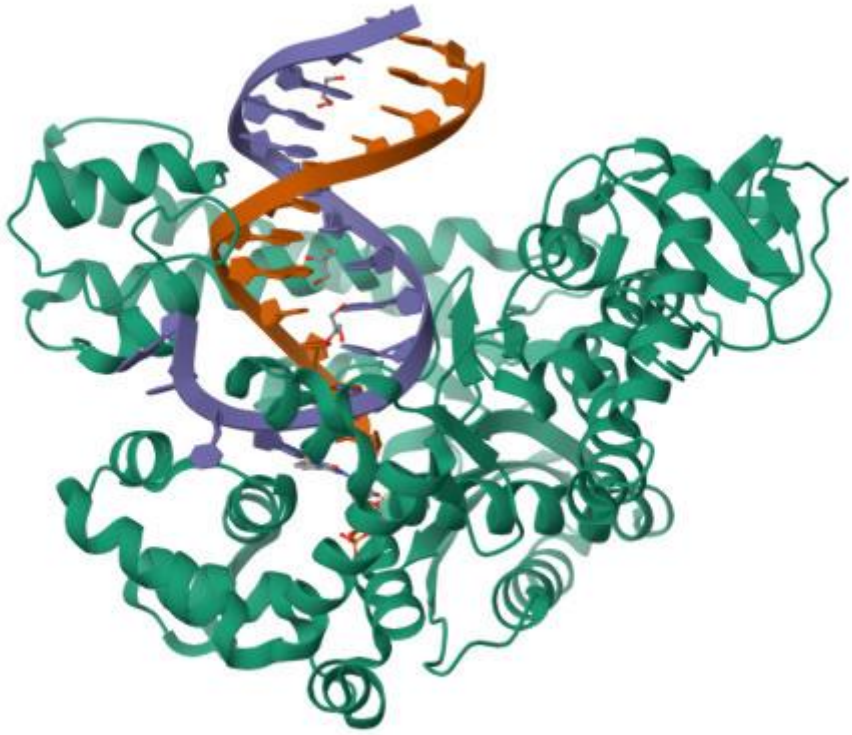

Figure 2: **Crystal structure of KlenTaq DNA Polymerase.**[12]

Figure 3 illustrates a schematic representation of the gene construct of KlenTaq polymerase. At the N-terminus of the gene construct there is a 19 AA long pre-signal sequence and a 66 AA long pro-signal sequence. This is followed by the His-Tag, which consists of 6 histidines and is therefore 6 AA long. Next comes the KlenTaq, which consists of 558 AA including the His-Tag. The DNA sequence of the KlenTaq DNA polymerase used in the work consists of 1659 bp, which corresponds to a molecular weight of approximately 62 kDa.

Figure 3: Schematic representation of the gene construct of KlenTaq polymerase. Consisting of a pre-sequence (19 AA), pro-sequence (66 AA), His-Tag (6 AA) and the KlenTaq (582 AA).

2.4 Upstream process

2.4.1 Bioreactor systems and general equipment

Bioreactors are central units in biotechnological production processes, providing a controlled environment for microbial cultivation and recombinant protein expression. Depending on the application, organism and production scale, different bioreactor systems are employed, which differ in design, hydrodynamics and achievable levels of process control.

Commonly used bioreactor types include stirred-tank reactors (STRs), bubble column reactors and airlift reactors. Among these, stirred-tank reactors represent the most widely applied system at laboratory and pilot scale. STRs consist of a cylindrical vessel equipped with one or more impellers that ensure efficient mixing, homogeneous nutrient distribution and effective gas–liquid mass transfer. Due to their high flexibility, scalability and compatibility with aerobic microorganisms, STRs are particularly well suited for yeast-based expression systems such as *P. pastoris*. [13]

Bubble column and airlift reactors, in contrast, rely on gas-induced circulation rather than mechanical agitation. These systems are characterized by lower energy consumption and reduced shear stress, which can be advantageous for shear-sensitive organisms. However, they typically offer less precise control over mixing and oxygen transfer compared to stirred-tank reactors.

Independent of the reactor type, modern bioreactors are equipped with a set of standard components that enable precise monitoring and control of critical process parameters. These typically include sensors for temperature, pH and dissolved oxygen tension (pO_2), as well as actuators such as stirring systems, gas flow controllers and dosing pumps for acids, bases, substrates and antifoam agents. Temperature control is commonly achieved via heating jackets or internal cooling coils, while oxygen supply is regulated through aeration rate and stirrer speed. [13]

In addition, advanced bioreactor systems are often connected to digital control units and supervisory software, allowing automated process control, data acquisition and alarm handling. This level of instrumentation is essential for reproducible operation and for maintaining defined cultivation conditions during batch, fed-batch and production phases.

Overall, the choice of bioreactor system and its equipment plays a decisive role in ensuring stable cultivation conditions, efficient biomass formation and reliable recombinant protein production.

2.4.2 Cultivation strategy

High cell density cultivation (HCDC) is applied to achieve high biomass concentrations within a limited process time, thereby enabling efficient product formation during the production phase. Using this strategy, cell concentrations of up to approximately 100 g/L can be reached. [14] The cultivation process is typically divided into three sequential phases: batch, fed-batch, and production, as illustrated in Figure 4.

The batch phase includes a lag phase followed by an exponential growth phase. During this phase, glycerol (S1) serves as the sole carbon source. At the beginning of cultivation, the dissolved oxygen tension (pO_2) decreases until the control system activates at a predefined setpoint, 25 % is commonly used. Once pO_2 regulation is activated, the stirrer speed increases to maintain constant oxygen availability. Under these conditions, cells grow at their maximum specific growth rate (μ_{max}), as neither substrate nor oxygen limitation occurs. Throughout the batch phase, the glycerol concentration in the liquid phase (c_{SL}) continuously decreases due to increasing biomass. The batch phase lasts until the substrate is completely depleted.

In the subsequent fed-batch phase, growth is intentionally limited by controlled substrate addition. Glycerol is supplied exponentially via F_{R1} to sustain a defined specific growth rate (μ_{w1}) while preventing substrate accumulation in the liquid phase. As a result, the substrate concentration can be assumed to be 0, whereas biomass formation continues and the stirrer speed increases accordingly to meet the rising oxygen demand.

The production phase is initiated by switching the carbon source from glycerol to methanol (S2), which also acts as an inducer for recombinant protein expression. Simultaneously, the cultivation temperature is reduced to decrease metabolic activity. During this phase, product formation increases, while biomass growth slows down significantly due to the lower maximum growth rate on methanol (μ_{w2}). Consequently, only a minor increase in cell mass is observed.

Throughout the entire cultivation process, the pH is maintained at a constant setpoint by controlled addition of acid or base. Despite its advantages, HCDC may be affected by limitations such as reduced cell viability, increased proteolytic activity, substrate limitation, or accumulation of inhibitory metabolic by-products, which can negatively influence overall process performance.[7]

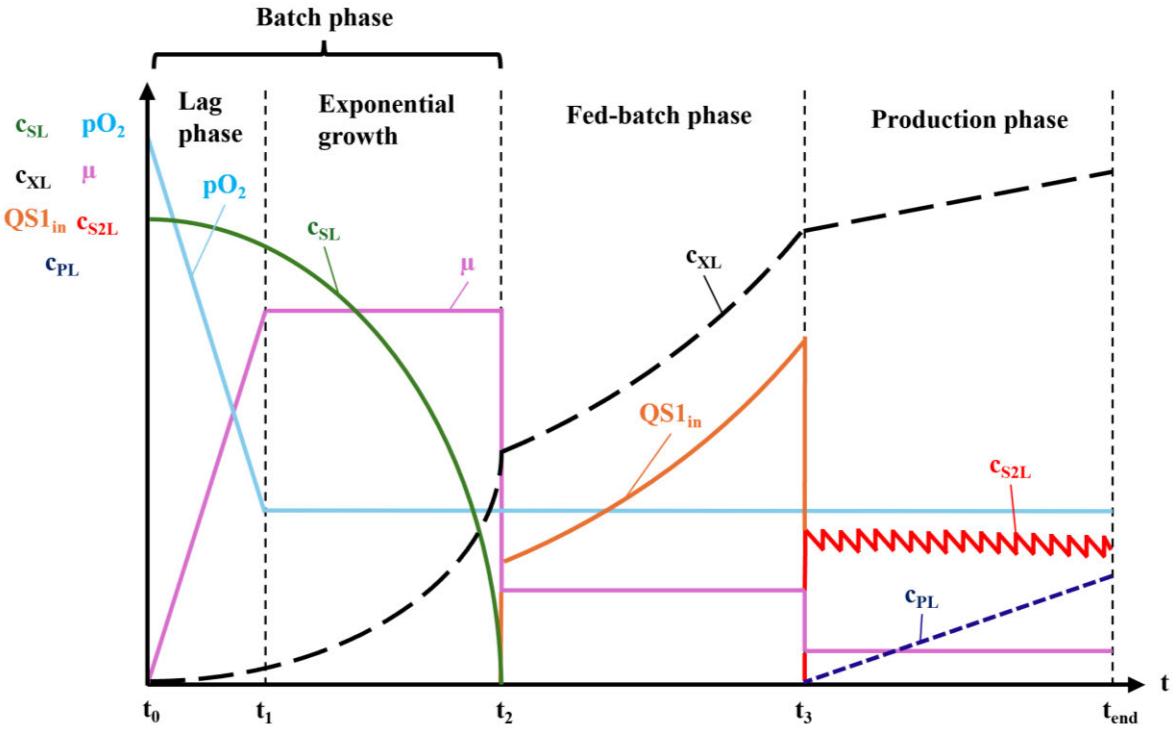

Figure 4: Schematic course of the three-stage cultivation process with P. pastoris. The batch-phase is separated into two phases, the lag phase (adaptation phase) and the exponential growth phase. In the adaptation phase the yeast adapts to the new cultivation environment, in the unlimited phase the yeast reaches unlimited growth (μ_{max}) due to the substrate surplus. In the fed-batch-phase the yeast grows at a controlled growth rate, to reach a high cell density. The production phase starts in this work with the induction of methanol. The graph shows the growth rate μ with different μ_{max} for each phase, the cell concentration c_{XL}, the glycerin concentration c_{SL}, the methanol concentration c_{S2L}, the product concentration c_{PL} and the oxygen partial pressure pO_2.

2.5 Downstream processing

Downstream processing (DSP) comprises all unit operations required to recover, purify and formulate a target protein from a complex biological matrix after cultivation. In biopharmaceutical manufacturing, DSP represents a major contributor to total production costs and is often considered the bottleneck of the overall process, particularly as upstream titers continue to increase.[15] The primary objectives of DSP are the removal of cells and cell debris, the reduction of process-related impurities, and the concentration and stabilization of the target protein.

Typically, downstream processing begins with a clarification step, which aims to separate biomass from the cultivation broth. This step is commonly performed using centrifugation and/or filtration. Centrifugation exploits density differences between cells and the surrounding liquid, enabling efficient removal of biomass even at high cell densities. Clarification is essential to protect subsequent purification steps from fouling and to ensure stable process performance.[16]

Following clarification, further purification and concentration steps are applied to increase product purity and adjust the formulation. Among membrane-based technologies, ultrafiltration and diafiltration operated in tangential flow mode (TFF) play a central role in

modern downstream processing. In TFF, the feed flows parallel to the membrane surface, reducing concentration polarization and membrane fouling compared to dead-end filtration. Ultrafiltration allows the retention of proteins above a defined molecular weight cut-off while smaller molecules such as salts, metabolites and residual medium components pass through the membrane. Diafiltration further enables controlled buffer exchange, which is critical for removing inhibitory substances and optimizing conditions for protein stability and activity.

Membrane-based filtration steps are widely used not only for concentration but also as final formulation steps in downstream processing cascades. Their scalability, gentle operating conditions and compatibility with continuous processing concepts make them particularly attractive for biopharmaceutical applications. Recent developments focus on improved process modeling, intensified filtration strategies and integration of ultrafiltration into continuous downstream workflows.

Additional purification steps, such as chromatography or precipitation, can further increase protein purity based on differences in size, charge, or affinity. Throughout all downstream steps, special attention must be paid to maintaining suitable pH, ionic strength, and temperature conditions to preserve protein functionality. [17]

Overall, downstream processing relies on a combination of mechanical separation techniques such as centrifugation and advanced membrane-based operations such as tangential flow filtration to ensure efficient recovery, purification and formulation of functional protein products.

2.5.1 Centrifugation

Centrifugation is a widely used separation technique in biotechnology that enables the clarification of cell suspensions by applying centrifugal force. Particles are separated based on differences in density, size, and shape, with denser components forming a pellet while the clarified liquid remains as the supernatant.

In bioprocessing, centrifugation is commonly applied for cell harvesting and removal of cell debris prior to downstream processing. The efficiency of separation depends on the applied relative centrifugal force and centrifugation time, while appropriate operating conditions are required to ensure effective separation without compromising product stability.[18]

2.5.2 Tangential flow filtration

Tangential Flow Ultrafiltration (TFUF) is a membrane-based separation technique commonly used for the concentration and buffer change of biomolecules. The process employs semi-permeable membranes characterized by their molecular weight cut-off (MWCO). Molecules with a hydrodynamic radius larger than the MWCO are retained by the membrane and remain in the retentate, whereas smaller molecules and solvents pass through the membrane as

permeate. Ultrafiltration membranes typically cover pore sizes ranging from approximately 0.002 µm to 0.2 µm, corresponding to MWCO values between 1,000 Da and 100,000 Da.[19]

In contrast to dead-end filtration, TFUF operates with a flow directed tangentially along the membrane surface. This flow configuration reduces concentration polarization and membrane fouling, thereby enabling stable filtration performance over extended process times. The driving force for mass transfer across the membrane is the transmembrane pressure (Δp_{TM}), defined as the average pressure on the feed and retentate side minus the permeate pressure, see Equation 2.1:

$$\Delta p_{TM}(t) = \frac{p_{Feed}(t)+p_{Ret}(t)}{2} - p_{Per}(t) \quad (2.1)$$

Δp_{TM} := Transmembrane pressure [bar]

p_{Feed} := Feed pressure [bar]

p_{Ret} := Retentate pressure [bar]

p_{Per} := Permeate pressure [bar]

An appropriately adjusted transmembrane pressure ensures a constant permeate flux while minimizing mechanical stress on the membrane. [20]

In addition to volume concentration, TFUF enables diafiltration, during which fresh buffer is added to the retentate at the same rate as permeate removal. The efficiency of buffer exchange is described by the number of diafiltration volumes (DV). The removal of low low-molecular-weight components such as salts, metabolites and residual medium constituents, follows an exponential relationship, with one DV removing approximately 63 % and three DV approximately 95 % of the original buffer.[21] Diafiltration thus enables a controlled buffer exchange without significant loss of product. [20]

2.6 Analytical methods

Analytical methods are a central component of bioprocess development, as they enable the monitoring, evaluation and optimization of microbial cultivations and downstream processes. Reliable analytical data are essential for understanding biomass formation, substrate consumption, product expression and product quality in recombinant protein production systems.

Analytical techniques in bioprocessing are commonly categorized as in-line, on-line, at-line and off-line methods, depending on their integration into the process and temporal resolution.[22] On-line methods such as off-gas analysis allow continuous monitoring of metabolic activity and respiratory behavior, providing insights into growth phases, substrate limitation and metabolic shifts. At-line and off-line methods, including optical density measurements and gravimetric biomass determination, are widely used for biomass quantification, although OD measurements require calibration and are limited at high cell densities.[23]

For recombinant protein processes, analytical methods must address both protein expression and functional activity. SDS-PAGE is routinely applied to confirm protein expression and molecular weight, while functional assays are required to assess biological activity, as expression alone does not guarantee functionality. In this context, activity-based assays such as PCR provide application-relevant information for DNA polymerases.

Modern bioprocess optimization relies on the integration of multiple analytical methods to derive key performance parameters such as specific rates and productivities.

2.6.1 Optical density measurements

The measurement of optical density (OD) is a widely used and rapid method for estimating cell concentration in microbial cultures. It is based on the attenuation of transmitted light caused by scattering and absorption when a cell suspension is illuminated with monochromatic light. In biotechnological applications, the optical density is typically measured at a wavelength of 600 nm (OD_{600}), as this wavelength minimizes absorption by cellular components while providing a reliable correlation with biomass concentration.

The measured optical density is proportional to the number of cells in suspension within a defined linear range. At low to moderate cell densities, a linear relationship between OD and biomass concentration can be assumed. However, at higher optical densities, multiple light scattering events occur, leading to non-linear signal behavior and increased measurement errors. Therefore, samples with high cell concentrations must be diluted to ensure that OD values fall within the linear measurement range of the photometer. [24]

To convert optical density values into absolute biomass concentrations, a strain- and system-specific conversion factor is required. This factor is typically determined by correlating OD measurements with gravimetrically determined biomass concentrations (Bio dry matter).

2.6.2 SDS-PAGE

Sodium dodecyl sulfate polyacrylamide gel electrophoresis (SDS-PAGE) is a widely used analytical technique for the separation of proteins according to their molecular weight. Prior to electrophoresis, protein samples are treated with sodium dodecyl sulfate (SDS), an anionic detergent that denatures proteins and confers a uniform negative charge proportional to the length of the polypeptide chain. This ensures that protein migration through the gel matrix is primarily determined by molecular size rather than intrinsic charge.

In addition, reducing agents such as dithiothreitol (DTT) are commonly applied to disrupt disulfide bonds, thereby ensuring complete unfolding of the protein structure. The denatured proteins are subsequently separated in a polyacrylamide gel under an applied electric field. Smaller proteins migrate faster through the gel pores than larger proteins, resulting in size-dependent separation. After electrophoretic separation, proteins are visualized using staining methods, most commonly Coomassie Brilliant Blue staining. [25]

2.6.3 Polymerase chain reaction

The polymerase chain reaction (PCR) is an enzymatic technique used for the exponential amplification of specific DNA fragments. It is based on repeated cycles of DNA denaturation, primer annealing and enzymatic strand extension, resulting in exponential increase of a defined target DNA sequence. Each PCR reaction requires a DNA polymerase, a template DNA that should be amplified, sequence-specific primers, deoxynucleotide triphosphates (dNTPs) and an appropriate reaction buffer.

The specificity of PCR is determined by short oligonucleotide primers that anneal to complementary regions on the DNA template. During the extension step, the DNA polymerase catalyzes the incorporation of dNTPs complementary to the template strand, thereby synthesizing a new DNA molecule. Repeated cycling results in exponential amplification of the target fragment. [26]

A successful PCR reaction can be detected by agarose gel electrophoresis, where the presence of a distinct DNA band at the expected DNA fragment size indicates enzymatic activity of the polymerase. In contrast, negative controls lacking active polymerase show no amplification product (band).

Figure 5 illustrates a schematic agarose gel electrophoresis used for the qualitative evaluation of PCR results. The marker lane serves as a size reference, while the negative control confirms the absence of contamination or unspecific amplification. The appearance of a clear band in the positive sample indicates successful DNA amplification and thus functional polymerase activity.

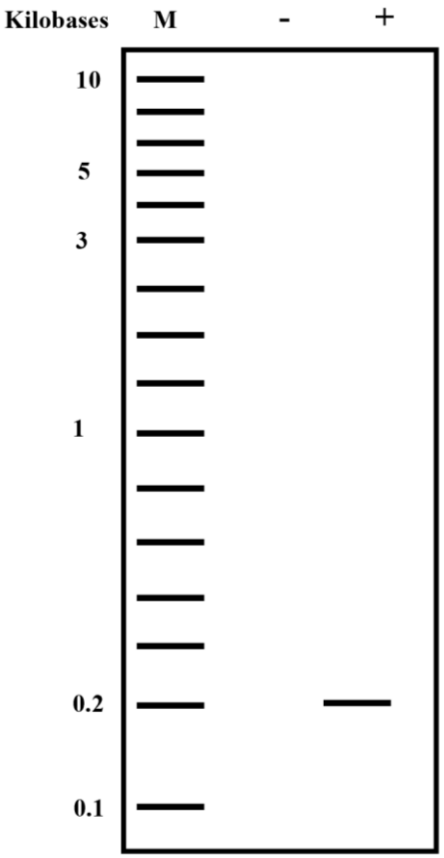

Figure 5: Schematic representation of an agarose gel electrophoresis used for the evaluation of PCR results. The marker lane (M) provides a reference for fragment size determination. The negative control (-) shows no band, confirming the absence of contamination or unspecific amplification. The positive sample (+) exhibits a distinct band at the expected fragment size, indicating successful DNA amplification and demonstrating the enzymatic activity of the DNA polymerase.

3. Materials

3.1 Primer and Plasmid for PCR

As a template for the PCR conducted the plasmid 0002 pRed/ET (c = 38 ng/µL) is used.

The primers used were primers 13 and 14:

Name	Sequence	T_M in °C
Primer 13	ACCCACAACTCAAAGGAAAAGG	57
Primer 14	GGGTTGAGTAGTGCCACACA	57

3.2 Cultivation

3.2.1 Bioreactor Biostat® Aplus 2

The bioreactor used is the Biostat® Aplus 2 manufactured by Sartorius Stedim Biotech GmbH. It is a 3 L autoclavable single-walled vessel with a working volume of 0.6 - 2 L including a Base Unit. The bioreactor and all its components are shown in Figure 7, Figure 8 illustrates the lid layout focusing on the probes.

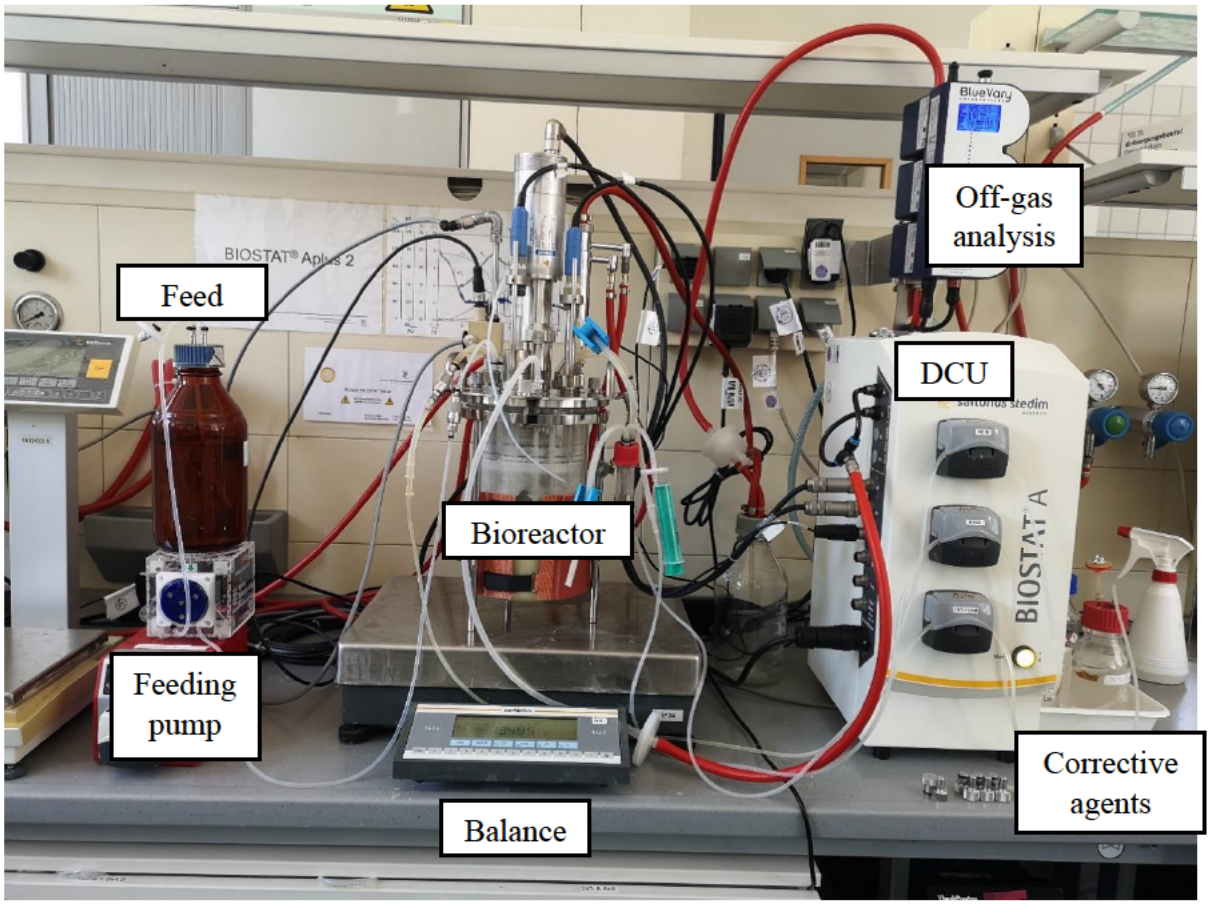

Figure 6: Bioreactor Biostat Aplus 2 with all its components, the feed as well as the feeding pump, bioreactor, balance, DCU, corrective agents and off-gas analysis are characterized. Components such as sampling, pO2, pH, antifoam, methanol probe, stirrer, heat jacket and cooling are not marked.

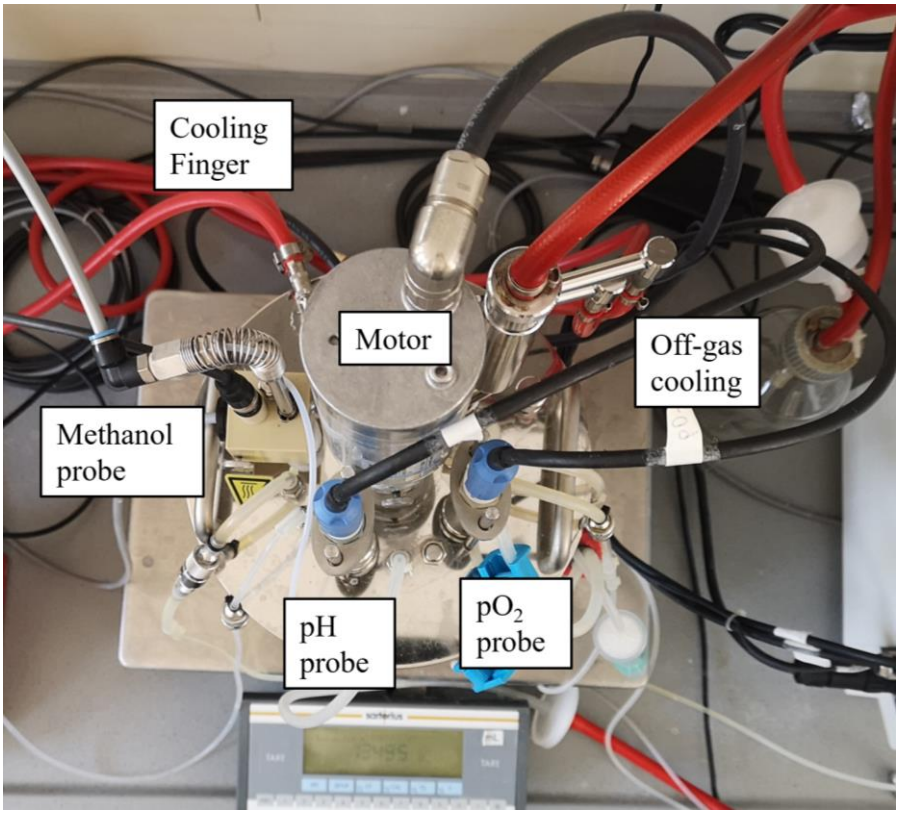

Figure 7: Lid layout of the Biostat® Aplus 2. The cooling finger, off-gas cooling, motor, methanol probe, pH probe, and pO2 probe are labeled. The inputs for corrective agents and feed, as well as sampling and supply air, are not labeled.

The total volume of the bioreactor, which consists of glass, is 3 L however the recommended working volume is 0.6 to 2 L. The temperature control consists of a heat jacket and a cooling finger. It also has an exhaust air cooler that leads to the off-gas analysis device, the BlueVary by BlueSens gas Sensor GmbH via a Schott bottle with a filter. Furthermore, the pO_2 probe Memosens COS81D by Endres+Hauser, the pH probe Memosens CPS171 by Endres+Hauser, a built-in house methanol probe and the level probe PB-20 by Sartorius Stedim Biotech are being used. The bioreactor can be closed with a stainless-steel lid, shown in Figure 8, which has 14 openings for various probes, cooling finger, exhaust cooler, stirrer with agitator shaft, sampling, gassing ring and more. The stirrer, which is located in the middle of the lid, is driven by the motor ECI 63.40-K4 by Breuell & Hilgenfeldt GmbH with revolutions of 30 -1,100 rpm. [27]

3.2.2 Measurements and automation

Figure 9 shows an overview of the measurements and instrumentation of the bioreactor system. During cultivation, the relevant process parameters are automatically monitored and controlled. The pH value is adjusted to the target value within a defined tolerance range by adding acid or base as required. The dissolved oxygen is controlled by automatically adjusting the stirrer speed as soon as the pO_2 value fells below the specified value.

The methanol concentration in the reactor is maintained between 1 and 2 g/L via a controlled substrate (S2) supply. The temperature is controlled using a heat jacket and a cooling finger,

with 30 °C set for the batch and fed-batch phases and 20 °C or 30 °C set for the production phase. The gas flow was kept constant during cultivation.

A foam sensor is used to ensure process reliability, enabling controlled addition of antifoam. The reactor pressure is regulated to ambient pressure via an exhaust gas pressure sensor.

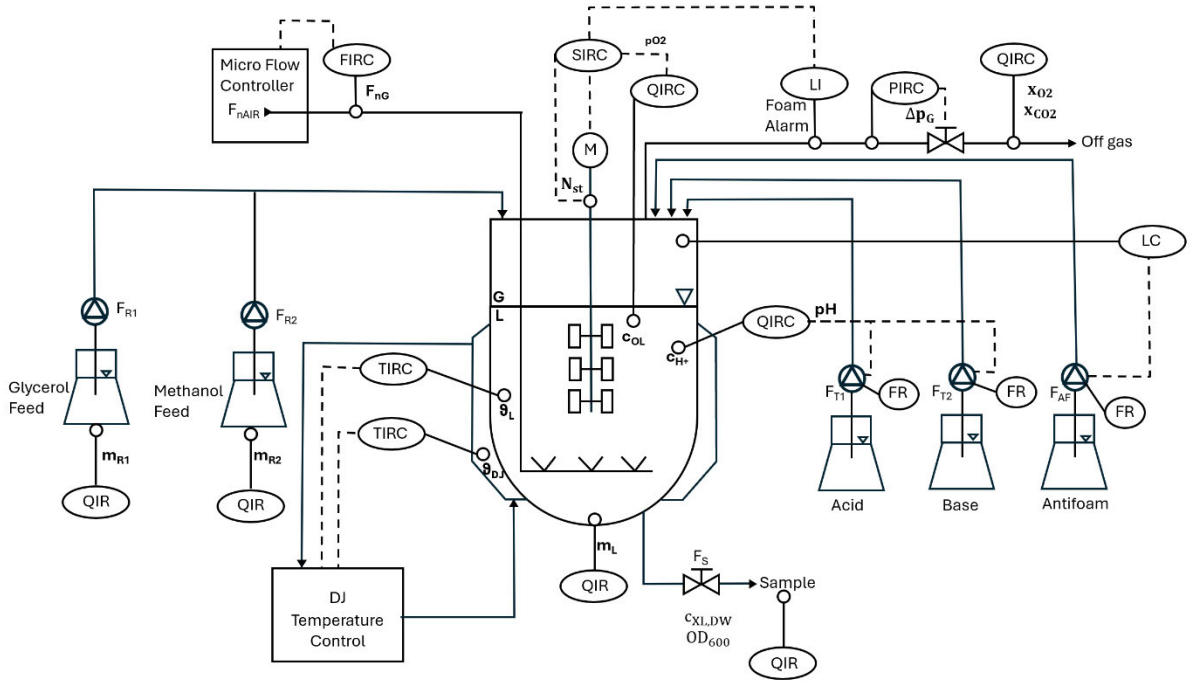

Figure 8: Instrumentation diagram of the used bioreactor system. Flows are represented as lines with arrows and dotted lines indicate regulation signals. G: Gas phase; L: Liquid phase, C: Control; DJ: Double jacket; F: Flow; I: Indication; P: Pressure; Q: Quality; R: Registration; T: Temperature.

3.2.3 DCU

The digital control unit, DCU for short, is the base unit of the bioreactor. It is used to control the process by regulating the process parameters. The DCU is equipped with three fast load pumps, which are used to add corrective agents to the reactor if necessary. Furthermore, the DCU has a gassing module which is regulated by a mass flow controller as well as connections for the heat jacket or probes such as pH, pO_2 and level control.

3.2.4 pO_2 Probe

The pO_2 probe used in the BIOSTAT® Aplus 2 bioreactor is manufactured by Endress+Hauser® and features Memosens technology, making it suitable for sterilization. The probe operates according to the amperometric measurement principle. Dissolved oxygen diffuses through a selective membrane into the sensor according to its partial pressure, while ions and other solutes are excluded, ensuring that the electrical conductivity of the medium does not influence the measurement.

The pO_2 probe is an electrochemical sensor, also known as a Clark electrode, which measures the concentration of dissolved oxygen in the liquid phase of the bioreactor. During operation, the probe is immersed directly in the cultivation medium. Inside the sensor, a gold cathode and a silver anode are immersed in an electrolyte. At the cathode, oxygen molecules are reduced to hydroxide ions, while at the anode, silver is oxidized to silver ions. This redox reaction generates an electrical current that is proportional to the dissolved oxygen concentration. The sensor transducer converts this current into a relative pO_2 signal expressed as a percentage of air saturation.[28]

For accurate measurement, the probe is calibrated using a two-point calibration under running aeration and stirring conditions, identical to those applied during cultivation. First, the bioreactor is aerated with pure nitrogen to remove dissolved oxygen and define the zero point (0 % pO_2). Subsequently, aeration with air is applied to establish the 100 % pO_2 reference value.

3.2.5 pH probe

The pH probe used is manufactured by Endress+Hauser® and is equipped with Memosens technology, providing digital signal stability and suitability for sterilization. Additionally, the probe contains an integrated temperature sensor, which allows for automatic temperature compensation during pH measurement.

The measurement principle is based on electrochemical potential differences. The probe consists of an inner silver/silver chloride electrode immersed in a potassium chloride buffer solution at pH 7 and enclosed by a pH-sensitive glass membrane. A surrounding reference electrode, also based on a silver/silver chloride system and containing the same buffer solution, ensures a stable reference potential. The reference system is separated from the cultivation medium by a diaphragm, which allows ionic contact while preventing direct mixing of solutions.[29]

When the probe is immersed in the liquid phase, hydronium ions from the medium interact with the hydrated outer layer of the glass membrane, while ions from the internal buffer interact with the inner layer. A potential difference is generated across the membrane when a pH gradient exists between the sample and the internal buffer. This potential difference is detected and converted into an electrical signal corresponding to the pH value of the sample.

Prior to use, the pH probe is calibrated using a two-point calibration with standard buffer solutions at pH 4 and pH 7. This calibration is performed before sterilization. After sterilization, the pH of the cultivation medium is measured using external reference pH probe, and the in-situ pH probe is subsequently adjusted in the digital control unit (DCU) to ensure accurate measurement.

3.2.6 Level sensor

The level sensor is used for foam detection in the bioreactor and enables automatic activation of the antifoam pump to reduce foam formation. Foam formation is unavoidable during aerobic cultivations due to agitation, aeration, medium composition and increasing cell concentration. Excessive foam can contaminate the off-gas cooling system and sterile filters, potentially compromising process sterility.

The foam level probe used is the PB-20 by Sartorius Stedim Biotech GmbH, a conductive foam detection sensor. This type of probe detects foam based on changes in electrical conductivity between the sensor electrode and the reactor wall, which typically serves as the counter electrode.

When only gas is present in the measuring range, the electrical circuit is interrupted and no foam is detected. As foam rises and wets the electrode, the conductivity increases due to the liquid phase in the foam, resulting in a measurable current. The signal is interpreted as foam detection and triggers the automatic addition of antifoam agent. Once the foam collapses the electrode surface dries, the electrical circuit is interrupted again, and the probe returns to its initial state. [30]

3.2.7 Methanol probe

The methanol probe used is built by the Bioprocess automatization (BPA) laboratory. The methanol probe has a carrier flow, which consists of compressed air, it flows through the sensor and fills the measuring cell. Figure 9 illustrates the probe immersed in the medium containing methanol. Methanol diffuses though a membrane into the measuring cell, where it is transported past the TGS2620 alcohol sensor by carrier flow. As methanol passes the sensor, it reduces the sensor`s electrical resistance, which means a higher methanol concentration results in lower resistance values.

The resistance is measured by a voltage drop and calculated back to a resistance value. Using a previously created calibration line, a percentage methanol concentration can be assigned to each resistance. These concentrations are displayed in MFCS/win as volume percent. To convert it to a mass concentration in g/L, the volume percent must be divided by the conversion factor 0.126 %/(g/L).

However, factors such as other volatile organic compounds, temperature, and humidity can interfere with the measurement, leading to possible cross-sensitivities.

$$c_{S2L}(t) = \frac{x_{S2L}(t) \cdot \rho_{S2}}{100\%} \tag{3.1}$$

c_{S2L} := Methanol concentration in liquid phase [g/L]

x_{S2L} := Mass fraction of methanol in the liquid phase [vol-%]

ρ_{S2} := Density of methanol at 22 °C [g/L]

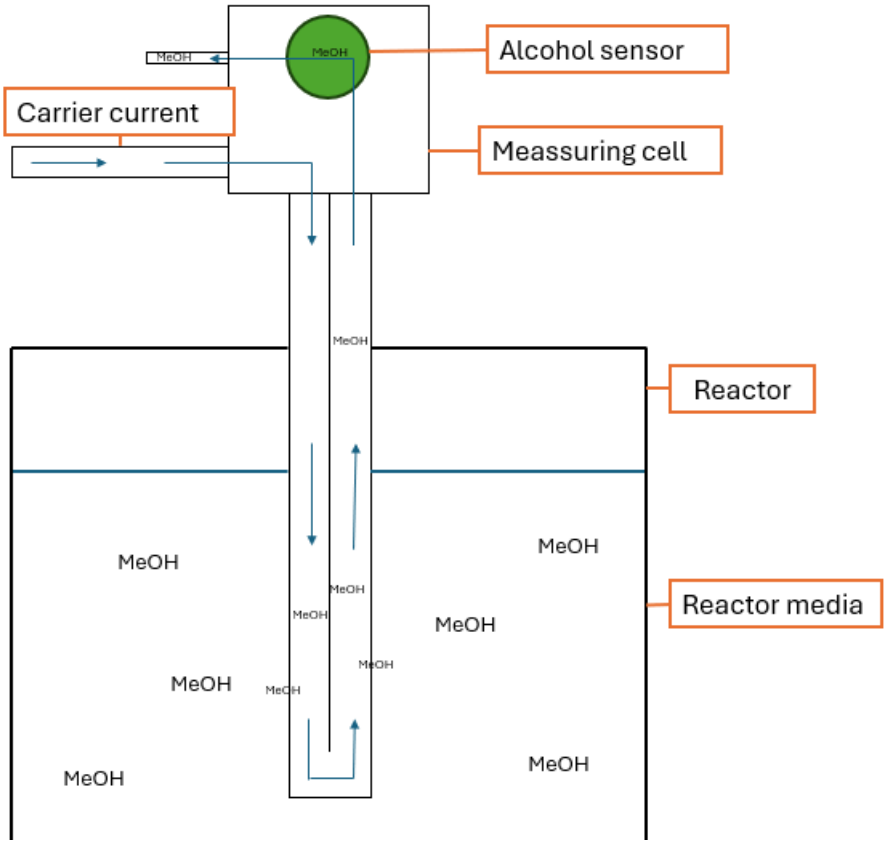

Figure 9: Schematic representation of the methanol probe. Methanol is transported to the alcohol sensor by the incoming carrier current and is measured in the measuring cell by an alcohol sensor TGS2620.[31]

3.2.8 Off-gas analysis system (BlueVis)

BlueVis is a complementary software and off-gas analysis system used for the quantitative monitoring of oxygen, carbon dioxide, pressure, and humidity in bioprocesses. The system enables continuous analysis of off-gas composition and provides information on cellular respiration and metabolic activity.

Oxygen concentration in the off-gas is measured using an electrochemical sensor capable of detecting oxygen levels down to the parts-per-million (ppm) range. Carbon dioxide concentration is determined using an infrared (IR) sensor. When the gas stream passes through the sensor, infrared light with a wavelength of 4.26 µm is emitted, which corresponds to a characteristic absorption band of carbon dioxide. The amount of absorbed infrared radiation increases with rising carbon dioxide concentration, allowing quantitative determination of the carbon dioxide content in the off-gas.

Pressure is measured using a piezoresistive silicon pressure sensor, which detects changes in electrical resistance induced by mechanical deformation of the sensor element. Humidity is measured with a capacitive polymer sensor. This sensor consists of two conductive electrode layers separated by a hygroscopic dielectric polymer. Absorption of water vapor by the dielectric material increases its dielectric constant, resulting in a corresponding increase in capacitance, Since the dielectric constant and capacitance are directly proportional to the water

content of the polymer, changes in capacitance can be directly correlated to the relative humidity of the gas stream.

3.2.9 Process control system MFCS/win

The Multi Fermenter Control System for Windows (MFCS/win) is a process control system from Sartorius Stedim Biotech GmbH. It is responsible for data acquisition and process control during cultivation. In the main menu, the MFCS/win shell, which can be seen in Figure 10, it is possible to open different client modules. With the help of these modules, it is possible to edit processes individually, for example with recipes for cultivation. The client module "Batch report" is used to create reports of already finished cultivations, i.e. it is possible to download certain recorded cultivation data such as the stirrer speed (N_{St}). The "Configuration Manager" is used to define, manage and maintain the system configuration. The "Batch management" module has the function of initializing new cultivations based on an existing recipe and managing the different cultivations. The "Operator Service" can be used to present configurable graphic overviews of sensors and variables or group variables. The "Plotting" module generates a graph from selected parameters of a running or already completed cultivation. The "Sample Data Management" is used to manage sample data and enables the entry of off-line measured value.

Figure 10: MFCS Shell application. From left to right: Batch Report, Configuration Manager, Batch Management, Operator Service, Plotting Module, Sample Data Management.

4. Methods

4.1 Creation of a cell bank

To create a cell bank, a plate with YPD medium (10 g/L Yeast extract, 20 g/L Peptone, 40 mL/L Glucose stock (500 g/L), 12 g/L Agar) is used on which the yeast *P. pastoris* BSY12MS_KlenTaq is plated on. This Plate was provided by the microbiology laboratory of HAW. The plate is incubated at 30 °C until visible single colonies can be seen on the plate. Two single colonies are removed using an inoculation loop and one single colony each is transferred into a 50 mL Erlenmeyer flask filled with 10 mL YPD medium (10 g/L Yeast extract, 20 g/L Peptone, 40 mL/L Glucose stock (500 g/L)). The Erlenmeyer flasks with the single colonies are incubated at 30 °C at 200 rpm in the shaking incubator 3032 by Gesellschaft für Labortechnik GmbH until the next morning.

The next morning the optical density of the overnight culture is determined using the photometer Genesys20 from Thermo Scientific, to calculate the inoculation volume of the main culture. The desired optical density at the start of the main culture is 0.2 AU. Equation 4.1 is used to calculate the inoculation volume for the main culture.

$$V_{OC} = \frac{OD_{MC}(t) \cdot V_{MC}}{OD_{OC}(t)} \tag{4.1}$$

V_{OC} := Volume of overnight culture [L]

OD_{PC} := Optical density of overnight culture [AU]

V_{MC} := Volume of main culture [L]

OD_{MC} := Optical density of main culture [AU]

The overnight culture is used for inoculation and the YPD medium is used as the medium for the main culture. For the main culture, two 500 mL Erlenmeyer flasks are filled with 50 mL YPD medium. The inoculated main cultures are incubated at 30 °C and 300 rpm and samples are taken every hour, from one of the two Erlenmeyer flasks, to determine the optical density. The desired optical density is 3 to 5 AU. Once the desired optical density is reached, the unopened Erlenmeyer flask, from which no samples are taken, is cooled to 4 °C using cooling spheres. The main culture is then transferred to a 100 mL screw-top flask filled with 11.11 g chilled sterile glycerol and mixed. For aliquoting, 1 mL at a time is filled into cryovials with the help of the multi-step pipette HandyStep® touch by Brand and then placed back on the cooling sphere for subsequent storage at -80 °C. The process described is illustrated in Figure 11.

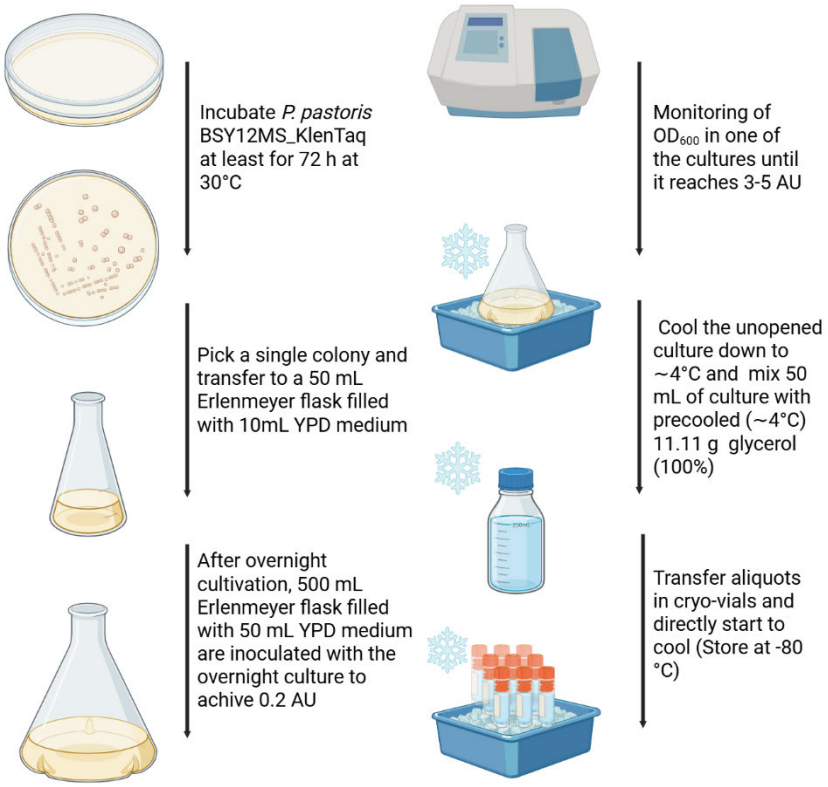

Figure 11: Schematic protocol for cell bank generation. *P. pastoris* BSY12MS_KlenTaq is plated on a plate with YPD medium. The plate is incubated at least 72 h at 30 °C until single colonies are visible. A single colony is picked from the plate and transferred into a 50m mL Erlenmeyer flask filled with 10 mL YPD medium, this culture is cultivated overnight. Next, the required volume of the overnight culture is calculated, which is necessary to inoculate 50 mL of YPD medium with the overnight culture to achieve a starting optical density of 0.2 AU. The optical density of the culture is then monitored until an OD of 3 to 5 AU is reached. Once a sufficient OD has been reached, the culture is cooled to approximately 4 °C using cooling balls and mixed with 11.11 g of pre-cooled glycerol. Finally, the cell suspension is transferred to cryovials using a multi-step pipette.

4.2 Determination of the optical density (OD)

At defined time intervals, samples are taken from the bioreactor or Erlenmeyer flask. For optical density (OD) measurements, 1 mL of the sample is transferred into a cuvette and measured at a wavelength of 600 nm using the photometer Genesys20 from Thermo Scientific. The measured optical density is used to determine the cell concentration.
The conversion of optical density to cell concentration requires a calibration based on biomass dry weight. Using this calibration, the cell concentration in the liquid phase is calculated according to Equation 4.2:

$$c_{XL}(t) = C_{X/OD} \cdot OD(t) \qquad (4.2)$$

$C_{X/OD}$:= Conversion coefficient for cell concentration from optical density [g/(L AU)]

To ensure accurate measurements, the optical density was maintained within a range of 0.1 – 0.6 AU, as higher cell densities can lead to significant measurement errors due to excessive light attenuation. If necessary, samples are diluted using appropriate dilution series to achieve

values within this range. Pipetting volumes below 100 µL are avoided to minimize pipetting inaccuracies.

All OD measurements are performed in duplicate. The mean value of the duplicate measurements is calculated and multiplied by the corresponding dilution factor to obtain the actual optical density of the sample.

4.3 Biomass dry matter

For the determination of biomass dry weight, pre-labeled micro reaction tubes are dried with the help of the drying cabinet 2711 from Köttermann GmbH at 100 °C at least 24 h prior to the first sampling. This step ensures that any residual moisture on and in the tubes is removed. After drying, the tubes must only be handled with gloves to avoid weight alterations due to moisture. Before using the tubes, their dry weight of each empty tube is measured with the analytical balance ABJ-NM/ABS-N from KERN & SOHN GmbH.

At defined time intervals, 1 mL of culture broth is transferred into each of two pre-dried micro reaction tubes (duplicate determination). The samples are then centrifuged at 10,000 rpm for 5 minutes. The supernatant is discarded, and the resulting pellet is dried in the drying cabinet at 100 °C for at least 24 h.

Following the drying step, the tubes containing the dried biomass are weighed. The mass of the empty tube is subtracted from the total mass, and resulting biomass is divided by the sample volume to calculate the cell concentration, as shown in Equation 4.3:

$$c_{XL}(t) = \frac{m_{BDM+E}(t) - m_E}{V_{sample}} \tag{4.3}$$

m_{BDM+E} := Mass of micro reaction tube and dried pellet [g]

m_E := Mass of micro reaction tube [g]

V_{sample} := Volume of sample [L]

The calculated biomass dry weight concentration is subsequently used to determine the conversion coefficient between optical density and cell concentration.

4.4 Protein expression of KlenTaq Polymerase in Erlenmeyer flasks

For the expression of KlenTaq polymerase in Erlenmeyer flasks the protocol by Finn-Lasse Koop is used.[32] To asses reproducibility, two parallel cultures (Flask 1 and Flask 2) are prepared. One cryovial is used to inoculate one Erlenmeyer flask with the preculture.

The contents of one cryovial is transferred into one 1 L Erlenmeyer flask containing 100 mL of BMGY medium (10 g/L Yeast extract, 20 g/L Pepton, 100 mL/L (1 M) PBB), 100 mL/L (10x) YNB, 40mL/L (50 %) Glycerol). The culture is incubated for 72 h at 30 °C and 300 rpm.

After incubation, the optical density at 600 nm is determined and is required to exceed 20 AU before further processing.

For induction of protein expression, the cultures are transferred from BMGY to BMMY medium (10 g/L Yeast extract, 20 g/L Pepton, 100 mL/L (1 M) PBB), 100 mL/L (10x) YNB, 100 mL/L (5 %) Methanol). To this end, 20 mL of the BMGY culture is transferred into sterile Falcon tubes and centrifuged at 6000 x g for 6 minutes. The supernatant is discarded, and the resulting pellets are resuspended in pre-warmed (30 °C) BMMY medium. Each pellet is resuspended in 12.5 mL BMMY medium. A 1 mL sample was taken for OD determination and stored at – 20 °C.

The resuspended pre-cultures are combined and transferred each into a 1 L Erlenmeyer flask, followed by incubation at 30 °C and 300 rpm for 72 h. Methanol feeding is performed: after 24 h 4 mL of 50 % (v/v) methanol is added and a sample is taken; after 48 h, an additional 2 mL of 50 % (v/v) methanol is added and another sample is collected.

After 72 h of induction, the culture supernatant is harvested by transferring 25 mL aliquots into sterile falcon tubes and centrifuging at 6000 x g for 5 minutes. For thermal purification, the supernatant is transferred to new falcon tubes and incubated at 75 °C for 30 minutes in a ThermoMixer C by Eppendorf at low shaking speed. Subsequently, the samples are cooled at 4 °C for 20 minnutes and centrifuged at 7745 x g and 4 °C for 20 minutes. The clarified supernatant is transferred to fresh falcon tubes.

For concentration and buffer exchange, 20 mL of the supernatant are filled into an Vivaspin 20 from Sartorius Stedim Biotech GmbH and centrifuged at 4015 x g for 40 minutes. The permeate is discarded, and the procedure is repeated with additional 20 mL clarified supernatant until the entire supernatant has been processed. During the final concentration step, 20 mL of KlenTaq buffer (20 mM Tris-HCl, 100 mM NaCl, 0.1 mM EDTA, pH 7.5) are added to the concentrator and centrifuged under the same conditions. This buffer exchange step is repeated three times until a final volume of approximately 1 mL of purified KlenTaq polymerase is obtained.

4.5 Recipe for cultivation

Figure 12 shows an overview of the recipe used in this thesis. It is divided into a total of five phases, three of which regulate cultivation and two, at the beginning and end of the recipe, serve to manage cultivation.

The recipe begins with the "init" phase, which serves to initialize cultivation. To do this, variables are initialized, calculations of required variables start, and control modes are defined. This is followed by three cultivation phases: the batch phase, the fed batch phase, and the production phase. At the end of cultivation, the "end" phase takes place, where calculations are stopped, controllers are turned off, and the recorded data is saved. For a more detailed insight into the recipe, it is deposited in Appendix A.5

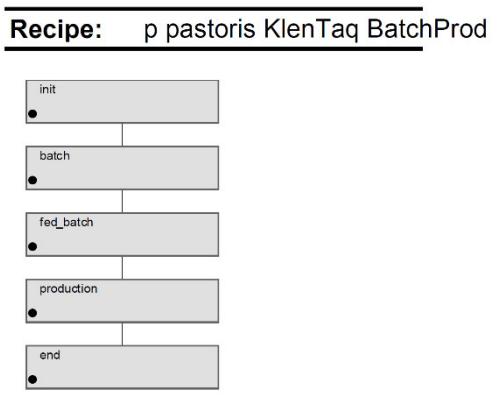

Figure 12: Overview of the recipe used in the thesis. The recipe "p pastoris KlenTaq BatchProd" divides into five phases. In the first phase, called "init," cultivation is initiated, for example, by activating data recording. This is followed by the batch phase, which also includes inoculation. This is followed by the fed batch and production phase. Finally, the "end" phase takes place, in which the process is terminated, and the recorded data is saved.

4.6 Batch phase

The batch phase, which is the first phase during cultivation, begins after the inoculum is transferred into the reactor. The inoculum consists of a defined cell amount to guarantee a reproducible initial biomass at the start of cultivation. Due to the new environment in the reactor, the cells undergo an adaptation phase in which the cells become accustomed to the new medium. The cells do not grow exponentially in the adaptation phase. The adaptation phase or lag phase can be shortened by using the same medium in the bioreactor as in the inoculum. After the cells have acclimatized to the new environment, they grow at the maximum specific growth rate μ_{max}, since sufficient substrate is present in the liquid phase. A defined quantity of substrate, here glycerol, is initially present in the culture medium. The dissolved oxygen tension (pO_2) is maintained at a minimum of 25 %, regulated through the stirrer speed (N_{St}). During the batch phase, the substrate concentration declines exponentially as a result of exponential cell growth. Upon substrate depletion, cellular proliferation ceases, accompanied by a sharp decrease in oxygen uptake. This distinct shift in oxygen consumption serves as an indicator for the end of the batch phase. This is evident from a steep rise in the pO_2 signal and a steep drop in the N_{St} signal. Equation 4.4 enables the estimation of cell concentration at any given time point during the batch phase with exponential cell growth, as well as the determination of the maximum specific growth rate.

$$c_{XL}(t) = c_{XL0} \cdot e^{\mu_{max} \cdot (t - t_0)} \tag{4.4}$$

c_{XL} := Cell concentration at process time t [g/L]

c_{XL0} := Cell concentration at t = 0 h [g/L]

μ_{max} := Maximum cell growth rate [1/h]

t := Process time [h]

t_0 := Start time [h]

It is also possible to calculate the time at which the substrate is completely used up. To do this, Equation 4.4 is rearranged and Equation 4.5 is obtained. With Equation 4.5 it is possible to calculate the end of the batch phase.

$$t = \frac{\ln\left(\frac{c_{XL}(t)}{c_{XL0}}\right)}{\mu_{max}} + t_0 \tag{4.5}$$

4.7 Fed-batch phase

During the fed-batch phase, cells grow in a controlled manner at a constant specific growth rate to avoid oxygen limitation. A defined feed medium is continuously added to the liquid phase, with the feed rate gradually increasing over time. Simultaneously, the stirrer speed is adjusted to maintain a constant level of dissolved oxygen tension (pO_2). Substrate limitation is intentionally imposed through the regulated addition of feed, thereby ensuring that cells grow at a defined specific growth rate μ_{1w}, which remains below the maximum growth rate ($\mu_{max} > \mu_{1w}$), while avoiding oxygen limitation. The required feeding rate can be calculated by performing a substrate mass balance, seen in Equation 4.6:

$$\dot{m}_{S1L}(t) = -q_{S1/X}(t) \cdot F_{R1}(t) \cdot c_{S1R1} \tag{4.6}$$

$\dot{m}_{S1L}$:= Change of substrate mass in liquid phase [g/h]

$q_{S1/X}$:= Cell specific substrate uptake rate at process time t [h^{-1}]

F_{R1} := Feeding rate of substrate from reservoir at process time t [L/h]

c_{S1R1} := Substrate concentration in reservoir [g/L]

Based on a substrate mass balance in the liquid phase, the cell-specific substrate uptake rate $q_{S1/X}$ can be expressed as a function of the substrate feed rate, the substrate concentration in the feed reservoir, the substrate concentration in the liquid phase, the reactor volume and the biomass concentration. This relationship is given by Equation 4.7:

$$q_{S1/X}(t) = \left(\frac{F_{R1}(t) \cdot c_{S1R1}}{V_L(t)}\right) \cdot \frac{1}{c_{XL}(t)} \tag{4.7}$$

The objective of the fed-batch phase is to supply the cells with substrate at a rate that matches their metabolic capacity at a given process time, thereby preventing substrate accumulation in the liquid phase. Under these substrate limited conditions, the substrate concentration can be assumed to be negligible ($c_{SL} \approx 0$ g/L). Based on this assumption, the required feeding rate can be calculated according to Equation 4.8:

$$F_{R1}(t) = \frac{q_{S1/X}(t)}{c_{S1R1}} \cdot c_{XL}(t) \cdot V_L(t) \quad (4.8)$$

4.8 Production phase

At the onset of the production phase, the carbon source is switched from glycerol (S1) to methanol (S2). An initial methanol pulse is applied to reach a concentration of approximately 5 g/L, allowing the cells to adapt to methanol metabolism. Following the adaptation phase, methanol is maintained at a low concentration of approximately 1 g/L to 2 g/L to avoid toxic effects associated with elevated methanol levels.

During the production phase, cell growth is intentionally limited and occurs at a specific growth rate significantly below the maximum growth rate on methanol ($\mu_{2w} < \mu_{1w} < \mu_{1max}$). Under these conditions, methanol primarily serves as a carbon and energy source for cellular maintenance rather than biomass formation. In addition, methanol acts as an inducer for KlenTaq polymerase expression, which is controlled by the methanol-inducible AOX1 promoter in *P. pastoris*.

4.9 Determination of protein concentration via Bradford assay

Protein concentrations are determined using the Bradford assay, which is based on the binding of Coomassie Brilliant Blue-G250 to proteins. Upon protein binding, the dye shifts to its anionic form, resulting in an increase in absorbance that can be measured photometrically at 595 nm.[33]

For protein quantification, the Roth® NanoQuant kit 5x is used according to the manufacturer's instructions. A calibration curve is prepared using bovine serum albumin (BSA) standards in the concentration range of 0-100 µg/mL. Standard solutions are prepared by serial dilution from a BSA stock solution, as summarized in Table 1.

For the assay, 50 µL of each standard and sample are pipetted into a 96-well microplate, followed by the addition of 200 µL of 1x NanoQuant reagent. After incubation for 5 min at room temperature, absorbance is measured at 590 nm and 450 nm using the microplate reader NanoQuant infinite M200 PRO by TECAN. Protein concentrations are calculated from the ratio OD_{590}/OD_{450} using the BSA standard curve obtained by linear regression.

Table 1: Preparation of BSA standard solutions for the Bradford assay.

BSA concentration [µg/ml]	BSA stock solution [µL]	dd-Water [µL]
0	-	200
1	20 µL from 10µL/ml	180
2.5	50 µL from 10µL/ml	150
5	100 µL from 10µL/ml	100
10	40 µL from 100µL/ml	360
25	50 µL from 100µL/ml	150
50	100 µL from 100µL/ml	100
75	150 µL from 100µL/ml	50
100	200 µL from 400µL/ml	600

4.10 SDS-PAGE

For sample preparation for an SDS-PAGE, a reducing sample buffer is prepared by adding 100 µL dithiothreitol (DTT) to 900 µL of 4x Laemmli sample buffer by BioRad. The protein samples are mixed with the prepared sample buffer in a ratio of 3:1 (15 µL sample and 5 µL sample buffer). The mixtures are heated at 95 °C for 5 minutes to ensure complete denaturation, followed by incubation at room temperature for 5 minutes. Subsequently, the samples are briefly centrifuged at 1,000 rpm to collect condensate.

Electrophoresis is performed using 16 % precast Mini-PROTEAN TGX gels by BioRad, which are mounted in a Mini-PROTEAN Tera Vertical Electrophoresis Cell by BioRad. The electrophoresis chamber is filled with running buffer (10x running buffer (1 M Tris, 1.92 M Glycine, SDS 1 %, pH 8.3). As a molecular weight reference, 5 µL of SeeBlue Plus 2 protein standard by invitogen is loaded into the first lane. The remaining lanes are each loaded with 20 µL of prepared sample. Electrophoresis is conducted at a constant voltage value of 150 V for 35 minutes.

Following electrophoresis, the gel is rinsed with deionized water and stained overnight on a laboratory shaker using Coomassie staining solution (200 mL/L Roti-Blue, 200 mL/L ethanol, 600 mL/L deionized water). Excess stain is removed by incubating the gel in decolorization solution (200 mL/L Roti-Blue, 200 mL/L ethanol, 600 mL/L deionized water) for at least 2 h under gentle shaking. After destaining, the gel is documented for further analysis.

4.11 Polymerase chain reaction (PCR)

For each PCR assay, all reaction components except the template DNA are combined to prepare a master mix (Table 2). For negative controls, the template DNA is replaced with nuclease-free water. Positive controls contained the target DNA and commercially available Hemo KlenTaq DNA polymerase by New England Biolabs, it is engineered to tolerate hemoglobin and other PCR inhibitors commonly present in blood. The term “Hemo” refers to its ability to enable direct PCR amplification from blood-containing samples without prior DNA purification.[34] For

all experimental samples, purified KlenTaq DNA polymerase obtained from the cultivation processes is used to assess enzymatic activity.

PCR reactions are performed in a FlexCycler^2 thermal cycler by analytikjena. The amplification protocol consisted of an initial denaturation step, followed by repeated cycles of denaturation, primer annealing, and extension, and a final elongation step. The specific temperature profile and cycle conditions are summarized in Table 3.

Table 2: Composition of the PCR assay for a 24 µL preparation of a check PCR with prepared KlenTaq DNA polymerase or Hemo KlenTaq DNA polymerase.

Component	Concentration	Volume, µL
Water	-	16.7
Hemo KlenTaq reaction buffer	5x	5
dNTPs	10 mM each	0.5
Primers	25 mM each	each 0.35
DNA Polymerase	-	1
Template	67 ng/µL	0.1

After amplification, PCR products are analyzed by agarose gel electrophoresis. A 1% (w/v) agarose gel is prepared and placed in an electrophoresis chamber filled with 1x TAE buffer (40 mM Tris, 20 mM acetate, 1 mM EDTA). A 1 kb DNA ladder by New England Biolabs is loaded as a molecular weight marker. PCR samples are mixed with 6x loading dye and applied to the gel. Electrophoresis is performed at 100 V until the tracking dye reaches the end of the gel. DNA bands are subsequently visualized and documented.

Table 3: PCR cycling conditions.

Step	Temperature, [°C]	Duration, [mm:ss]	Repetitions
Denaturation	95	03:00	1
	95	00:20	
Annealing	60	00:30	30
	68	01:18	
Extension	68	10:00	1
Cooling	4	00:00	-

4.12 Calibration of Methanol probe

The methanol probe is calibrated prior to cultivation using defined methanol concentrations in the bioreactor. For this purpose, one liter of cultivation medium is added to the bioreactor, which is then operated under standard process conditions with agitation and aeration activated.

Defined amounts of methanol are subsequently added stepwise to achieve predetermined target methanol concentrations in the liquid phase. The theoretically required methanol volumes are calculated in advance. Methanol is added using a syringe, and the exact amount added is determined by weighing the syringe before and after methanol addition.

For each calibration point, the corresponding sensor signal (resistance, RS) and the methanol concentration (vol -%) are recorded. These data are used to generate a calibration curve for the methanol probe. A logarithmic representation of RS and methanol concentration is applied, as the sensor response follows a logarithmic relationship within the relevant concentration range.

4.13 Tangential Flow Ultrafiltration (TFUF)

The TFUF setup used in this study is shown in Figure 13 and consists of a retentate tank, a hollow fiber membrane module, and a permeate tank. The first step is to rinse the module with deionized water, as the module has been stored in 0.1 M NaOH. The module is rinsed with deionized water until the water flowing from the permeate and retentate has a neutral pH value, to check the pH, pH strips are used. Subsequently the thermally purified supernatant is circulated through the membrane module using a peristaltic pump. The permeate flow is controlled via valves V1 and V2, while valve V3 is used to adjust the retentate backpressure and thereby regulate the transmembrane pressure.

For the experiments conducted in this work, a hollow fiber ultrafiltration cartridge (UFP 10 C 4X2MA, Cytiva – Global Life Sciences Solutions Austria GmbH & Co. KG) was used.

For membrane equilibration, permeate valves V1 and V2 were initially closed, and the concentrated supernatant was transferred to the retentate tank and circulated through the module. After equilibration, permeate flow was initiated and the feed and retentate pressures were adjusted to approximately 1 bar.

For diafiltration, fresh buffer was continuously added to the retentate tank while permeate was removed at the same rate, maintaining a constant retentate volume. After completion of the filtration process, the system was rinsed with isotonic saline solution to recover residual proteins from the membrane surface, followed by a final rinse with deionized water. The ultrafiltration module was subsequently stored in 0.1 M NaOH.

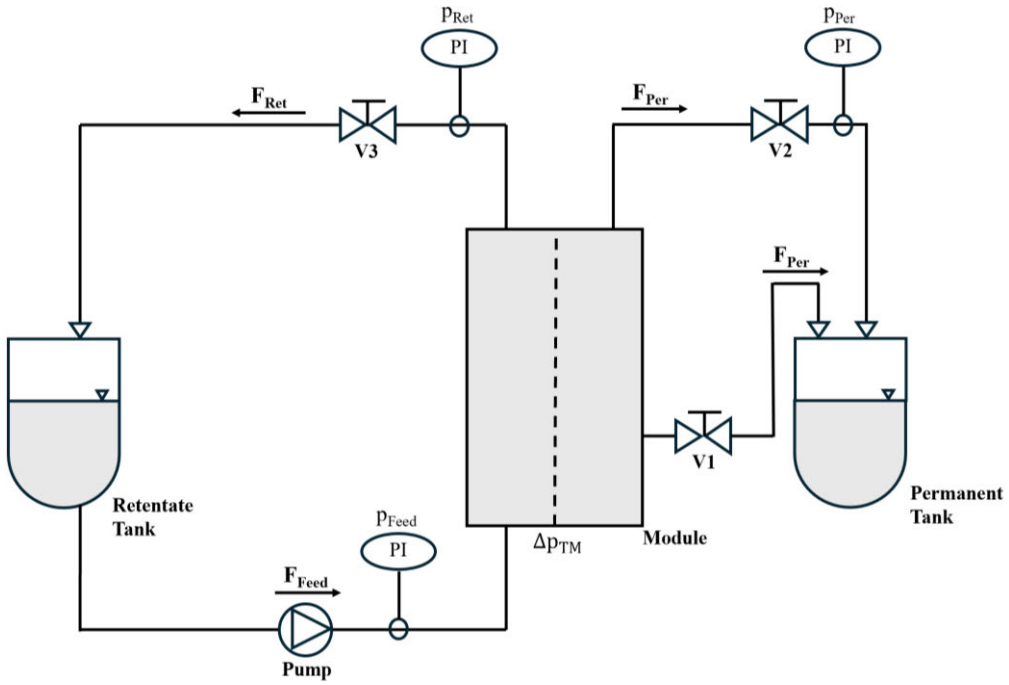

Figure 13: Schematic Illustration of Tangential Flow filtration system. The hollow fiber cartridge UFP 10 C 4X2MA module is installed in the filtration system. A peristaltic pump is used to create a feed flow from the retentate tank. In total three valves are used in the filtration system to adjust the pressure. Two valves are located at the permeate site and one at the retentate site. A pressure gauge is installed in both the retentate and feed lines to monitor the pressure set using the valves. F: Flow; P: Pressure; I: Indication; V: Valve.

4.14 Ultrafiltration using centrifugal Concentrators

Centrifugal concentrators are devices for the preparation of biomolecules, combining the principles of centrifugation and ultrafiltration in one process. This enables gentle and solution-free concentration of samples.

Centrifugal concentrators usually consist of falcon tubes of various designs, equipped with a semi-permeable membrane. This membrane has a defined molecular weight cut-off (MWCO), typically between 1,000 and 100,000 Da. Molecules whose molecular weight is greater than the MWCO cannot pass through the membrane and are retained, resulting in the retentate. Molecules whose molecular weight is less than the MWCO can pass through the membrane and enter the filtrate area (permeate).

The centrifugal concentrators used are Vivaspin 20 from Sartorius Stedim Biotech GmbH, which has a MWCO of 10 kDa. It is possible to add 20 mL of sample above the membrane and then centrifuge the tube in the Tabletop centrifuge at 6000 x g until a desired retentate is left above the membrane.

Figure 14 shows the protocol used to purify samples using centrifugal concentrators. First, 20 mL of the thermally purified supernatant was added via the membrane of the Vivaspin 20 and then centrifuged at 6000 x g until 1 mL of the retentate remained above the membrane, the permeate is discarded. This procedure was carried out twice. For diafiltration, 19 mL of KlenTaq buffer is added to the 1 mL of concentrated supernatant and centrifuged at 6000 x g

until 1 mL remains above the membrane. The diafiltration procedure is repeated a total of three times. This results in an approximate 57-fold change in buffer.

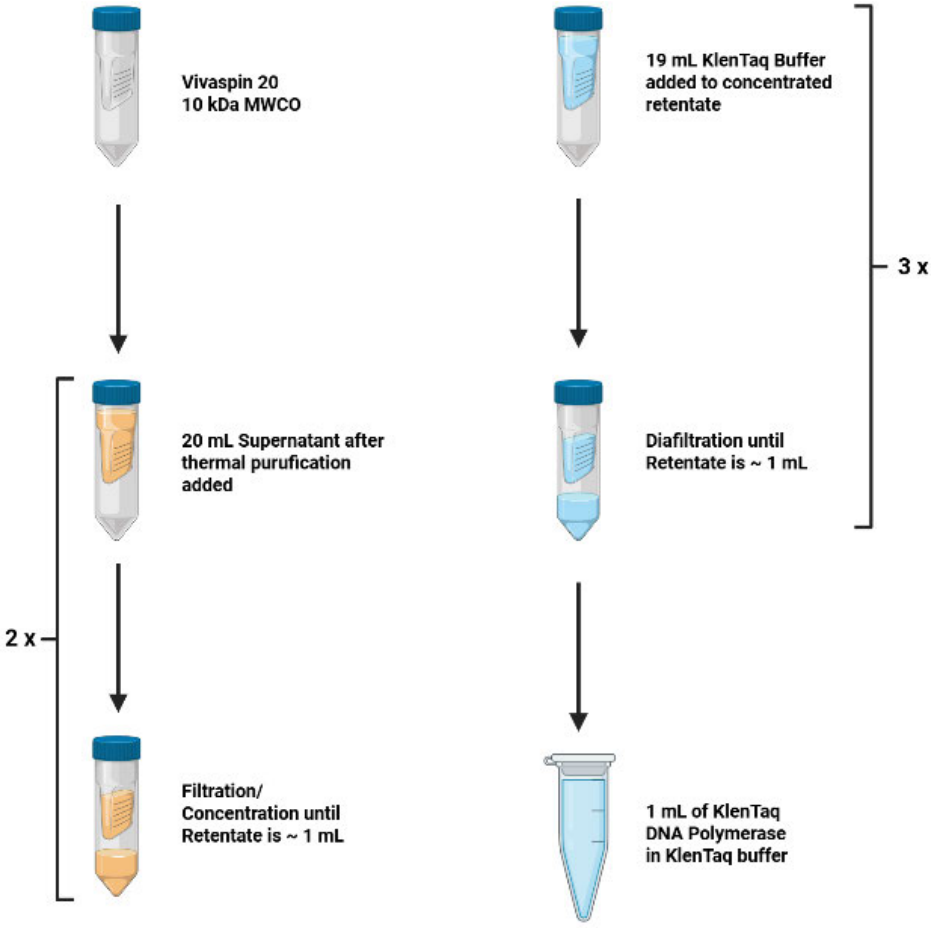

Figure 14: Protocol used for ultra- and diafiltration using centrifugal concentrators Vivaspin 20. First, 20 mL of sample is added to the centrifugal concentrators above the membrane. The concentrator is then centrifuged at 6000 x g until the retentate corresponds to approximately 1 mL. This process is repeated twice. 19 mL of KlenTaq buffer is added to the sample concentrated to 1 mL and centrifuged at 6000 x g until the retentate is 1 mL. This process is repeated three times and then remove 1 mL of purified KlenTaq polymerase from the concentrator.

4.15 Calculation of yield for processes

To evaluate and compare the performance of the different cultivation processes, polymerase production was assessed using biomass-specific yield and specific productivity parameters. The polymerase concentration in the culture supernatant was determined after completion of the respective cultivation and subsequent thermal clarification of the supernatant. Based on the measured polymerase concentration and the final culture volume, the total polymerase mass was calculated.

To relate polymerase formation to biomass formation, the biomass-specific yield was calculated. The total biomass mass was determined from the final cell concentration $c_{XLend}$and the final culture volume V_L. The biomass-specific yield $Y_{P/X}$is expressed as milligrams of polymerase per gram of biomass, as seen in Equation 4.9.

In addition, the specific productivity was calculated to evaluate polymerase formation with respect to both biomass concentration and process time. Specific productivity describes the rate of product formation per unit biomass and time and is therefore a suitable parameter for comparing different process strategies with varying cultivation durations. The specific productivity was calculated by dividing the total produced polymerase mass by the product of the final biomass concentration and the effective production time, shown in Equation 4.10:

$$Y_{P/X}(t) = \frac{c_{PL}(t)}{c_{XL,end}} \tag{4.9}$$

$$q_{P/X}(t) = \frac{c_{PL}(t)}{c_{XLend} \cdot t_{prod}} \tag{4.10}$$

4.16 Calculation of volumetric substrate feeding rate (Q_{S1in})

To quantitatively describe the substrate supply to the culture during the fed-batch phase, the volumetric substrate feeding rate Q_{S1in} was calculated. This parameter represents the amount of substrate S1 (glycerol) that is fed into the bioreactor per unit reactor volume and time and therefore reflects the actual substrate availability for the cells during exponential feeding.

Q_{S1in} is derived from the feed pump rate, the substrate concentration in the feed solution and the actual reactor volume at each time point. Since the feed rate (F_{R1}) and the liquid volume (V_L) were recorded at different sampling intervals by the process control system, both data sets were first interpolated onto a common time vector. Prior to interpolation, duplicate time points and outliers were removed to ensure numerical stability.

The volumetric substrate feeding rate was calculated according to equation 4.11:

$$Q_{S1in}(t) = \frac{F_{R1}(t) \cdot c_{SR1}}{V_L(t)} \tag{4.11}$$

5. Results

5.1 Creation of a Cell bank

The cell bank (CB) was prepared according to the instructions described in section 4.1. Two individual colonies were removed from the plate and used for the inoculation of the precultures in two Erlenmeyer flasks. The measurements of the precultures are shown in Table 4.

Table 4: Optical density measurements of Erlenmeyer flask 1 and 2 for the MCB. 10 mL of YPD medium in a 50 mL Erlenmeyer flask are inoculated with a single colony off the cultivation plate.

Preculture Flask	Time, [h]	OD_{600} (mean value), [AU]
1	22.34	1.29
2	22.43	1.59

Using preculture 2, the main cultures A and B were inoculated for the preparation of CB. The main culture A was used for the CB while samples were taken from the main culture B to determine the optical density. The optical density measurements of main culture A are shown in Figure 15.

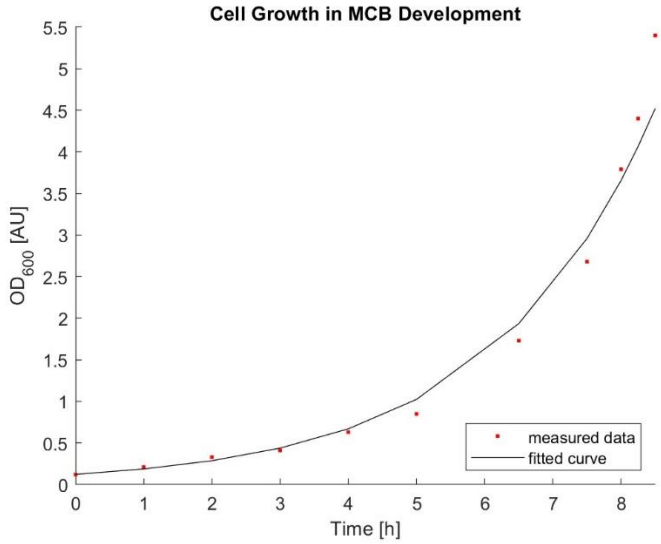

Figure 15: **OD measurements of the Erlenmeyer flask for MCB development.** 46 mL of YPD medium are inoculated with 4 mL of preculture. The exponential fit was created by logarithmic linearization.

Figure 15 shows that the cultivation of the main culture was stopped after 8.5 h, as a sufficient OD was achieved. Subsequently, the 50 mL of the main culture was mixed with 11.11 g mL sterile chilled glycerol and aliquoted as finished CB as 1 mL each into cryovials. The final optical density of the CB was 4.43 AU.

5.2 Protein expression of KlenTaq Polymerase in Erlenmeyer flasks

The expression of KlenTaq polymerase in Erlenmeyer flasks was performed as described in section 4.4. Table 5 illustrates the measurements of the optical density of the two Erlenmeyer flasks in which the expression of KlenTaq polymerase takes place.

Table 5: Measurements of the optical density of *P. pastoris* cultures in Erlenmeyer flasks for the KlenTaq polymerase expression. The Table shows the optical density measurements taken at various points during cultivation in the two Erlenmeyer flasks. The first measurement was taken after 72 hours in BMGY medium, after which the cells were transferred to BMMY medium, and a new measurement is taken. At the 72-hour mark (BMMY), the cultivation had been running for a total of 144 hours.

Time, [h]	OD_{600} Flask 1, [AU]	OD_{600} Flask 2, [AU]
72 (BMGY)	23.23	21.45
0 (BMMY)	17.89	16.93
24 (BMMY)	20.19	19.65
48 (BMMY)	20.92	20.10
72 (BMMY)	21.03	20.32

The measurements in Table 5 show that the cells exhibit a reduction in optical density when transferred from BMGY medium to BMMY medium. This effect can be attributed to incomplete resuspension of the cells in BMMY medium. Furthermore, the cells no longer show significant growth after 24 hours in BMMY medium, which suggests that they have reached the stationary phase.

Figure 16 shows the SDS-PAGE of the samples taken during and after protein expression of KlenTaq polymerase in Erlenmeyer flasks. The gel has the protein marker in the first lane (not marked), to the right of which is the supernatant at the time straight after methanol induction (lane 1). This is followed by three further samples taken during cultivation, the second after 24 hours (lane 2), the third after 48 hours (lane 3), and the last after 72 hours (lane 4). The fifth sample is the supernatant, which was thermally purified at the end of cultivation and concentrated using centrifugal concentrators. Furthermore, a 1:2 and a 1:4 dilution was prepared from the concentrated sample (lane 6 and 7). The KlenTaq DNA polymerase from NEB was used as a reference for the last sample (lane 8).

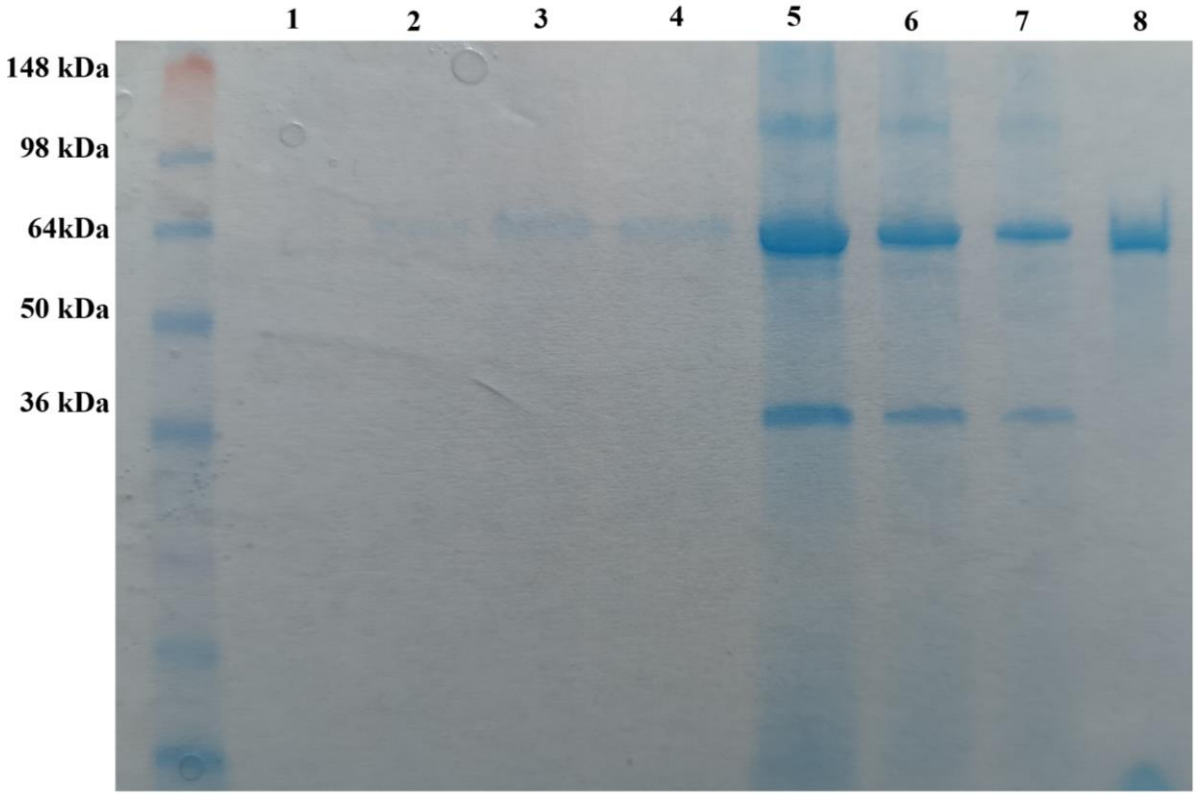

Figure 16: SDS- PAGE gel of all samples taken during the protein expression of the KlenTaq Polymerase in Erlenmeyer flasks. Samples: 1: Supernatant after centrifugation at t = 0 h after methanol induction, 2: Supernatant after centrifugation at t = 24 h after methanol induction, 3: Supernatant after centrifugation at t = 48 h after methanol induction, 4: Supernatant after centrifugation at t = 72 h after methanol induction, 5: concentrated KlenTaq polymerase, 6: KlenTaq polymerase 1:2 diluted, 7: KlenTaq polymerase 1:4 diluted, 8: Hemo KlenTaq polymerase

Figure 17 shows the agarose gel of the PCR assay performed with the thermally purified KlenTaq polymerase obtained from the Erlenmeyer flask cultivation. The molecular weight marker (M) was used for size estimation. No amplification product was detected in the negative control (-), confirming the absence of contamination. In contrast, a clear DNA band of the expected size was observed in the positive control (+), as well as in the sample containing the thermally purified Erlenmeyer flask supernatant. This demonstrates that the produced and thermally purified KlenTaq polymerase was enzymatically active and capable of catalyzing DNA amplification.

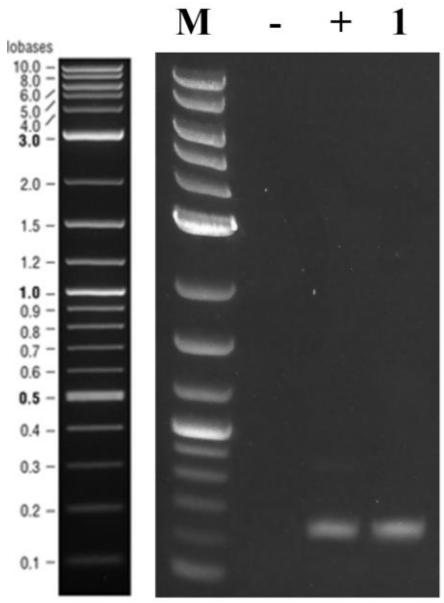

Figure 17: PCR assay of Erlenmeyer flask sample. M: Marker -: negative control, +: positive control, 1: Erlenmeyer flask supernatant (thermally purified)

Table 6 summarizes the absorbance values measured for the BSA standard series at 590 nm and 450 nm as well as the calculated OD_{590}/OD_{450} ratios. Increasing BSA concentrations resulted in a proportional increase of the OD_{590}/OD_{450} ratio.

Table 6: Mean values of the BSA standard series of the Brandford assay. The BSA concentrations of the standard series, the measured OD_{590} and OD_{450}, and the calculated OD_{590}/OD_{450} ratio. The measurements were performed in duplicate.

BSA concentration, [µg/mL]	OD_{590}, [AU]	OD_{450}, [AU]	OD_{590}/OD_{450}, [-]
100	0.8826	0.4532	1.947
75	0.7723	0.5034	1.534
50	0.6981	0.6054	1.153
25	0.5837	0.6545	0.8918
10	0.4544	0.6538	0.6951
5	0.4969	0.6583	0.7548
2.5	0.4428	0.6471	0.6843
1	0.4152	0.6627	0.6265
0	0.3968	0.6575	0.6035

The corresponding calibration curve is shown in Figure 18. A linear relationship between the BSA concentration and the OD_{590}/OD_{450} ratio was obtained over the investigated concentration range (0-100 µg/mL). Linear regression yielded a high coefficient of determination of R^2 = 9.854, indicating good linearity and suitability of the calibration for protein quantification.

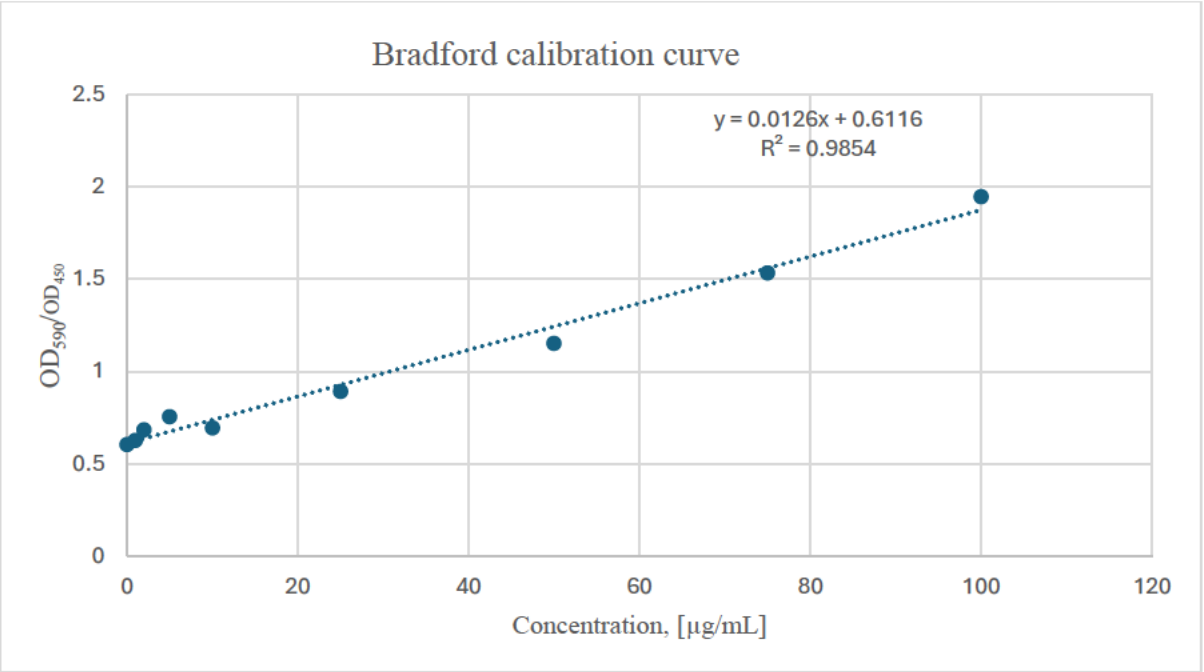

Figure 18: BSA calibration curve for protein determination. The known standard series concentrations were plotted against the ratio of the two optical densities. The linear regression function and coefficient of determination are displayed in the Figure.

Table 7 presents the measured absorbance values and calculated protein concentration of the KlenTaq polymerase samples at different dilutions. The determined protein concentration increased with decreasing dilution factors, confirming the consistency of the Bradford assay. After correction of the dilution factors, the undiluted KlenTaq polymerase concentration ranged between 196.9 and 213.4 µg/mL. Minor deviations between the calculated concentrations can be attributed to pipetting inaccuracies and assay variability.

Table 7: Optical density measurements of the Erlenmeyer flask supernatant (thermally purified). The measured optical densities of the samples and the calculated density ratio are shown. The concentrations were calculated using linear regression and the actual concentration was calculated using dilution.

Sample	OD_{590}, [AU]	OD_{450}, [AU]	OD_{590}/OD_{450}	Concentration, [µg/mL]	Undiluted concentration, [µg/mL]
KlenTaq 1:30	0.4462	0.6364	0.7012	7.112	213.4
KlenTaq 1:10	0.4919	0.5622	0.8749	20.89	208.9
KlenTaq 1:5	0.6401	0.5777	1.108	39.39	196.9

5.3 Calibration of methanol probe

The bioreactor is filled with 1 liter of medium, then it is operated under normal process conditions and the required volumes of methanol, which can be seen in Table 8, are added to the bioreactor one after the other to achieve the theoretical methanol concentrations in the reactor.

Table 8: Theoretical methanol calibration data.

Theoretical calibration concentration, [g/L]	Calculated weight, [g]	Needed volume, [mL]	Theoretical concentration, [Vol%]
0.5	0.5	0.6329	0.063
1	0.5006	0.6337	0.126
1.5	0.5013	0.6345	0.189
2	0.5019	0.6353	0.252
2.5	0.5025	0.6361	0.315
6	3.5127	4.446	0.756

Methanol is added to the bioreactor using the calculated data from Table 8. The actual weight added is calculated and thus the actual methanol concentration in the reactor could also be calculated, which can be seen in Table 9.

Table 9: Actual data for methanol probe calibration.

Theoretical concentration, [g/L]	Actual added weight, [g]	Actual resulting concentration [g/L]
0.5	0.6066	0.4735
1	0.6139	0.9527
1.5	0.6223	1.4385
2	0.5879	1.9287
2.5	0.6453	2.4324
6	5.6439	6.8383

Table 10 shows the actual methanol concentration during the calibration and their corresponding measured resistance and concentration in volume percent as well as their logarithm. Using the measured resistance and concentration in percent and the calculated logarithm the methanol calibration curve can be created, which can be seen in Figure 19 and 20.

Table 10: Actual methanol concentration in the bioreactor as well as the measured resistance and concentration in percent by volume and their logarithm.

Actual concentration, [g/L]	RS, [Ohm]	Concentration measured, [Vol%]	RS, [log(Ohm)]	Concentration measured, [log(Vol%)]
0.4735	6209.78	0.9264	3.7930	-1.0332
0.9527	4779.65	0.1424	3.6793	-0.8170
1.4385	4085.09	0.2165	3.6112	-0.6645
1.9287	3675.62	0.2667	3.5653	-0.5739
2.4324	3353.77	0.3253	3.5255	-0.4877
6.8383	2198.89	0.7046	3.3422	-0.1520

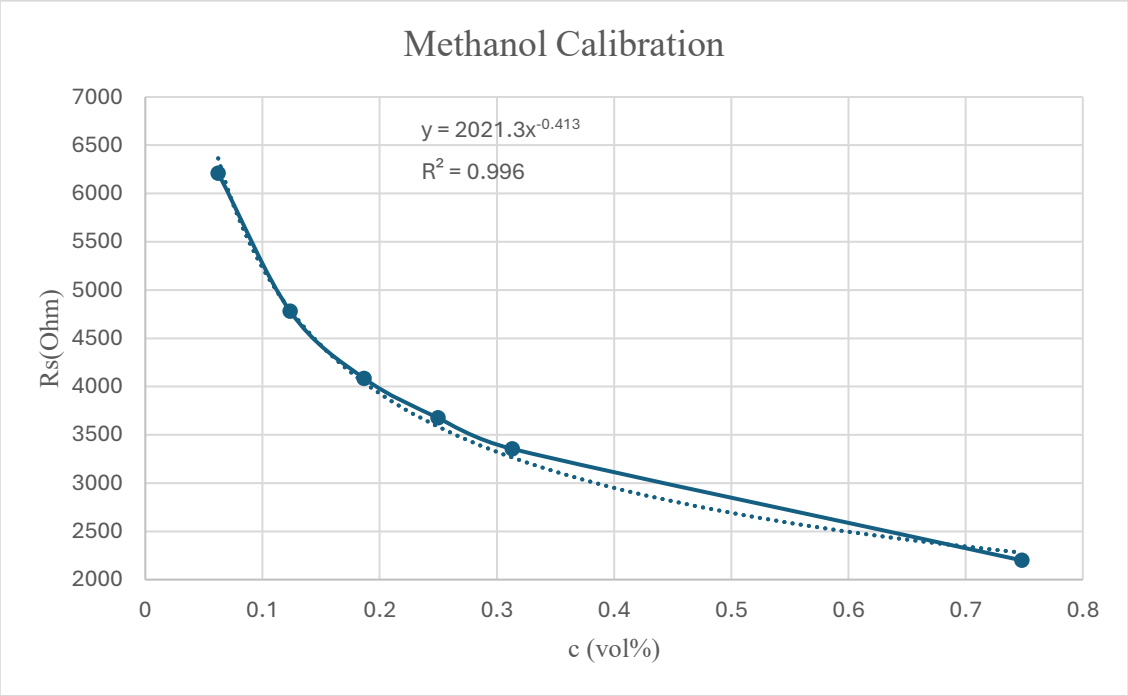

Figure 19: Methanol calibration curve. The calibration curve shows a falling resistance whilst increasing the methanol concentration

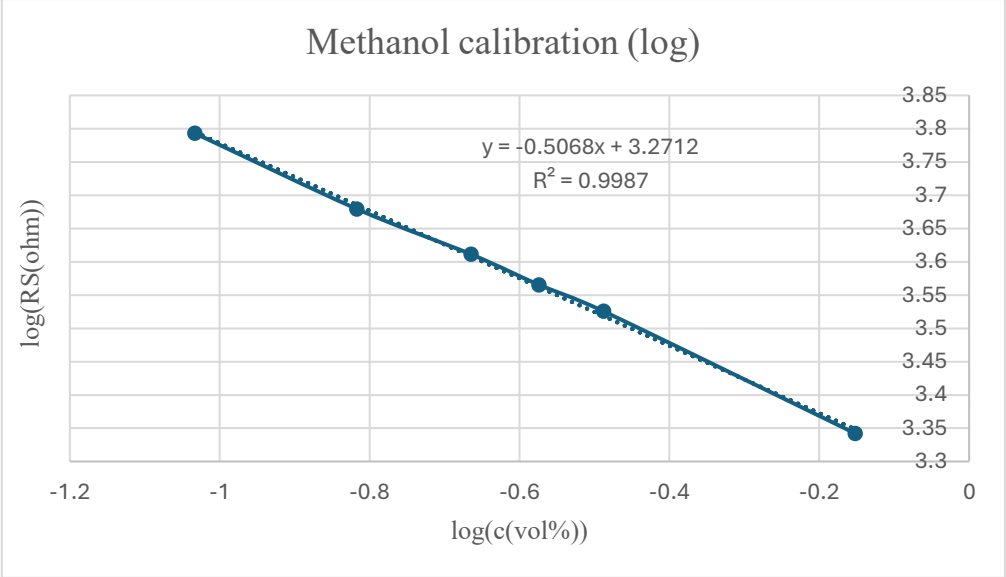

Figure 20: Logarithmic methanol calibration curve.

5.4 Upstream Processing using Biostat A plus 2

The recipe provided in Appendix A.5 was used for the cultivations carried out.

5.4.1 Process JW_4725

The cultivation process JW_4725 was initiated in the morning to enable sampling throughout the day. The process was conducted as a complete cultivation run comprising a batch phase, a fed-batch phase and a subsequent production phase. Cultivation was performed using the minimal medium FM22. Throughout the entire process, the pH value was actively regulated at 6.5, and the temperature was maintained at a constant setpoint of 30 °C. The total process duration was 64.8 h. The transition from batch to fed-batch phase occurred after 13.7 h, while the production phase was initiated after 32 h. The parameters of the cultivation process are illustrated in Figures 21-23.

The batch phase, depicted in Figure 21, exhibited behavior consistent with theoretical expectations. The pH value was maintained at 6.5 by controller addition of ammonia and phosphoric acid, while the temperature remained constant at 30 °C throughout the batch phase. Following inoculation at an initial cell concentration of 0.89 g/L, the dissolved oxygen tension (pO_2) decreased from 100 % to the setpoint of 25 % within approximately 7.5 h. Upon reaching this setpoint, pO_2 was actively regulated by increasing the stirrer speed, as shown in Figure 21. Substrate depletion in the liquid phase was indicated by a sharp increase in pO_2 accompanied by a corresponding decrease in stirrer speed, thereby signaling the end of the batch phase. The measured cell concentration exhibited clear exponential growth throughout the batch phase.

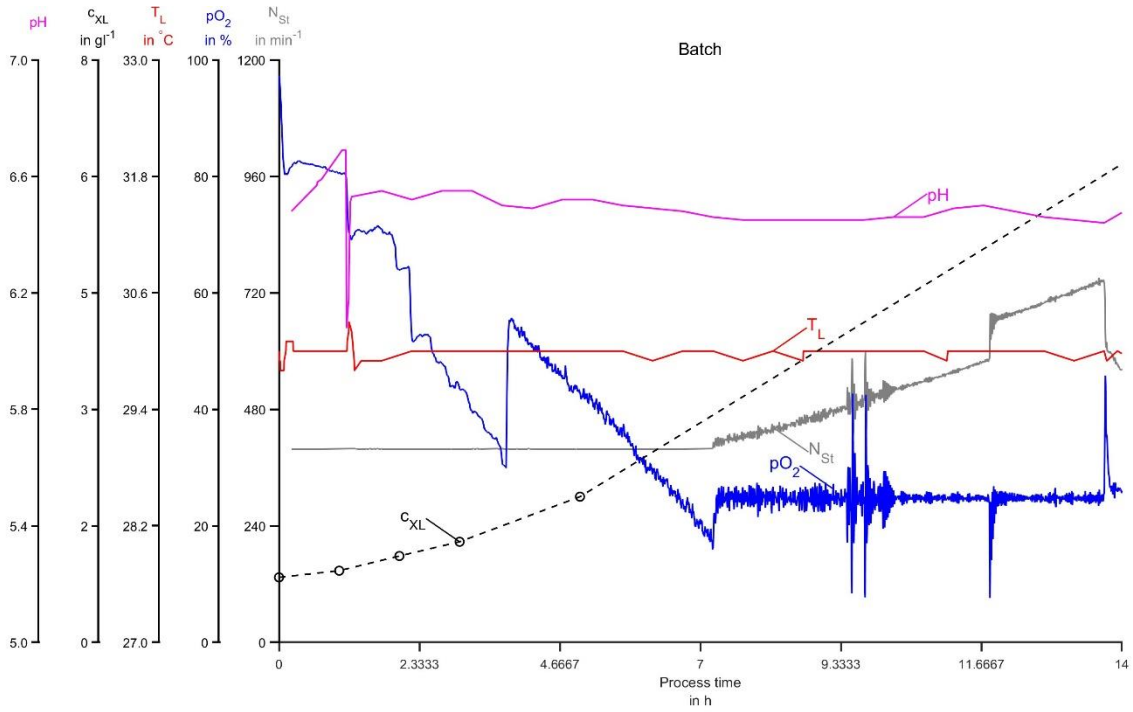

Figure 21: Batch phase of JW_4725. Shown are the temporal courses of cell concentration (c_{XL}), pH value, temperature (ϑ_L), stirrer speed (N_{St}) and dissolved oxygen (pO_2). The pH and temperature are controlled at their set value the entire batch phase. After reaching 25 %, the dissolved oxygen is regulated by adjusting the stirrer speed, which increases over the course of the batch phase. Cell concentration shows exponential growth.

During the fed-batch phase, shown in Figure 22, the dissolved oxygen tension (pO_2) was initially regulated at the setpoint 25 % until approximately 15.5 h. Afterwards, pO_2 increased from 25 % to approximately 78 % over a period of about 5.5 h. This behavior was caused by a malfunction of the feed pump, which failed to deliver substrate into the reactor due to a mechanical failure. As a result, substrate limitation occurred, leading to reduced oxygen consumption and a corresponding rise in pO_2. Following the repair of the feed pump at approximately 21 h process time, substrate feeding was resumed, which resulted in in an immediate decrease of pO_2. Thereafter, pO_2 was again regulated at 25 %. Towards the end of the fed-batch phase, pO_2 decreased to values around 10 %, indicating increased metabolic activity at elevated cell concentrations. The stirrer speed reduced to 400 rpm at the beginning of the fed batch phase and remained constant until approximately 18 h. Subsequently, it increased continuously and reached a maximum value of 1110 rpm at the end of the fed-batch phase.

The parameter Q_{S1in} represents the substrate feeding profile, describing the rate at which substrate was added to the liquid phase. Due to the initial feed pump malfunction, no substrate was added during the early fed batch phase, consequently the increase in Q_{S1in} observed up to approximately 21 h does not reflect the actual feeding conditions. After correction of the error, feeding was resumed with an increased specific feed rate (μ_{w1} raised from 0.1 to 0.3 1/h) to compensate for the lost feeding time and to complete the fed batch phase within the same day.

This adjustment is reflected by the steeper increase in the Q_{S1in} profile at later time points.

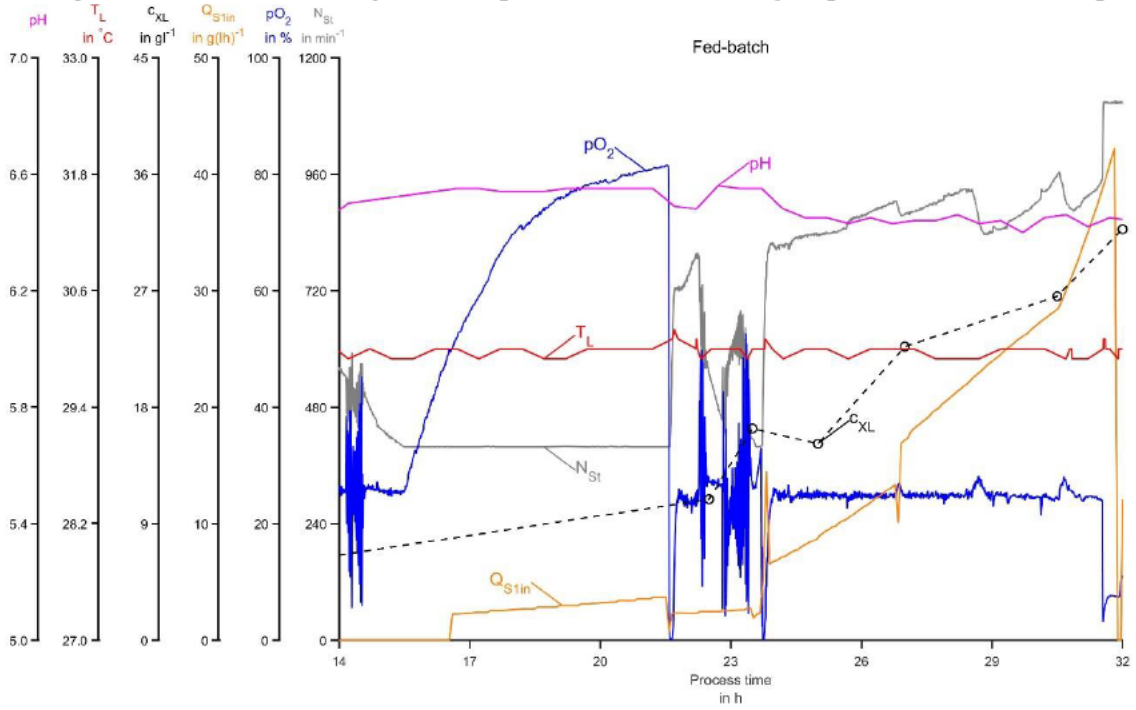

Figure 22: Fed batch phase of JW_4725. Shown are the temporal courses of specific substrate supply rate (Q_{S1in}), cell concentration (c_{XL}), pH value, temperature (ϑ_L), stirrer speed (N_{St}) and dissolved oxygen (pO_2). The pH and temperature are controlled at their set value during the fed batch phase. pO_2 was regulated at 25 % but experienced an increase to 78 % due to an unwanted substrate limitation, as the substrate limitation ended the pO_2 was maintained at 25 % again. Specific substrate supply rate follows the feeding profile, which was elevated to achieve a μ_{w1} = 0.3 1/h. Cell concentration shows growth during the fed batch phase.

During the production phase (Figure 23), the pH was maintained at 6.5 and the temperature was kept constant at 30 °C. At the onset of this phase, the carbon source was switched from glycerol (S1) to methanol (S2). To facilitate cellular adaptation to methanol metabolism, an initial methanol pulse was applied. While an initial concentration of 5 g/L was targeted, an actual concentration of approximately 4 g/L was achieved. Subsequently, additional methanol pulses were intended to maintain the methanol concentration between 1 and 2 g/L. However, due to a software error, the additional methanol pulses added the same volume as the initial methanol pulse, resulting in higher methanol concentrations as anticipated.

At the transition from the fed-batch to the production phase, the dissolved oxygen tension (pO_2), which had already decreased towards the end of the fed batch phase, dropped further to 0 %. At this point, the stirrer speed had reached its maximum limit and was therefore unable to regulate pO_2 at the setpoint of 25 %. Following adaptation of the cells to methanol utilization and a shift from biomass formation towards product formation, the cellular oxygen demand decreased. Consequently, the stirrer speed declined to approximately 650 rpm, allowing pO_2 to be regulated back to 25 % for the remainder of the cultivation. After the second methanol addition, a moderate increase in stirrer speed to approximately 900 rpm was observed, which can be attributed to residual biomass growth during production phase.

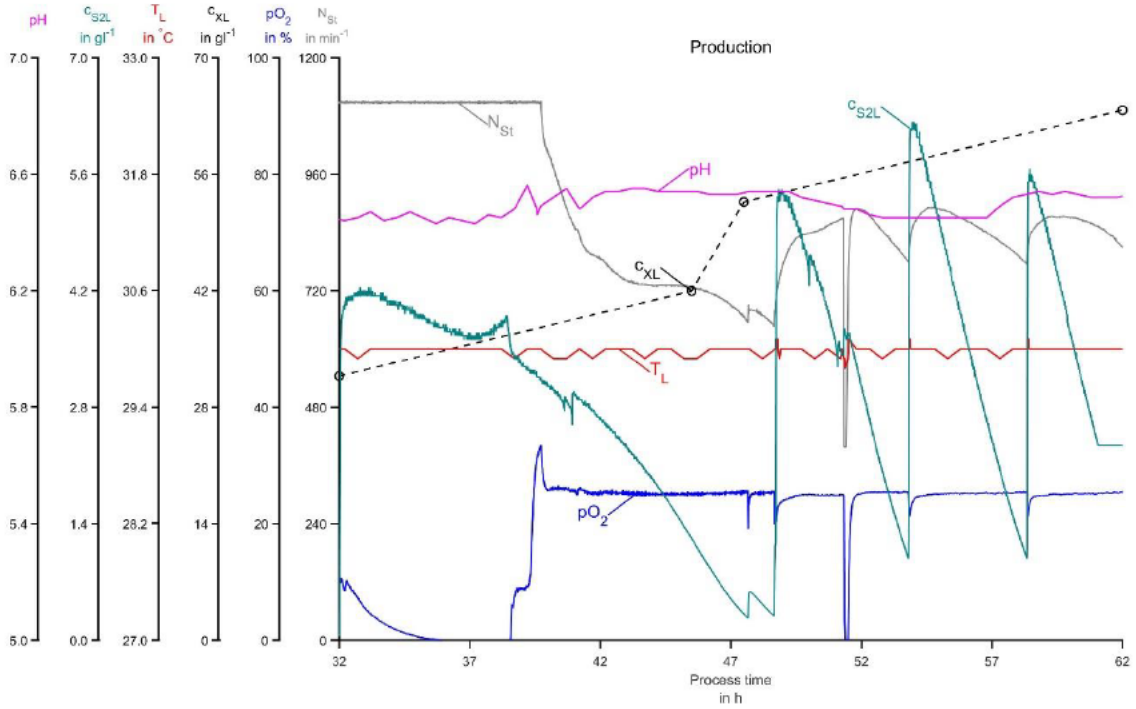

Figure 23: Production phase of JW_4725. Shown are the temporal courses of methanol concentration (c_{S2L}), cell concentration (c_{XL}), pH value, temperature (ϑ_L), stirrer speed (N_{St}) and dissolved oxygen (pO_2). pH and temperature are maintained at the set values during the production phase. As the methanol concentration reaches 1 g/L, a new addition of methanol via pulse occurs. The pO_2, which was initially at 0 %, recovers and is then regulated at 25 % by the stirrer speed throughout the production phase. Cell concentration still increases in this phase.

Process JW_4725 resulted in a final biomass concentration of 63.67 g/L. The polymerase concentration in the supernatant is 332.2 mg/mL, corresponding to a total product mass of 4.413 mg. No enzymatic activity was detected prior to downstream processing.

5.4.1.1 Verification of expression through SDS-PAGE

Figure 24 shows the SDS gel to which samples of process JW_4725 are applied. A total of six samples were applied. The first sample is the supernatant at the end of the process. The supernatant was thermally purified as described in section 4.4. Ultrafiltration was carried out with 500 mL after the supernatant had been thermally purified. Concentration was carried out until 450 mL of permeate and 50 mL of retentate were obtained. This corresponds to a 10-fold concentration increase, the ultrafiltration sample is sample 2. Diafiltration was performed with 50 mL of the concentrated retentate and 4000 mL of KlenTaq buffer (Tris-HCl 20m M, NaCl 100 mL, EDTA 0.1 mM, pH 7.5) until the retentate volume was 100 mL, of which four same samples were applied (samples 3-6). Diafiltration corresponded to a 40-fold buffer change.

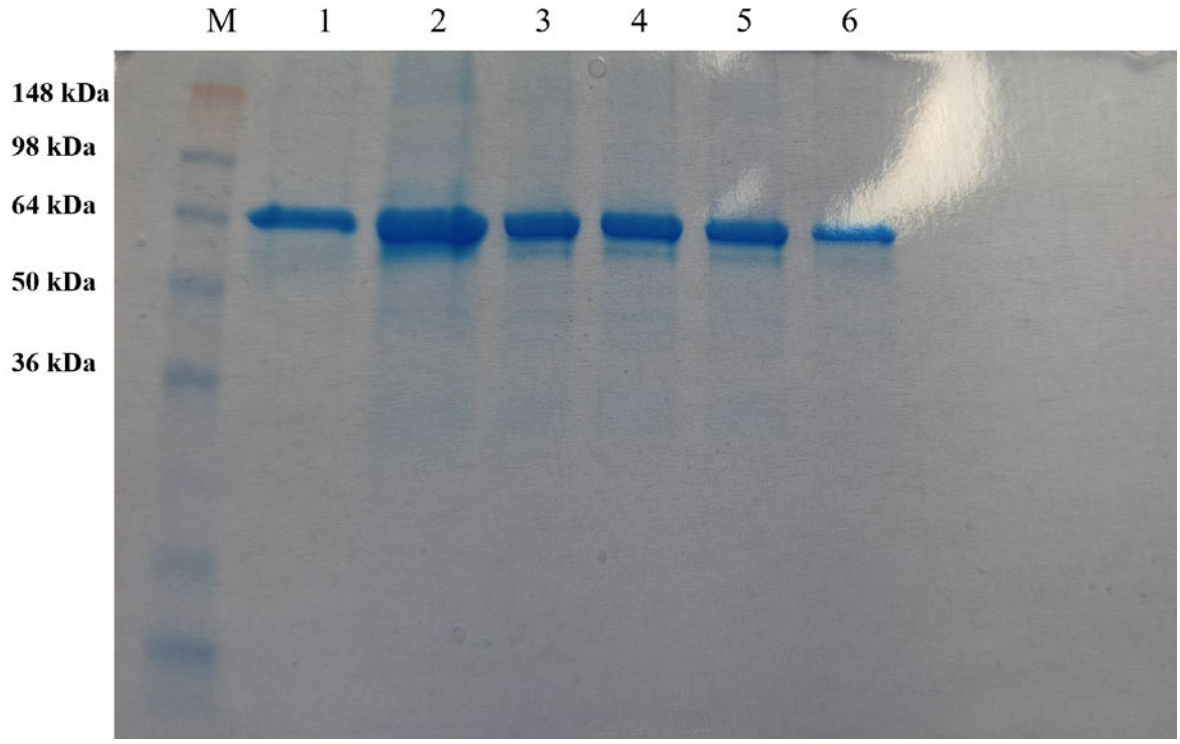

Figure 24: SDS-PAGE gel of samples from process JW_4725. Samples: M: Marker, 1: thermally purified supernatant at the end of cultivation, 2: 10x concentrated supernatant (ultrafiltration), 3-6: Diafiltrated concentrate with 40x buffer change**.**

Figure 24 shows the SDS-PAGE analysis of samples obtained during downstream processing of process JW_4725. In all analyzed samples. A dominant protein band with an apparent molecular weight of approximately 63 kDa is visible, corresponding to the expected size of the KlenTaq DNA polymerase.

Lane 1, representing the thermally purified supernatant at the end of cultivation, already exhibits a distinct band at the target molecular weight, indicating successful expression of the KlenTaq polymerase. Following ultrafiltration (lane 2), the intensity of the target band is noticeably increased, reflecting effective concentration of the polymerase. Lanes 3 to 6 show samples after diafiltration with a cumulative 40-fold buffer exchange. The target band remains clearly detectable in all diafiltrated samples, while no additional prominent protein bands are observed. This suggests a high degree of purity of the polymerase after combining ultrafiltration and diafiltration. No significant degradation products or higher-molecular-weight aggregates are visible under the applied conditions.

Overall, the SDS-PAGE analysis confirms the successful expression during upstream processing and the concentration and purification of the KlenTaq DNA polymerase during downstream processing of process JW_4725, yielding a protein product dominated by a single band at the expected molecular weight.

5.4.1.2 Verification of KlenTaq polymerase activity

The enzymatic activity of the expressed KlenTaq DNA Polymerase was assessed by PCR amplification of the plasmid 0002 pRed/ET (c = 38 ng/µL) using primer 13 and 14. Figure 25 shows the PCR gel obtained from samples of process JW_4725 at different downstream processing stages.

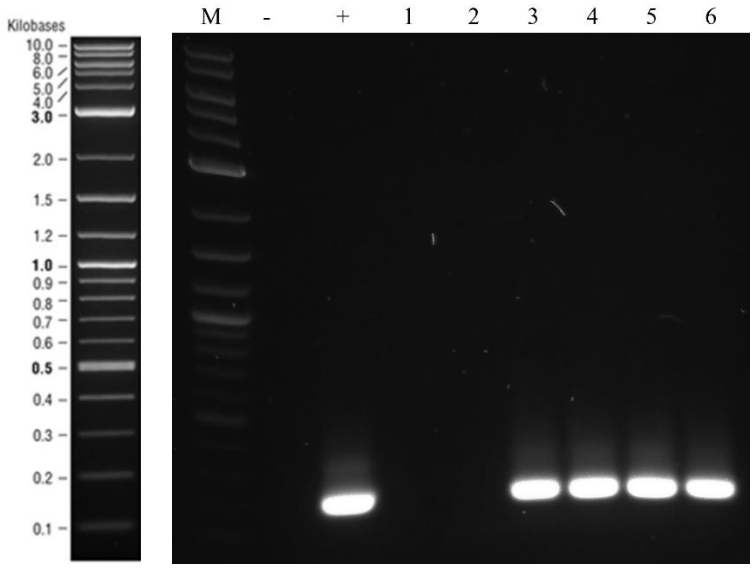

Figure 25: PCR gel from process JW_4725. M: Marker, -: negative control, + positive control, 1 JW_4725 thermally purified supernatant, 2: concentrated supernatant (ultrafiltration), 3-6: Diafiltration samples (4 same samples as confirmation).

No amplification product was detected in the negative control, confirming the absence of contamination. The thermally purified supernatant (lane 1) at the end of cultivation did not show detectable polymerase activity, as no PCR product was observed. Similarly, the ultrafiltration step alone (lane2), resulting in a tenfold concentration of the supernatant, was insufficient to yield a detectable amplification signal. In contrast, clear PCR products were obtained from samples that underwent diafiltration (lane 3-6) with an extensive buffer exchange (40-fold). These results demonstrate that enzymatic activity of the KlenTaq DNA polymerase could only be detected after sufficient buffer exchange during diafiltration.

The presence of distinct amplification bands after diafiltration indicates that inhibitory substances present in the cultivation broth were effectively removed during downstream process. Thus, while expression of the polymerase was achieved during cultivation, functional activity was only recovered after appropriate downstream processing.

5.5 Comparison of processes

Table 11 provides an overview of the bioreactor cultivation processes performed for the production of KlenTaq DNA polymerase. The Table summarizes the key process parameters that were systematically varied throughout this study, including medium composition, pH value and its regulation, process management strategy, and production temperature.

Both the minimal medium FM22 and the complex medium BGGY were applied to evaluate their influence on polymerase production. The investigated processes covered a pH range from 5.0 to 6.6, with both regulated and non-regulated conditions. In addition, two different process strategies were implemented, namely two-stage and three-stage processes. Production temperatures of either 20 °C or 30 °C were applied during the expression phase.

The experimental design enabled a direct comparison of the effects of individual process parameters on polymerase production by varying one or more conditions between the different processes. In particular, the Table highlights the differences between early processes conducted at lower production temperatures and the acidic pH values and later processes employing higher production temperatures and regulated pH conditions closer to the reported optimum of the enzyme.

In addition to the overview summarized in Table 11, time-resolved process plots were generated for all processes listed in the table. These plots illustrate the temporal evolution of key process parameters and are provided in the Appendix A.6.1-A6.5.

Table 11: Overview of the most important cultivation processes carried out to produce KlenTaq polymerase. The Table shows the names of the processes and the process parameters that were varied. Variations were made between the complex medium BGGY and the minimal medium FM22, as well as the pH value and its regulation, process management, and finally the production temperature.

Process	Media	pH	Process management	Production temperature
JW_2825	FM22	5, regulated	Three stage	20
JW_3125	BGGY	5, regulated	Three stage	20
JW_3625	BGGY	6.6, regulated	Two stage	20
JW_3825	BGGY	6.5, regulated	Three stage	30
JW_4025	BGGY	6.5, not regulated	Two stage	30
JW_4725	FM22	6.5, regulated	Three stage	30

Table 12 summarizes the measured polymerase concentrations, calculated total product masses, final biomass concentrations and productivity parameters obtained from the different cultivation processes. In addition to biomass-specific yields ($Y_{P/X}$), the specific productivity ($q_{P/X}$) was evaluated in order to assess the polymerase production rate per cells volume and time. These data are complemented by the graphical representation of the biomass-specific yields shown in Figure 26, allowing a direct comparison of product efficiencies between the individual processes.

The measured polymerase concentrations in the supernatants ranged from 131.9 µg/mL (JW_3625) to 408.3 µg/mL (JW_3825). Correspondingly, the calculated total product mass varied considerably between the processes, with the highest product mass achieved in process

JW_3825 (540.6 mg) and the lowest in process JW_4025 (105.3 mg). Process JW_4725 also showed a comparably high total product mass of 441.1 mg, despite being conducted in the minimal medium FM22.

Final biomass concentration c_{XLend} ranged from 12.56 g/L to 86.15 g/L, indicating substantial differences in biomass formation under the applied cultivation conditions. The resulting biomass-specific yields $Y_{P/X}$ varied markedly between the processes, as shown in Table 12 and illustrated in Figure 26. The lowest biomass-specific yield was observed for process JW_2825 (3.103 mg/g), while the highest value was obtained for process JW_4025 (11.98 mg/g). Intermediate yields were measured for processes JW_3625 (6.208 mg/g), JW_3825 (9.005 mg/g) and JW_4725 (5.217 mg/g).

In addition to biomass-specific yields, the specific productivity $q_{P/X}$ was used as a key performance indicator to evaluate the rate of polymerase formation per cells and time. As shown in Table 12, $q_{P/X}$ values ranged from 0.026 mg/(g h) for process JW_2825 to 0.369 mg/(g h) for process JW_3825. High specific productivities were observed for processes JW_3825 (0.369 mg/(g h)) and JW_4025 (0.323 mg/(g h)), whereas lower productivities were determined for processes JW_2825 and JW_3125.

The comparison of $Y_{P/X}$ and q_P highlights that processes exhibiting high biomass-specific yields did not necessarily result in the highest volumetric productivities. For example, process JW_4025 showed the highest $Y_{P/X}$ but only an intermediate total product mass, whereas process JW_3825 combined a high biomass-specific yield with the highest specific productivity and total polymerase mass. These results indicate that specific productivity provides a more comprehensive measure of overall process performance than biomass-specific yield alone, as it accounts for both production efficiency and cultivation duration.

Table 12: Overview of samples from the various processes and the parameters calculated for them. The protein concentration was measured for the samples, and this parameter was used to calculate the total product mass of the processes. The cell concentration used to calculate the biomass-related yield is also shown.

Sample	Measured concentration, [µg/mL]	Product mass, [mg]	$c_{XLend,}$ [g/L]	$Y_{P/X}$, [mg/g]	$q_{p/X}$, [mg/(g h)]
JW_2825 Supernatant	267.3	372.9	86.15	3.103	0.02636
JW_3125 Supernatant	220.6	316.5	60.36	3.654	0.1343
JW_3625 Supernatant	131.9	139.3	21.24	6.208	0.3059
JW_3825 Supernatant	408.3	540.6	45.34	9.005	0.3691
JW_4025 Supernatant	150.4	150.3	12.56	11.98	0.3228
JW_4725 Supernatant	332.2	441.1	63.67	5.217	0.1721

The graphical comparison of biomass-specific yields highlights that processes with high biomass formation did not necessarily result in the highest production efficiency per unit biomass. Instead, substantial differences in $Y_{P/X}$ were observed across the investigated processes, indicating that polymerase production efficiency was strongly dependent on the applied process conditions rather than biomass concentrations alone.

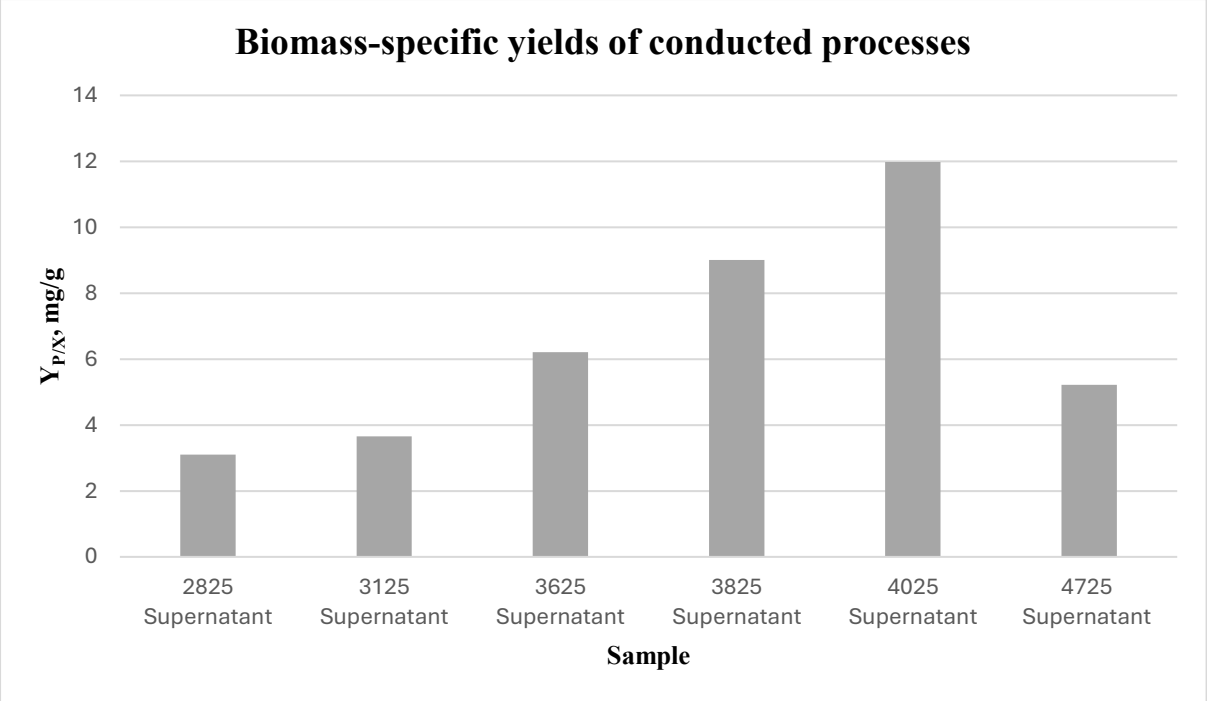

Figure 26: Biomass-specific product yields ($Y_{P/x}$) of the investigated cultivation processes. The yields were calculated based on the polymerase concentration in the culture supernatants and the final biomass concentration at the end of each process. Considerable differences in biomass-specific productivity were observed between the individual processes, indicating a strong influence of process conditions on KlenTaq polymerase production efficiency.

5.6 Summary of conditions leading to a successful process

Table 13 summarizes the cultivation, downstream processing and analytical conditions which led to a successful process and highlights the parameters associated with successful production of enzymatically active KlenTaq DNA polymerase. The results demonstrate that successful polymerase production was not determined by a single parameter, but rather by the combination of suitable upstream and downstream conditions.

High biomass concentrations were obtained with both minimal and complex media, however, these did not consistently correlate with high polymerase yields or enzymatic activity. Processes operated with a three-stage cultivation strategy, controlled pH values around 6.5 and production temperatures of approximately 30 °C showed more robust and reproducible performance compared to two-stage processes.

A decisive factor for enzymatic activity was the downstream processing strategy. While polymerase expression was detectable in all processes by SDS-PAGE, enzymatic activity was only observed after extensive ultrafiltration combined with sufficient diafiltration. In particular, high buffer exchange volumes were required to remove inhibitory medium components and enable polymerase functionality.

Overall, the comparison of the processes investigated show that active KlenTaq DNA polymerase production required a balanced process design combining suitable medium selection, controlled cultivation conditions, effective downstream processing and appropriate analytical validation, as summarized in Table 13.

Table 13: Overview of process conditions associated with successful KlenTaq DNA polymerase production. Overview of media composition, cultivation parameters, downstream processing conditions and analytical methods applied in order to achieve optimal production processes. The table summarizes the conditions that resulted in detectable enzymatic activity of KlenTaq DNA polymerase.

Process aspect	Parameter	Successful conditions in this study
Medium	Carbon source (growth)	Glycerol based media (FM22 or BMGY) suitable for biomass formation
	Carbon source (production)	Methanol suitable as inducer and substrate
Cultivation conditions	Process strategy	Three-stage process (batch, fed-batch, production)
	Production temperature	30 °C during production
	pH setpoint	pH ≈ 6.5 during production
Downstream processing	Clarification	Centrifugation sufficient for biomass removal
	Rough purification	Thermal purification removes remaining impurities.
	Concentration method	Ultrafiltration (TFUF), 10 kDa MWCO
	Buffer exchange (KlenTaq Buffer)	Extensive diafiltration (≥ 40 DV)
Analytical methods	Expression analysis	SDS-PAGE
	Activity assessment	PCR assay

6. Discussion

The present study aimed at establishing a biotechnological production process for the recombinant KlenTaq DNA polymerase using *Picha pastoris*, covering the entire workflow from cultivation to downstream processing and analysis. The results demonstrate that both upstream cultivation parameters and downstream processing steps substantially influence not only the overall polymerase yield, but more importantly, the functional quality of the final polymerase product.

Influence of cultivation conditions on biomass formation and polymerase expression.

The comparison of the different bioreactor processes, summarized in Table 11, clearly shows that cultivation parameters such as production temperature, pH control and process strategy strongly affect biomass formation and polymerase expression. While both minimal and complex media enabled high cell density cultivations, a high final biomass concentration alone did not necessarily result in improved process performance. This observation confirms that biomass formation alone is not a sufficient indicator for productive efficiency.[35]

An illustrative example is provided by processes JW_2825 and JW_3125, which both achieved high final cell concentrations but exhibited low biomass-specific yields. In contrast, process JW_3825 reached a lower cell concentration while displaying an approximately threefold higher biomass-specific yield. This indicates that polymerase production efficiency is strongly influenced by the applied cultivation strategy rather than biomass formation alone.

The initial transfer of conditions established in Erlenmeyer flask experiments to the bioreactor, particularly the use of complex medium BGGY, a production temperature of 30 °C and a pH setpoint of 6.5, did not result in an enzymatically active polymerase, despite detectable expression levels. This highlights the limited transferability of small-scale cultivation results to controlled bioreactor systems and underlines the importance of systematic process optimization at larger scales.[36]

Adjustments of the cultivation parameters, including increased production temperature, modification of pH setpoints and altered process strategies (two-stage versus three-stage processes), resulted in significant differences in polymerase concentrations and biomass-specific yields. In particular, three-stage processes with controlled pH values around 6.5 showed more stable and reproducible outcomes, as observed in processes JW_3825 and JW_4725. [37]

Discrepancy between polymerase expression and enzymatic activity

A key finding of this work is that KlenTaq DNA polymerase expression alone was not sufficient to obtain an active enzyme. In all bioreactor processes, the presence of the KlenTaq polymerase could be confirmed by SDS-PAGE analysis (Figure 24 and Figures 46 – 48), whereas no enzymatic activity was detected in the thermally purified supernatants, 5x concentrated or diafiltrated samples with a 20-fold buffer exchange (Figure 52). This indicates that the lack of activity was not caused by insufficient expression but rather by factors affecting enzyme functionality after expression.[38]

Possible explanations include unfavorable buffer conditions, the presence of inhibitory medium components or host-derived impurities, as well as stress induced misfolding or partial inactivation of the enzyme during cultivation. However, as the expression of the polymerase was consistently observed, the results strongly suggest that downstream-related factors played a decisive role in determining enzymatic activity.

The corresponding PCR gel, provided in the Appendix (Figure 49), demonstrates that the presence of untreated bioreactor supernatant led to reduced amplification signals. This strongly suggests that inhibitory medium components interfered with polymerase functionality.

Critical role of downstream processing on polymerase activity

The most significant improvement in polymerase activity was achieved by modifying the downstream processing strategy. A high degree of ultrafiltration combined with extensive diafiltration led to the successful enzymatic activity for polymerases obtained from several processes (JW_3125, JW_3625, JW_3825 and JW_4025). The PCR results presented in the Appendix (Figure 50) clearly show that polymerase activity was only detectable when a sufficiently high degree of buffer exchange was applied. This clearly demonstrates that the activity of the KlenTaq DNA polymerase is highly dependent on the surrounding buffer system and on the effective removal of inhibitory substances.

Experiments comparing different diafiltration extents showed that a 40-fold buffer exchange was required to obtain active enzyme, whereas a 20-fold buffer exchange was insufficient (Figure 51). The successful activity detection after extensive buffer exchange indicates that salts, residual medium components or other low-molecule-weight compounds likely interfered with polymerase function.[39] These findings emphasize the importance of considering downstream processing not merely as a concentration step, but as a critical determinant of final product quality.

The activity detected in process JW_4725 further confirms this conclusion. Although this process was again based on the minimal medium FM22, which initially yielded inactive polymerase, enzymatic activity could be detected after thorough diafiltration. This demonstrates that minimal media can be used for KlenTaq production, provided that appropriate downstream processing strategies are applied.

Evaluation of polymerase yield and process performance

The comparison of the investigated cultivation processes clearly demonstrates that a high final cell concentration does not necessarily result in a high polymerase yield. In particular, the comparison of processes JW_2825 and JW_3125 indicates that the transition from minimal medium to complex medium alone had no significant effect on the biomass-specific yield.

A pronounced influence was observed for the applied process strategy. Two-stage processes (JW_3625 and JW_4025) consistently resulted in lower final biomass concentrations, which is in line with expectations for this process design. Despite reduced biomass formation, these processes exhibited increased biomass-specific yields, indicating enhanced polymerase production per cell. However, this increased biomass-specific yield did not necessarily translate into high total product amounts or high specific productivities $q_{P/X}$, highlighting the limitations of evaluating process performance based solely on biomass-specific yield.

In contrast, three-stage processes with controlled pH values around 6.5 and elevated production temperatures achieved the highest overall polymerase amounts. This was particularly evident for process JW_3825, which combined moderate cell concentrations with high specific productivity, indicating a more balanced relationship between growth and productivity. [37]

The comparison between processes JW_3825 and JW_4025 further emphasizes the importance of end biomass concentration for volumetric productivity. Although JW_4025 exhibited the highest biomass-specific yield, its total polymerase mass remained limited due to the lower cell concentration. Conversely, JW_4725 demonstrated that high polymerase amounts can also be achieved using minimal medium.

Overall, these findings underline that process optimization should not be restricted to maximizing biomass formation or biomass-specific productivity alone. Instead, an integrated evaluation considering specific productivity $q_{P/X}$, enzyme functionality and process robustness is required. The superior performance of three-stage processes with controlled pH conditions highlights the importance of such an integrated approach for establishing an efficient and reproducible bioreactor-based production process for KlenTaq DNA polymerase.

Summary

This study aimed to establish a complete biotechnological production process for recombinant KlenTaq DNA polymerase in *Pichia pastoris*, covering upstream cultivation, downstream processing, and analytical evaluation of enzyme functionality. The results demonstrate that successful production of an active polymerase is not solely dependent on high expression levels or biomass formation, but rather on the careful coordination of cultivation strategy, process control, and downstream purification.

The comparison of different bioreactor cultivations revealed that high final cell concentrations did not necessarily correlate with high polymerase yields. Instead, differences in biomass-specific yields and specific productivity were observed depending on medium composition, pH control, temperature, and process strategy. In particular, three-stage processes with controlled pH values around 6.5 and elevated production temperatures provided the most balanced relationship between biomass formation and polymerase productivity.

A key finding of this work is the clear discrepancy between polymerase expression and enzymatic activity. Although SDS-PAGE analysis consistently confirmed the presence of KlenTaq polymerase in all bioreactor cultivations, no activity could be detected in thermally purified or insufficiently diafiltrated samples. This demonstrated that the limiting factor was not expression, but the biochemical environment surrounding the enzyme after cultivation.

The decisive improvement in polymerase activity was achieved through extensive ultrafiltration and diafiltration. Only after applying a sufficiently high degree of buffer exchange was enzymatic activity detectable in PCR assays. These findings underline the critical importance of downstream processing for the functional quality of the final product and demonstrate that inhibitory medium components or low-molecular-weight substances significantly affected polymerase functionality.

Overall, this work shows that the establishment of a robust production process for KlenTaq DNA polymerase in *P. pastoris* requires an integrated approach that considers not only biomass

formation and protein expression, but also the decisive role of downstream processing in ensuring enzyme activity.

Outlook

If further work were to be conducted, several aspects could be investigated to further improve and optimize the production process for active KlenTaq DNA polymerase.

First, systematic studies of the diafiltration process should be performed to determine the minimum number of diafiltration volumes required to reliably obtain enzymatically active polymerase. This would allow a more efficient downstream process design while maintaining enzyme functionality.

Second, the application of Design of Experiments (DoE) approaches could help identify critical cultivation parameters that maximize both polymerase yield and activity. Parameters such as pH, temperature, feeding strategy, and dissolved oxygen control could be evaluated furthermore in a structured manner to determine optimal operating conditions.

Furthermore, quantitative enzymatic assays should complement the qualitative PCR-based activity assessment. This would allow a more precise evaluation of polymerase performance under different process conditions and provide deeper insight into factors influencing enzyme functionality.

Finally, the long-term stability and usability of the purified KlenTaq polymerase should be assessed by performing repeated PCR applications over extended periods. This would demonstrate the practical robustness of the produced enzyme and its suitability for routine molecular biology applications.

These investigations would contribute to a deeper understanding of the interaction between upstream cultivation, downstream processing, and enzyme functionality, and could further enhance the efficiency and reliability of recombinant polymerase production in *P. pastoris*.

7. References

1. Nielsen, J., Tillegreen, C. B. & Petranovic, D. Innovation trends in industrial biotechnology. *Trends Biotechnol.* **40**, 1160–1172 (2022).

2. Karbalaei, M., Rezaee, S. A. & Farsiani, H. Pichia pastoris: A highly successful expression system for optimal synthesis of heterologous proteins. *J. Cell. Physiol.* **235**, 5867–5881 (2020).

3. Cereghino, J. L. & Cregg, J. M. Heterologous protein expression in the methylotrophic yeast Pichia pastoris. *FEMS Microbiol. Rev.* **24**, 45–66 (2000).

4. Wollborn, D. *et al.* Predicting high recombinant protein producer strains of Pichia pastoris MutS using the oxygen transfer rate as an indicator of metabolic burden. *Sci. Rep.* **12**, (2022).

5. Jahic, M., Veide, A., Charoenrat, T., Teeri, T. & Enfors, S. O. Process technology for production and recovery of heterologous proteins with Pichia pastoris. *Biotechnol. Prog.* **22**, 1465–1473 (2006).

6. Zahrl, R. J., Peña, D. A., Mattanovich, D. & Gasser, B. Systems biotechnology for protein production in Pichia pastoris. *FEMS Yeast Res.* **17**, 68 (2017).

7. Cornelissen, G. Pharmaceutical Biochemical Engineering. *PBE Scr.* **1**, 1–235 (2021).

8. Karbalaei, M., Rezaee, S. A. & Farsiani, H. Pichia pastoris: A highly successful expression system for optimal synthesis of heterologous proteins. *J. Cell. Physiol.* **235**, 5867–5881 (2020).

9. Lee, J. D. & Komagata, K. TAXONOMIC STUDY OF METHANOL-ASSIMILATING YEASTS. *J. Gen. Appl. Microbiol.* **26**, 133–158 (1980).

10. Allen, D. J., Darke, P. L. & Benkovic, S. J. Fluorescent Oligonucleotides and Deoxynucleotide Triphosphates: Preparation and Their Interaction with the Large (Klenow) Fragment of Escherichia coli DNA Polymerase I. *Biochemistry* **28**, 4601–4607 (1989).

11. Barnes, W. M. The fidelity of Taq polymerase catalyzing PCR is improved by an N-terminal deletion. *Gene* **112**, 29–35 (1992).

12. RCSB PDB - 7OWF: KlenTaq DNA polymerase in a ternary complex with primer/template and the fluorescent nucleotide analog BFdUTP. https://www.rcsb.org/structure/7OWF.

13. Regonesi, G. *BIOREACTORS : A Complete Review*. https://www.researchgate.net/publication/373708124_BIOREACTORS_A_Complete_Review (2023).

14. Marquard, D. *et al.* In situ microscopy for online monitoring of cell concentration in Pichia pastoris cultivations. *J. Biotechnol.* **234**, 90–98 (2016).

15. Li, Y. *et al.* Emerging biomaterials for downstream manufacturing of therapeutic

proteins. *Acta Biomater.* **95**, 73–90 (2019).

16. Gaughan, C. L., Christopher, B. & Gaughan, L. The present state of the art in expression, production and characterization of monoclonal antibodies. *Mol. Divers. 2015 201* **20**, 255–270 (2015).

17. Schwaminger, S. P., Zimmermann, I. & Berensmeier, S. Current research approaches in downstream processing of pharmaceutically relevant proteins. *Curr. Opin. Biotechnol.* **77**, 102768 (2022).

18. Sharifian Gh., M. & Norouzi, F. Guidelines for an optimized differential centrifugation of cells. *Biochem. Biophys. Reports* **36**, 101585 (2023).

19. Van Reis, R. & Zydney, A. Membrane separations in biotechnology. *Curr. Opin. Biotechnol.* **12**, 208–211 (2001).

20. van Reis, R. & Zydney, A. Bioprocess membrane technology. *J. Memb. Sci.* **297**, 16–50 (2007).

21. Schwartz, L. Diafiltration for Desalting or Buffer Exchange. *Bioprocess Int.* 43–49 (2003).

22. Reyes, S. J., Durocher, Y., Pham, P. L. & Henry, O.: Modern Sensor Tools and Techniques for Monitoring, Controlling, and Improving Cell Culture Processes. *Process. 2022, Vol. 10, Page 189* **10**, 189 (2022).

23. Dambruin, N. A., Pronk, J. T. & Klijn, M. E.: Application of process analytical technology for real-time monitoring of synthetic co-culture bioprocesses. *Anal. Bioanal. Chem.* **417**, 5611 (2025).

24. Sutton, S. Microbiology Topics. ABOUT THE AUTHOR Measurement of Microbial Cells by Optical Density. *46 J. Valid. Technol.* (2011).

25. Nowakowski, A. B., Wobig, W. J. & Petering, D. H. Native SDS-PAGE: High Resolution Electrophoretic Separation of Proteins With Retention of Native Properties Including Bound Metal Ions. *Metallomics* **6**, 1068 (2014).

26. Garibyan, L. & Avashia, N. Research Techniques Made Simple: Polymerase Chain Reaction (PCR). *J. Invest. Dermatol.* **133**, e6 (2013).

27. BIOSTAT ® A Ihr professioneller Einstieg in Zellkultur und mikrobielle Fermentation.

28. Dissolved Oxygen Probe How It Works? - Apure. https://apureinstrument.com/blogs/dissolved-oxygen-probe-how-it-works/.

29. pH Meter - Instrument - Holme Research Group - Iowa State University. https://group.chem.iastate.edu/Holme/augmented-reality-in-educational-laboratories/ph-meter/.

30. Delvigne, F. & Lecomte, J. Foam Formation and Control in Bioreactors. *Encycl. Ind. Biotechnol.* 1–13 (2010) doi:10.1002/9780470054581.EIB326.

31. Iff, Y. Etablierung der Berechnung von Abgaskennwerten bei der Kultivierung von Pichia pastoris in einem Laborfermenter.

32. Koop, F.-L. Etablierung eines Laborprotokolls zur Hefe-basierten Herstellung von KlenTaq DNA Polymerase. (Hochschule für Angewandte Wissenschaften, 2021).

33. ROTI®Nanoquant, 500 ml, 2000 Assays (Küvetten) | Proteinquantifizierung | Proteinbiologie | Life Science | Carl ROTH - Deutschland. https://www.carlroth.com/de/de/proteinquantifizierung/rotinanoquant/p/k880.1.

34. Hemo KlenTaq® | NEB. https://www.neb.com/en/products/m0332-hemo-klentaq.

35. Ahmad, M., Hirz, M., Pichler, H. & Schwab, H. Protein expression in Pichia pastoris: recent achievements and perspectives for heterologous protein production. *Appl. Microbiol. Biotechnol. 2014 9812* **98**, 5301–5317 (2014).

36. Xia, J. *et al.* Understanding the scale-up of fermentation processes from the viewpoint of the flow field in bioreactors and the physiological response of strains. *Chinese J. Chem. Eng.* **30**, 178–184 (2021).

37. Joseph, J. A., Akkermans, S. & Van Impe, J. F. M. Effects of Temperature and pH on Recombinant Thaumatin II Production by Pichia pastoris. *Foods* **11**, 1438 (2022).

38. Dako, E., Bernier, A.-M., Dadie, A. T. & Jankowski, C. K. The Problems Associated with Enzyme Purification.

39. Vijayaraghavan, P., Raj, S. R. F. & Vincent, S. G. P. Industrial Enzymes: Recovery and Purification Challenges. *Agro-Industrial Wastes as Feed. Enzym. Prod. Apply Exploit Emerg. Valuab. Use Options Waste Biomass* 95–110 (2016) doi:10.1016/B978-0-12-802392-1.00004-6.

8. Appendix

A.1 Equipment

Table 14: Used equipment during the thesis

Name	Manufacturer	Model
Analytical balance KERN	KERN & SOHN GmbH	ABJ-NM/ABS-N
Autoclave	Systec GmbH	VX-150
Balance	Various	
Base unit	Sartorius Stedim Biotech GmbH	
Bioreactor	Sartorius Stedim Biotech GmbH	Biostat A plus 2
Centrifuge	Eppendorf SE	Centrifuge 5417R
Centrifuge filter unit	Sartorius Stedim Biotech GmbH	Vivaspin 20
Drying cabinet	Köttermann GmbH	2711
Heating block	Eppendorf	ThermoMixer C
IMAC	Cytiva – Global Life Sciences solutions Austria GmbH & Co. KG.	ÄKTA™ avant
Level probe	Sartorius Stedim Biotech GmbH	PB-20
Magnetic stirrer	Janke und Kunkel KG IKA Wert	IKA-COMBIMAG REO/RCO
Microplate reader	TECAN	NanoQuant infinite M200 pro
Off-gas sensor	BlueSens gas Sensor GmbH	BlueVary
pH probe	Endres+Hauser	Memosens CPS171
pH-Meter	METTLER TOLEDO	FiveEasy
Photometer	Thermo Scientific	Genesys20
pO_2 probe	Endres+Hauser	Memosens COS81D
SDS-Page	BioRad	Mini-PROTEAN Tetra Vertical Electrophoresis Cell

Shaking incubator	Gesellschaft für Labortechnik GmbH	3032
Sterile filter	Sartorius Stedim Biotech GmbH	
Sterile workbench	Heraeus Instruments	HERA Safe
Stirrer with agitator shaft	Sartorius Stedim Biotech GmbH	
Temperature module	Sartorius Stedim Biotech GmbH	BB-8822002
TFUF hollow fiber cartridge	Cytiva – Global Life Sciences solutions Austria GmbH & Co. KG.	UFP 10 C 4X2MA
Thermal cycler	analytikjena	FlexCycler^2
Vortexer	IKA Works Inc.	MS2 Minishaker

A.2 Buffers

Table 15: Buffer used for this thesis.

Name	Chemicals	Concentration
KlenTaq Buffer	Tris-HCl	20mM
	NaCl	100 mM
	EDTA	0.1 mM
	pH 7.5, sterile filtrated, 4°C	
10x Running buffer	Tris	1 M
	Glycine	1.92 M
	SDS	1 %
	pH 8.3	
Coloring solution	Roti-Blue (Coomassie 5x)	200 mL/L
	Ethanol	200 mL/L
	VE-Water	800 mL/L
Decolorizing solution	Ethanol	100 mL/L
	Acetic acid	100 mL/L
	VE-Water	800 mL/L

A.3 Media

Table 16: Used Media during the Master thesis

Name	Chemicals	Concentration
YPD media	Yeast extract	10 g/L
	Pepton	20 g/L
	Glucose stock (500 g/L)	40 mL
buffered-glycerol-complex media (BMGY)	Yeast extract	10 g/L
	Pepton	20 g/L
	Added after autoclaving:	
	PPB (1M)	100 mL 10
	YNB (10x)	100 mL 10
	Glycerol (50%)	40 mL
buffered-methanol-complex media (BMMY)	Yeast extract	10 g/L
	Pepton	20 g/L
	Added after autoclaving:	
	PPB	100 mL
	YNB	100 mL
	Methanol (5%)	100 mL
FM22 media (preculture)	$C_3H_8O_3$	20 g
	KH_2PO_4	25.7 g
	$(NH_4)_2SO_4$	5 g
	K_2SO_4	8.6 g
	$Ca_3SO_4 \cdot 2H_2O$	1.4 g
	$MgSO_4 \cdot 27O$	16.4 g
	$Na_3 - citrate \cdot 2H_2O$	5.88 g
	Added after autoclaving:	
	Biotin Stock (0.2 g/L)	8 mL
	PTM4 Stock	4 mL
	10xYNB	100 mL
FM22 media (feed)	$C_3H_8O_3$	150 g
	KH_2PO_4	25.7 g
	$(NH_4)_2SO_4$	5 g
	K_2SO_4	8.6 g
	$Ca_3SO_4 \cdot 2H_2O$	1.4 g
	$MgSO_4 \cdot 27O$	16.4 g
	$Na_3 - citrate \cdot 2H_2O$	5.88 g
	Added after autoclaving:	
	Biotin Stock (0,2 g/L)	8 mL
	PTM4 Stock	4 mL
	10xYNB	100 mL

Methanol feed media	Methanol	790 g
	Biotin Stock (0.2 g/L)	8 mL
	PTM4 Stock	4 mL

A.4 Matlab source code

A.4.1 Exponential fit for cell bank

```
%Exponential fit for cell bank

M = load('MCB.txt');
x = M(:,1);
y = M(:,2);

z = log(y);
p = polyfit(x,z,1);
A = p(1);
C = exp(p(2));

F =@(t)C*exp(A*x);
s =F(x);

hold on
plot(x,y,'r.');
plot(x,s,'k-');
xlabel('Time [h]');

ylabel('OD_{600} [AU]');
xlim([0 8.5]);
ylim([0 5.5]);
title('Cell Growth in MCB Development');
legend('measured data', 'fitted curve', 'Location', 'southeast');
hold off
```

A.4.2 Data processing for plots

```
%Import data
pO2=readmatrix('pO2.txt'); %[%]
cXL=readmatrix('cXL.txt');
FAIR=readmatrix('FnAIR.txt'); %[L/min]
AF=readmatrix('FOAM.txt'); %[on/off]
FR2=readmatrix('FR2.txt'); %[%]
Nst=readmatrix('NSt.txt'); %[1/min]
pH=readmatrix('pH.txt'); %[-]
TL=readmatrix('TL.txt'); %[°C]
cSL2 = readmatrix('MeOH_c.txt'); %[g/L]
cSL2r = cSL2(:,2)./0.126;
VL = readmatrix('VL.txt');

%constant parameters
FR2max=0.780; %[L/h]
cS1R1=150; %[g/L]
cS2R=790; %[g/L]
xOAIR=0.2094; %[-]
xCAIR=0.0003; %[-]
xOGcal=xOAIR; %[-]
MO2= 32; %[g/mol]
Vnm=22.414; %[L/mol]
```

A.4.3 QS1in calculation for Fed Batch phase

QSin calulation

```
% Time and value of FR2
timeFR2 = FR2(:,1);
FR2_val = FR2(:,2);

% remove dublivate time points
[timeFR2, idxFR2] = unique(timeFR2);
FR2_val = FR2_val(idxFR2);

% remove dublivate VL values
timeVL = VL(:,1);
VL_val = VL(:,2);
[timeVL, idxVL] = unique(timeVL);
VL_val = VL_val(idxVL);

% Common time vector
timeCommon = linspace(max(min(timeFR2), min(timeVL)), ...
                      min(max(timeFR2), max(timeVL)), 1000);

% Remove outliers in FR2 and VL     ONLY NEEDED IN FED BATCH PHASE
outliersFR2 = isoutlier(FR2_val);
FR2_val(outliersFR2) = [];
timeFR2(outliersFR2) = [];

outliersVL = isoutlier(VL_val);
VL_val(outliersVL) = [];
timeVL(outliersVL) = [];

% Interpolation
FR2_interp = interp1(timeFR2, FR2_val, timeCommon, 'linear');
VL_interp  = interp1(timeVL,  VL_val,  timeCommon, 'linear');

% QS1in calculation
QS1in = (((FR2_interp./100).*0.780) .* cS1R1) ./ VL_interp;
QS1in_matrix = [timeCommon(:), QS1in(:)];
```

A.4.4 Creation of Plots using multi-Y-axis plots (Tom R. (2025) (https://www.mathworks.com/matlabcentral/fileexchange/67349-plot-with-multiple-y-axes)

JW4725 Batch

```
pO2 = smoothdata(pO2, 'movmean', 10);
Nst = smoothdata(Nst, 'movmean', 10);

linecolors={'#0072BD' '#D95319' '#A2142F' '#7E2F8E' '#77AC30'};
fh = figure('Units','normalized','Position',[0.25 0.25 .6 .55]);
 hci=plotNy({pO2(:,1),Nst(:,1),TL(:,1), pH(:,1), cXL(:,1)}, ...
            {pO2(:,2),Nst(:,2),TL(:,2), pH(:,2), cXL(:,2)}, ...
            [1 2 3 4 5],...
 'XAxisLabel','Time[h]', ...
 'YAxisLabels',{'pO_2[%]' 'N_{st}[rpm]' '\vartheta_L [°C]' 'pH' 'c_{XL}[g/L]'},...
 'LineColor',linecolors,...
 'Linewidth',1.5,...
 'FontSize',14,...
 'Grid','off',...
 'Parent',fh,...
 'LegendLoc','none',...
 'Xlim',[0 13.75],...
 'Ylim',[0 100; 0 1110; 25 33; 5.5 6.7; 0 8]);
 for i=1:length(hci.ax)
    set(hci.ax(i),'ycolor',linecolors{i});
 end

 text(6.5,96,'Batch','FontSize',14)
```

JW4725 FEDBATCH

```
pO2 = smoothdata(pO2, 'movmean', 10);
Nst = smoothdata(Nst, 'movmean', 10);

cS1R1 = 150;
linecolors={'#0072BD' '#D95319' '#A2142F' '#7E2F8E' '#77AC30' 'b'};
fh = figure('Units','normalized','Position',[0.25 0.25 .6 .55]);
 hci=plotNy({pO2(:,1),Nst(:,1),TL(:,1), pH(:,1), cXL(:,1), QS1in_matrix(:,1)}, ...
            {pO2(:,2),Nst(:,2),TL(:,2), pH(:,2), cXL(:,2), QS1in_matrix(:,2)}, ...
            [1 2 3 4 5 6 ],...
 'XAxisLabel','Time[h]', ...
 'YAxisLabels',{'pO_2[%]' 'N_{st}[rpm]' '\vartheta_L [°C]' 'pH' 'c_{XL}[g/L]' 'QS1in [g/L*h]'},...
  'LineColor',linecolors,...
  'Linewidth',1.5,...
  'FontSize',14,...
  'Grid','off',...
 'Parent',fh,...
 'LegendLoc','none',...
 'Xlim',[13.75 32],...
'Ylim',[0 100; 0 1110; 27 33; 5.5 6.7; 5 45; 0 45]);
 for i=1:length(hci.ax)
    set(hci.ax(i),'ycolor',linecolors{i});
 end

 text(22,96,'Fedbatch','FontSize',14)
```

JW4725 Production

```
pO2 = smoothdata(pO2, 'movmean', 20);
Nst = smoothdata(Nst, 'movmean', 20);

linecolors={'#0072BD' '#D95319' '#A2142F' '#7E2F8E' '#77AC30' 'b'};
fh = figure('Units','normalized','Position',[0.25 0.25 .6 .55]);
 hci=plotNy({pO2(:,1),Nst(:,1),TL(:,1), pH(:,1), cXL(:,1), cSL2(:,1)}, ...
            {pO2(:,2),Nst(:,2),TL(:,2), pH(:,2), cXL(:,2), cSL2r(:,1)}, ...
            [1 2 3 4 5 6 ],...
 'XAxisLabel','Time[h]', ...
 'YAxisLabels',{'pO_2[%]' 'N_{st}[rpm]' '\vartheta_L [°C]' 'pH' 'c_{XL}[g/L]' 'c_{SL2} [g/L]'  },...
  'LineColor',linecolors,...
  'Linewidth',1.5,...
  'FontSize',14,...
  'Grid','off',...
 'Parent',fh,...
 'LegendLoc','none',...
 'Xlim',[32 62],...
'Ylim',[0 100; 0 1110; 27 33; 5.4 6.7; 30 70; 0 7 ]);
 for i=1:length(hci.ax)
    set(hci.ax(i),'ycolor',linecolors{i});
 end

 text(44,96,'Production','FontSize',14)
```

A.5 MFCS/win Recipe for cultivation

MFCS/win | **Recipe List** | **Printed:** *04-Dez-2025* 15:03:04 Mitteleuropäische Zeit

Recipe: p pastoris KlenTaq BatchProd
Version: 10.000
Status: APPROVED

MFCS Rev. 78,001

Operation : init

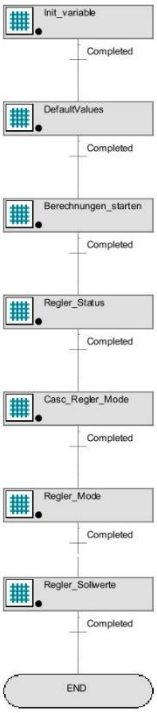

Operation : batch

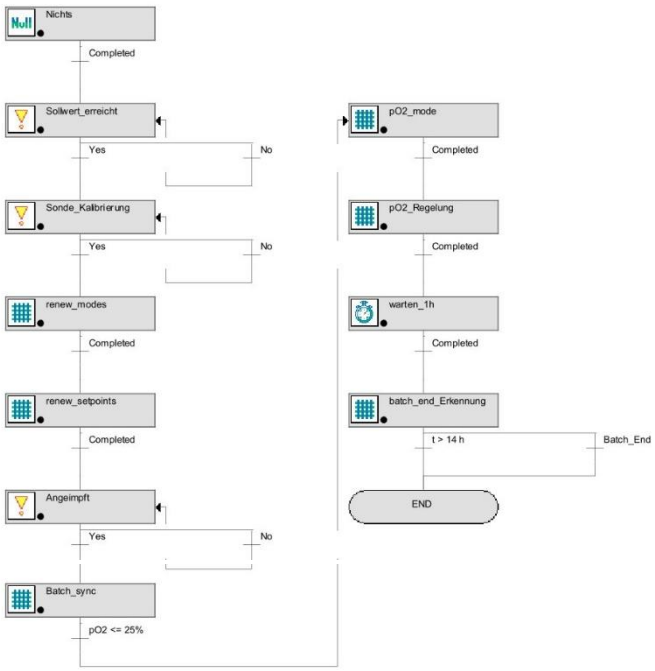

MFCS/win **Recipe List** **Printed:** *04-Dez-2025* 15:03:04 Mitteleuropäische Zeit

Recipe: p pastoris KlenTaq BatchProd MFCS Rev. 78,001

Version: 10.000

Status: APPROVED

Operation : fed_batch

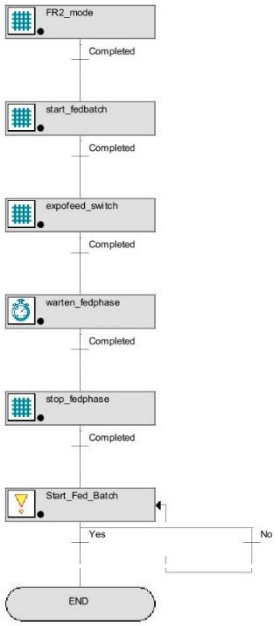

MFCS/win | **Recipe List** | **Printed:** *04-Dez-2025* 15:03:04 Mitteleuropäische Zeit

Recipe: p pastoris KlenTaq BatchProd
Version: 10.000
Status: APPROVED

MFCS Rev. 78,001

Operation : production

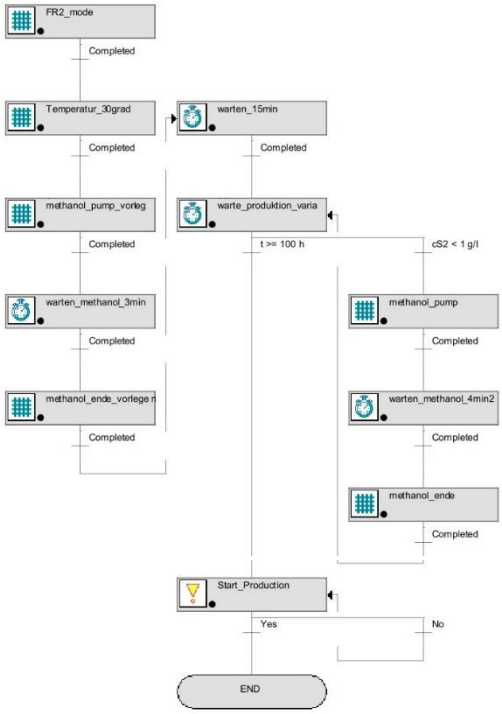

MFCS/win | **Recipe List** | **Printed:** *04-Dez-2025* 15:03:04 Mitteleuropäische Zeit

Recipe: p pastoris KlenTaq BatchProd
Version: 10.000
Status: APPROVED

MFCS Rev. 78,001

Operation : end

Figure 27: Used MFCS/win recipe for cultivations.

A.6 Cultivations

A.6.1 Process JW_2825

In the cultivation JW_2825, the process was initiated in the morning to enable systematic sampling throughout the day. The process comprised a complete cultivation run, including a batch phase, a fed batch phase, and a production phase, and was conducted using the minimal medium FM22. The total process duration was 135 h, with the fed-batch phase starting after 5.35 h and the production phase initiated after 23 h. The progression of the individual cultivation phases is shown in Figures 28-31.

The batch phase, depicted in Figure 28, generally corresponded to the expected process behavior. The pH was successfully regulated at a constant value of 5 by the controlled addition of ammonia and phosphoric acid. Following inoculation, a pronounced decrease in the dissolved oxygen tension (pO_2) was observed, which can be attributed to the initial cell concentration of 1.41 g/L. This elevated starting biomass was deliberately chosen to shorten the batch phase, as previous cultivations had experienced technical issues with the feed pump during the transition to the fed-batch phase.

Towards the end of the batch phase, both the pO_2 and the stirrer speed (N_{St}) signals exhibited increased noise. Under normal conditions, complete substrate depletion is indicated by a sharp rise in pO_2 accompanied by a decrease in N_{St}. In this case, the end of the batch phase could not be identified based on these signals, due to a shutdown computer, which resulted in a deactivation of the pO_2 control. Nevertheless, the observed increase in N_{St} over the course of the batch phase reflects the expected increase in biomass, which is also confirmed by the measured cell concentration shown in Figure 28.

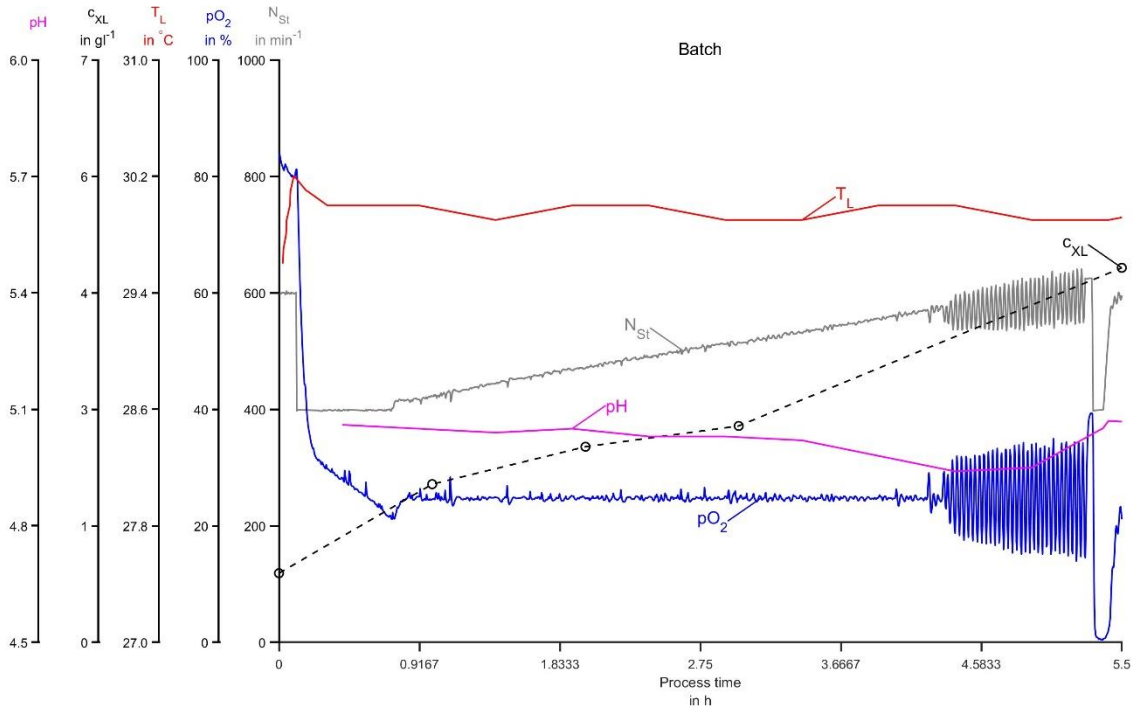

Figure 28: Batch phase of JW_2825 cultivation. This graph shows the course of the variables: c_{XL}: cell concentration by dry weight determination, pH, pO_2 and N_{St}. The pH value has a clear regulation around the value 5 throughout the batch phase. The pO_2 decreases over the batch phase until pO_2 reaches 25 %, then the pO_2 regulation is activated and the stirrer speed increases to introduce more oxygen into the liquid phase. Due to noise in the pO_2 and N_{St} signals, the end of the batch cannot be detected, and it is assumed that the end of the batch was triggered incorrectly. The cell concentration increased exponentially over the batch phase.

During the fed-batch phase, the pH was regulated at the setpoint of pH 5, while the temperature remained constant at its target value. At the beginning of the fed-batch phase, the dissolved oxygen tension (pO_2) exhibited a noisy signal, which stabilized shortly after continuous feed addition was established. A distinct, sharp decrease in pO_2 was observed at approximately 8.5 h; this event is most likely attributable to measurement artefacts rather than biological effects.

The stirrer speed responded inversely to the pO_2 signal, decreasing during transient pO_2 increases and rising when pO_2 dropped. Overall, the stirrer speed increased progressively over the course of the fed-batch phase, reflecting an increasing oxygen demand associated with biomass formation. From approximately 14.5 h onwards, the pO_2 continuously declined as the stirrer speed reached its upper limit, resulting in oxygen limitation. Despite this limitation, pH and temperature remained stably regulated at their respective setpoints. The measured cell concentration continued to increase during the fed-batch phase, indicating ongoing biomass growth.

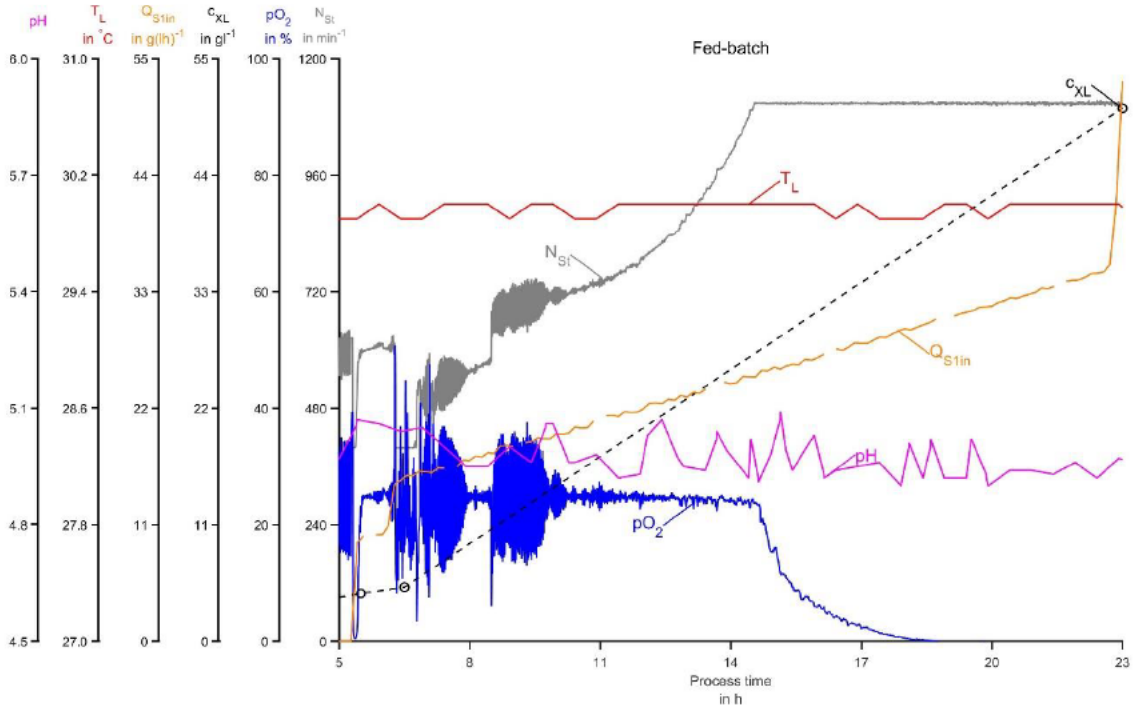

Figure 29: Fed-batch phase of JW_2825 cultivation. The Figure shows the course of the variables: c_{XL}: cell concentration by dry weight determination, pH value, pO_2: dissolved oxygen and N_{St}: stirrer speed during the fed batch phase. The cell concentration increases steadily over time, indicating continuous growth under substrate-limited conditions. The pO_2 signal is maintained at a stable level by automatic adjustment of the stirrer speed, only at the beginning are the signals very noisy, but they calm down after a short time. The pH is regulated to 5, becomes acidic over time as the base became empty, but the pH recovers to 5 after the base has been filled up.

The first production phase, depicted in Figure 30, was initiated at 23 h. At the onset of this phase, a methanol pulse was applied to achieve an initial methanol concentration of approximately 5 g/L (0.62 vol%) in the bioreactor. For this purpose, the F_{R1} feed pump was operated at 50 % for 1 minute. This initial pulse served to introduce sufficient methanol into the liquid phase to allow cellular adaptation to the new substrate and to induce the expression of enzymes required for methanol metabolism.

Following the initial pulse, methanol was metabolized by the cells and the concentration decreased to approximately 1 g/L (0.126 vol%). At this point, an additional methanol pulse is applied to increase concentration to approximately 2 g/L (0.252 vol%). Throughout the impulse driven production phase, both pO_2 and pH were maintained at their respective setpoints. The stirrer speed showed a increase to approximately 32.5 h, followed by a moderate decrease.

The pronounced increase in cell concentration observed during the production phase is not characteristic for methanol-induced protein expression, where biomass formation is usually limited. A plausible explanation for this behavior is the occurrence of oxygen limitation during the preceding fed-batch phase. As the maximum stirrer speed was reached, oxygen availability likely became limiting, potentially preventing complete consumption of glycerol. Residual glycerol may therefore have remained available at the start of the production phase and could have been preferentially metabolized by the cells, resulting in continued biomass growth despite the switch to methanol feeding.

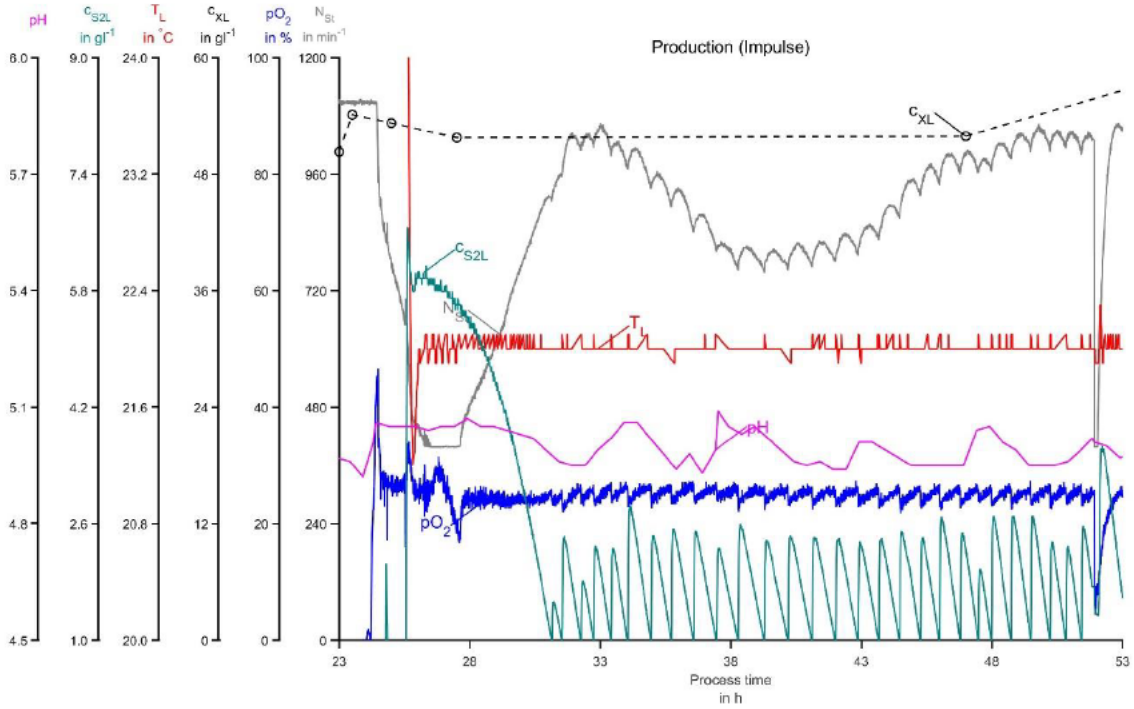

Figure 30: Impulse driven production phase of process JW_2825. The graph of the impulse driven production phase shows the variables: c_{S2L}, c_{XL} pH, temperature, N_{St} and pO_2. The pH is still regulated at 5 in the production phase, while the temperature is reduced to 22 °C and both are maintained. In the production phase, methanol (S2) is added to the medium. The graph shows an initial addition of methanol, which results in an increase in the methanol concentration. The methanol is then consumed by the cells until a concentration of 1 g/L is reached, which leads to a further addition of methanol so that a concentration of around 2 g/L is reached. The cell concentration increases, as can be also seen from the pO_2 and N_{St} values. The pO_2 is constantly regulated at 25 % by the stirrer speed, which increases during the impulse driven production phase.

After completion of the impulse-driven production phase, a second production phase was initiated at 53 h, in which the methanol concentration was regulated using a PI controller. This phase is illustrated in Figure 31. Over the entire duration of the PI-controlled production phase, pH, pO_2, methanol concentration, and stirrer speed remained largely constant, indicating stable and well controlled process conditions. The measured cell concentration suggests that biomass growth continued during this phase.

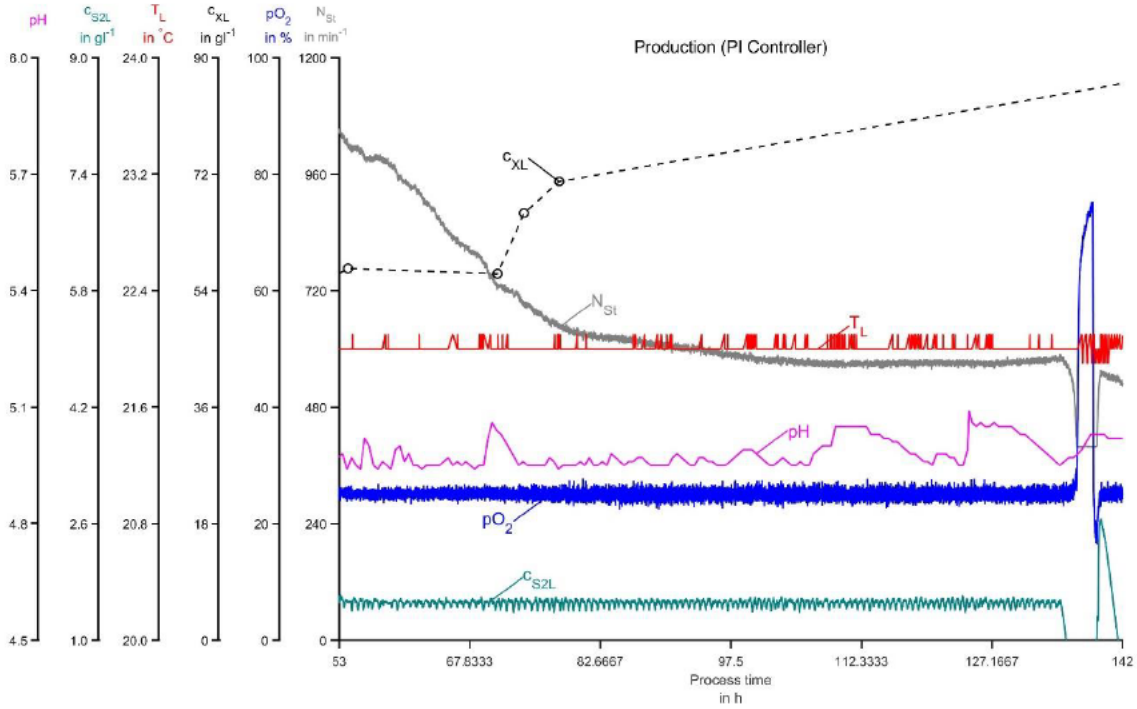

Figure 31: PI Controller regulated production phase of process JW_2825. The graph of the PI controller regulated production phase shows the variables: c_{S2L}, c_{XL} pH, temperature, N_{St} and pO_2. The temperature, pH, pO_2 and c_{S2L} are regulated at their respected setpoints. The stirrer speed shows a clear decrease during this production phase, which conversely means that the cells show less growth. Nevertheless, the cells show recognizable growth.

A.6.1.1 SDS-PAGE

Figures 32 and 33 show two SDS gels to which samples of process JW_2825 are applied. A total of seven samples were applied. The first sample that was applied was taken 20 h after the start of production at a process time of 54 h, the second after 47 h after the start of production at a process time of 71 h and the last sample of the current process was taken at a process time of 142 h or after 118 h of the start of production. The samples mentioned above were thermally purified as described in section 4.4. Ultrafiltration was carried out with the entire volume at the end of the thermal purification. The retentate and the permeate are shown in the Figures. After ultrafiltration, a diafiltration was performed with the KlenTaq buffer (20mM Tris-HCl, 100 mL NaCl, 0.1 mM EDTA, pH 7.5) and the retentate and permeate are shown in the Figure 33.

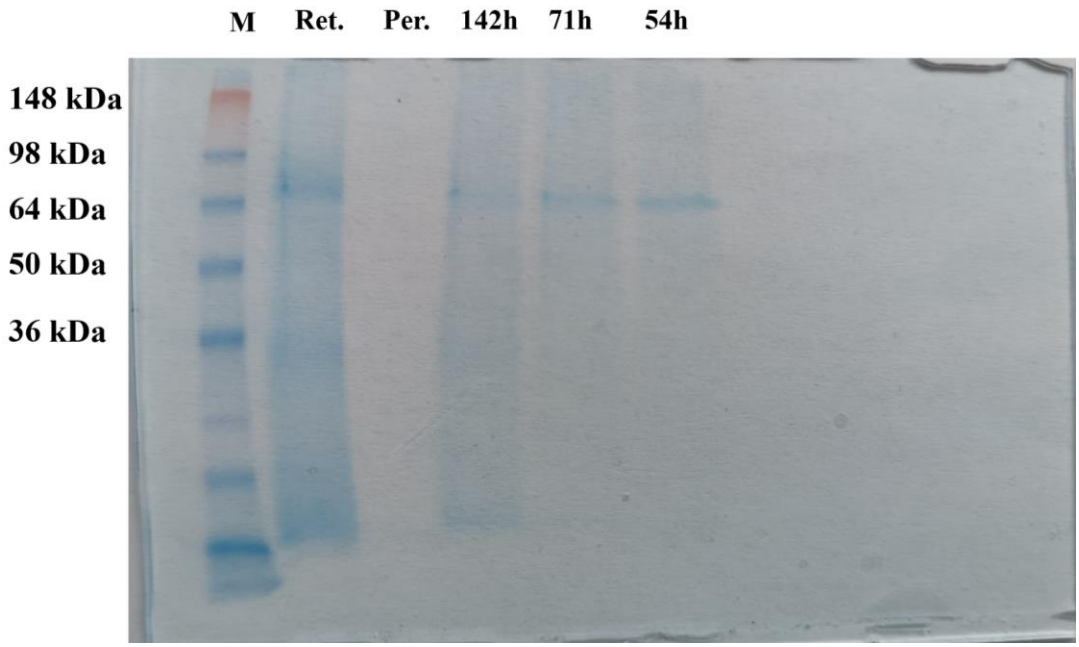

Figure 32: SDS- PAGE gel of samples taken during the cultivation JW_2825. Samples: M: Marker, Ret.: Retentate of ultrafiltration of the purified culture supernatant, Per.: Permeate of ultrafiltration of the purified culture supernatant, 142 h: Purified culture supernatant at the process time 142 h, 71 h: Purified culture supernatant at the process time 71 h, 54 h: Purified culture supernatant at the process time 54 h.

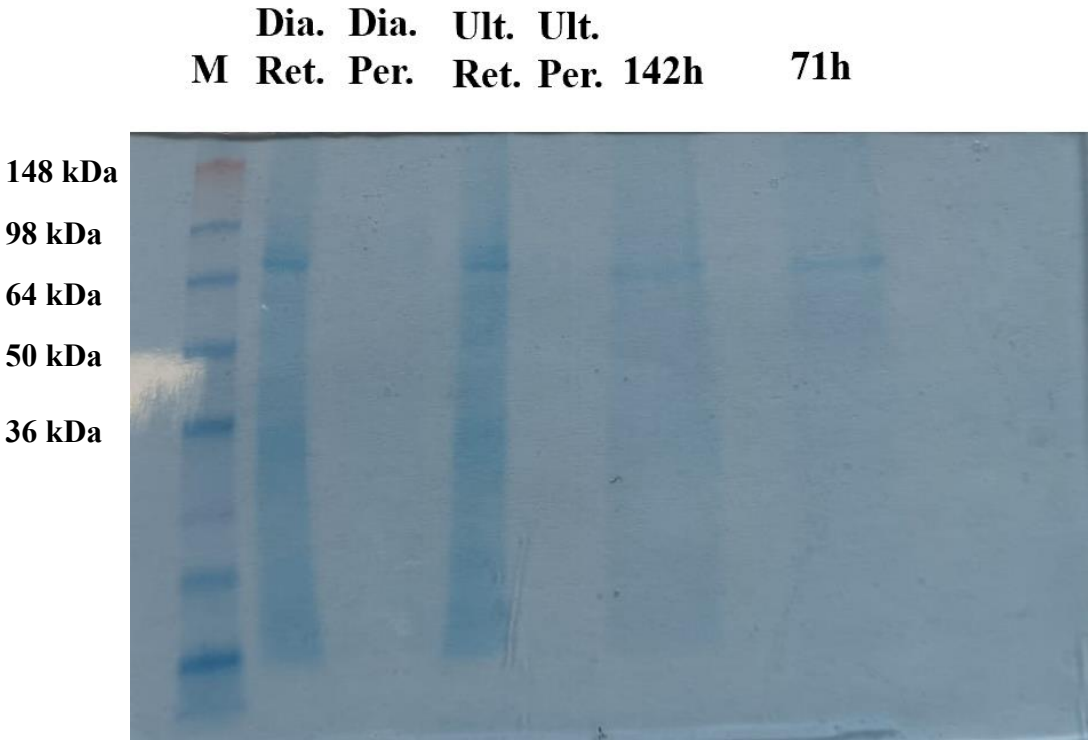

Figure 33: SDS- PAGE gel of samples taken during the cultivation JW_2825. Samples: M: Marker, Dia. Ret.: Retentate of diafiltration of the retentate of the Ultrafiltration, Dia. Per.: Permeate of diafiltration of the retentate of the ultrafiltration, Ult. Ret.: Retentate of ultrafiltration of the purified culture supernatant, Ult. Per.: Permeate of ultrafiltration of the purified culture supernatant, 142 h: Purified culture supernatant at the process time 142 h, 71 h: Purified culture supernatant at the process time 71 h.

A.6.2 Process JW_3125

The cultivation JW_3125 was initiated in the morning with a batch phase at an initial cell concentration of 0.87 g/L. The process comprised a complete run, including a batch phase, a fed-batch phase, and a production phase. In contrast to cultivations performed in minimal medium, the complex medium BGGY was used, identical to the medium applied in the Erlenmeyer flask experiment (see section 4.4). The total duration was 51 h, with the fed batch phase starting after 4.7 h and the production phase initiated after 23.2 h. The overall course of the cultivation is shown in Figures 34-36.

The batch phase of cultivation JW_3125 followed the expected theoretical course. The pH value was successfully maintained at 5 through the controlled addition of ammonia and phosphoric acid, while the temperature of the liquid phase was constantly regulated at 30 °C using the cooling finger and heating jacket.

After inoculation, the dissolved oxygen tension pO_2, initially at 100 %, decreased rapidly due to increasing cellular respiration, which is expected during exponential growth in the batch culture. Upon reaching a pO_2 value of 25 % the pO_2 control was activated via the stirrer speed. Consequently, the stirrer speed increased continuously to maintain the dissolved oxygen level at the setpoint.

Complete depletion of the substrate in the medium resulted in a sharp increase in pO_2 accompanied by a corresponding decrease in the stirrer speed N_{St}, marking the end of the batch phase at approximately 4.7 h, as shown in Figure 34. During the batch phase the cell concentration increased exponentially, which is consistent with the observed oxygen demand.

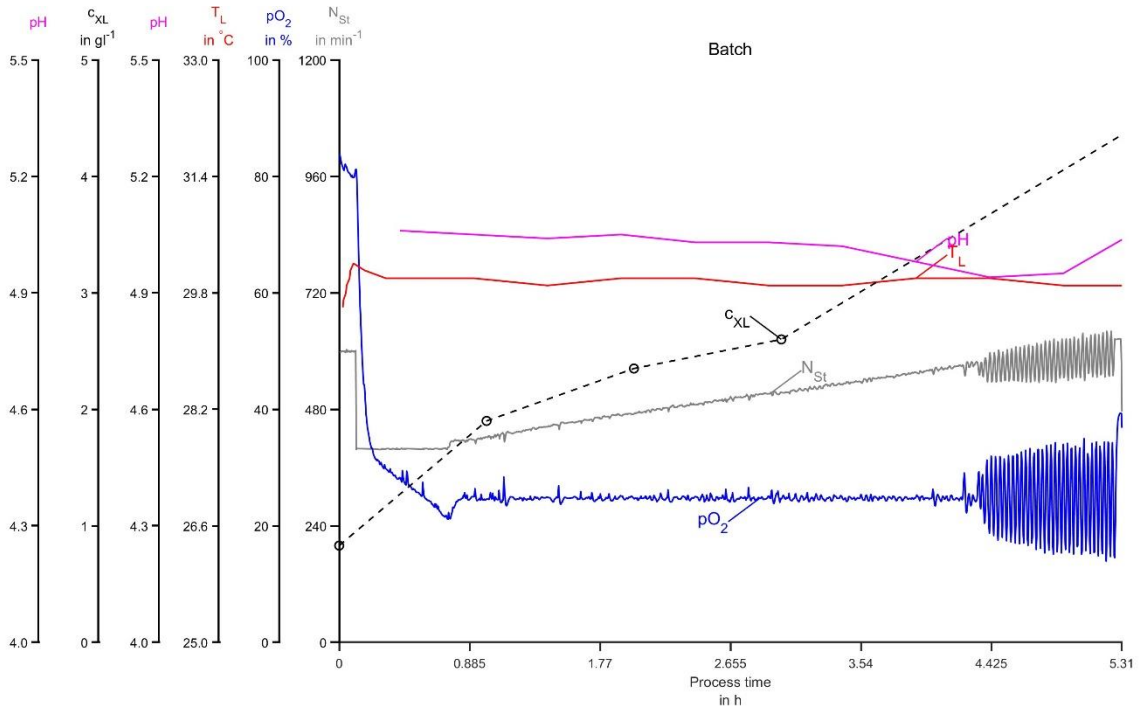

Figure 34: Batch phase of JW_3125 cultivation. This graph shows the course of the variables: c_{XL}: cell concentration by dry weight determination, pH, pO_2, N_{St} and temperature. The pH value shows a constant value of 5 throughout the batch phase. The temperature also shows a constant behavior at 30 °C due to the regulation. The pO_2 decreases over the batch phase until pO2 reaches 25%, then the pO2 regulation is activated which leads to an increase of the stirrer speed. At 4.6 h the pO_2 value increases and thus the N_{St} value decreases, which indicates the end of the batch phase, as the glycerol in the medium has been used up. The cell concentration increased over the batch phase exponentially.

During the fed-batch phase, pH and temperature remained constant at their respective setpoints in the batch phase. At the beginning of the fed batch phase, the pO_2 signal exhibited considerable noise but stabilized at approximately 25 % shortly thereafter. From a process time of around 12 h onwards, oscillations in the pO_2 signal were observed, which led to corresponding oscillations in stirrer speed.

At approximately 16 h, a sharp decrease in pO_2 occurred, triggering a rapid increase in stirrer speed to its maximum value of 1110 rpm. Throughout the remainder of the fed batch phase, the pO_2 could no longer be maintained at the setpoint of 25 % and instead oscillated strongly around a lower value of approximately 10 %. The fed batch phase concluded after 23.2 h.

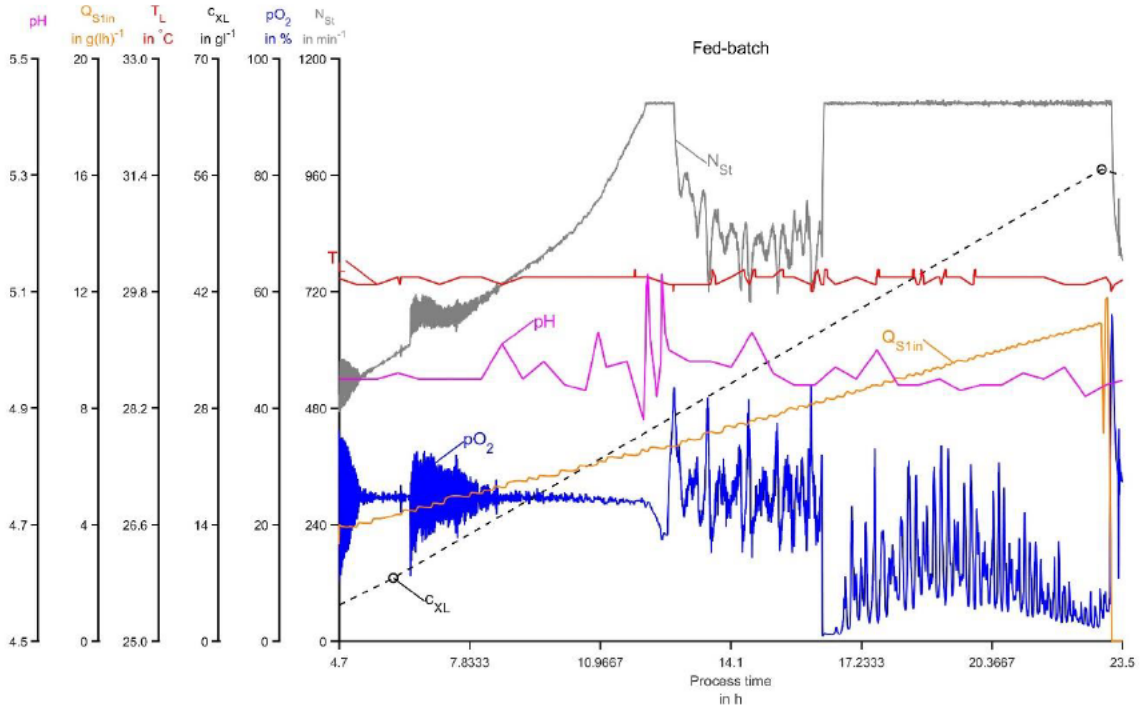

Figure 35: Fed-batch phase of JW_3125 cultivation. The graph of the fed batch phase contains the variables: Q_{S1in}: specific substrate supply rate, c_{XL}: cell concentration by dry weight determination, pH, temperature, N_{St} and pO_2. The pH is regulated to the value of 5 and the temperature is kept at 30 °C in the fed batch phase. Q_{S1in} shows the feeding profile with which glycerol is added to the liquid phase in the fed batch phase. This is increasing exponentially, as the cells also show exponential growth. The pO_2 signal and the N_{St} signal are initially very noisy at times, but the pO_2 is regulated to 25 % after a short time. The N_{St} shows a clear increase during this time until it reaches the limit of 1110. Subsequently, the pO_2 signal fluctuates strongly, as does the stirrer speed. After that the N_{St} reaches its limit again and the pO_2 is not regulated anymore at 25 %.

The production phase was initiated after 23.2 h, as shown in Figure 36. During the initial methanol pulse, a technical malfunction of the feed pump led to the addition of a substantially higher amount of methanol than intended. As a result, an initial methanol concentration of approximately 20 g/L was reached instead of the targeted 5 g/L.

Following adaptation to the new substrate, cells began to metabolize methanol, requiring approximately 13 h. to reduce the methanol concentration to 1 g/L. Once this concentration was reached, small methanol pulses were applied to increase the concentration back to approximately 2 g/L. Throughout the entire production phase, the pH remained stable at 5 and the temperature was maintained at 22 °C. The pO2 was successfully regulated at 25 %, and the stirrer speed remained relatively constant, indicating stable metabolic activity.

No significant increase in cell concentration was observed during the production phase, which is consistent with the expectations for methanol-induced protein expression, where metabolic activity is primarily directed toward recombinant protein production rather than biomass growth.

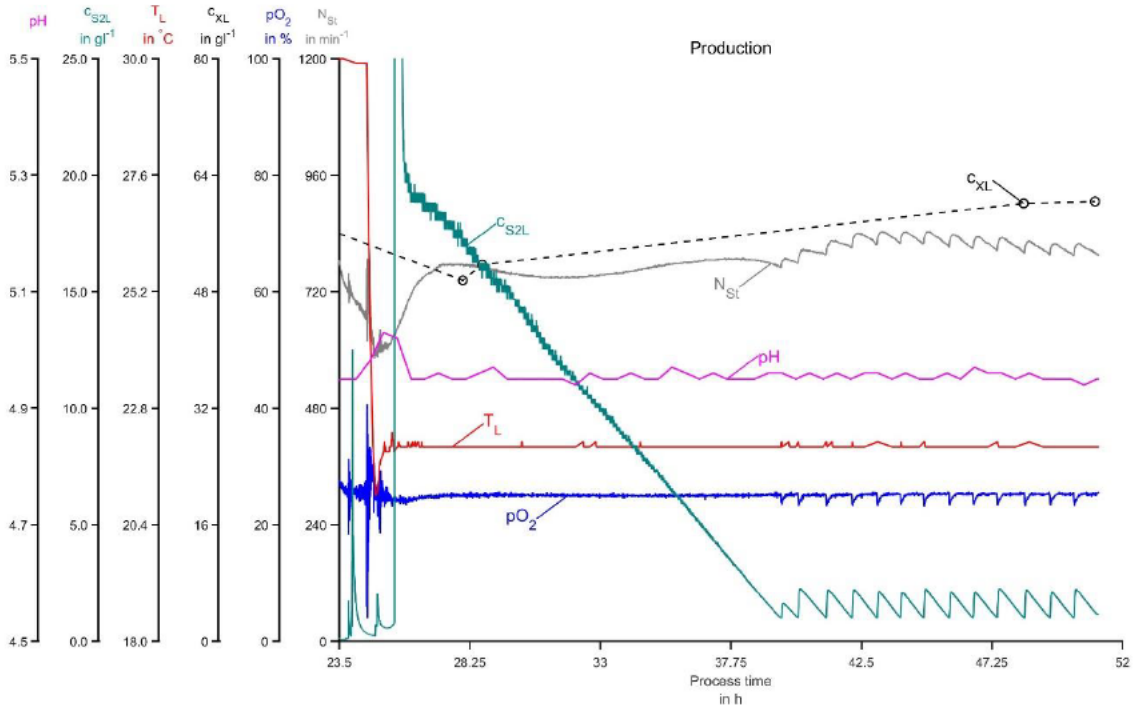

Figure 36: Production phase of JW3125 cultivation. The graph of the production phase shows the variables: c_{S2L}, c_{XL} pH, temperature, N_{St} and pO_2. The pH is still regulated to 5 in the production phase, while the temperature is reduced to 22 °C and maintained. In the production phase, methanol (S2) is added to the medium. The graph shows an initial addition of methanol, which results in an increase in the methanol concentration. The methanol is then consumed by the cells until a concentration of 1 g/L is reached, which leads to a further addition of methanol so that a concentration of around 2 g/L is reached. The cell concentration does not increase, as can be also seen from the pO2 and N_{St} values. The pO_2 is constantly regulated at 25 % by the stirrer speed, which remains constant during the production phase.

A.6.2.1 SDS-PAGE

Figure 37 shows the SDS gel that was performed with the sample taken during the process JW_3125. On this gel only one sample was applied, to verify the expression of the KlenTaq DNA polymerase. The sample was taken at the process time 51 h which subsequently means it has been taken 24h after the start of production. In Figure 37, the sample shows a visible band at 64kDa.

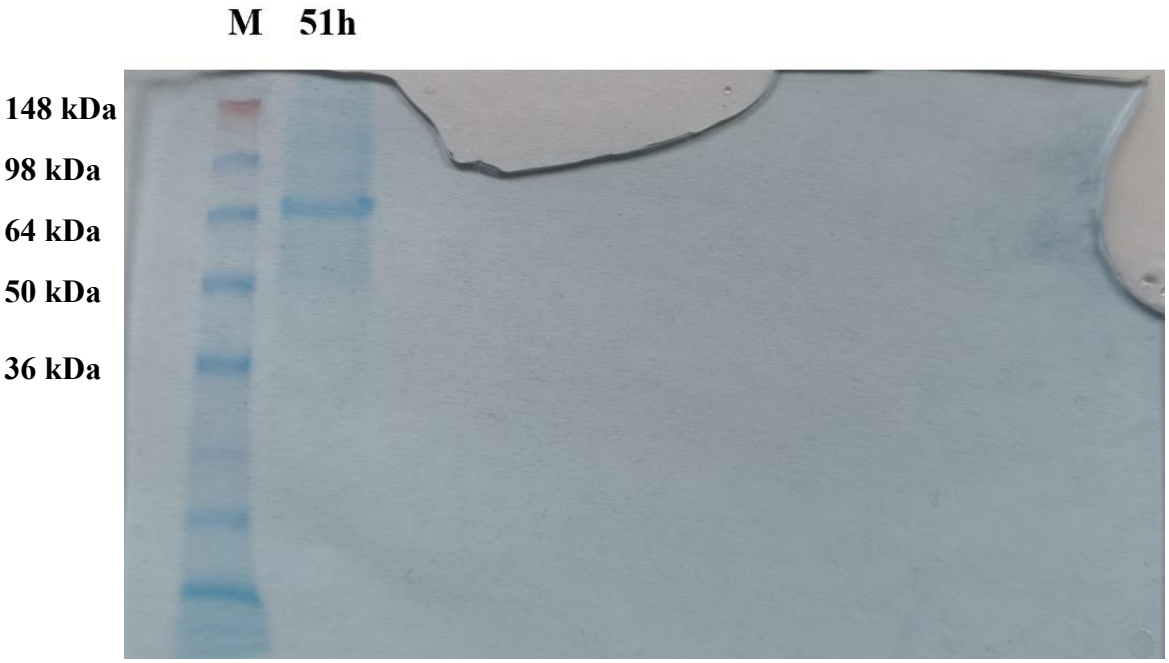

Figure 37: SDS- PAGE gel of sample taken during the cultivation JW_3125. Samples: M: Marker, 51 h: Purified culture supernatant at the process time 51 h.

A.6.3 Process JW_3625

The cultivation JW_3625 was initiated in the morning with an initial cell concentration of 0.79 g/L. Compared to previous cultivations, the process was modified and consisted only of a batch phase followed directly by a production phase, a fed-batch phase was started. In addition, the culture pH setpoint was increased from 5.0 to 6.6 in order to more closely match the optimum of KlenTaq DNA polymerase. The total cultivation time was 25.8 h. The batch phase ended after approximately 5.5 h, resulting in a production phase duration of about 20.4 h. The complete cultivation profile is shown in Figures 38-39.

Figure 38 illustrates the batch phase of cultivation JW_3635. The pH value was regulated to 6.6 and remained constant throughout the batch phase. Similarly, the temperature was maintained at a constant setpoint of 30 °C.

After process start, the dissolved oxygen tension (pO_2) gradually decreased from 100 % to approximately 25 % over a period of about 2.5 h. From this point onward, pO_2 control was activated and the value was successfully maintained at the setpoint of 25 %. Correspondingly, the stirrer speed began to increase at a process time of approximately 2.5 h

Towards the end of the batch phase, no distinct batch end signal could be identified due to pronounced signal noise, which led to an incorrect triggering of the batch end detection. Despite this limitation, the cell concentration during the batch phase exhibited exponential growth, indicating successful biomass formation.

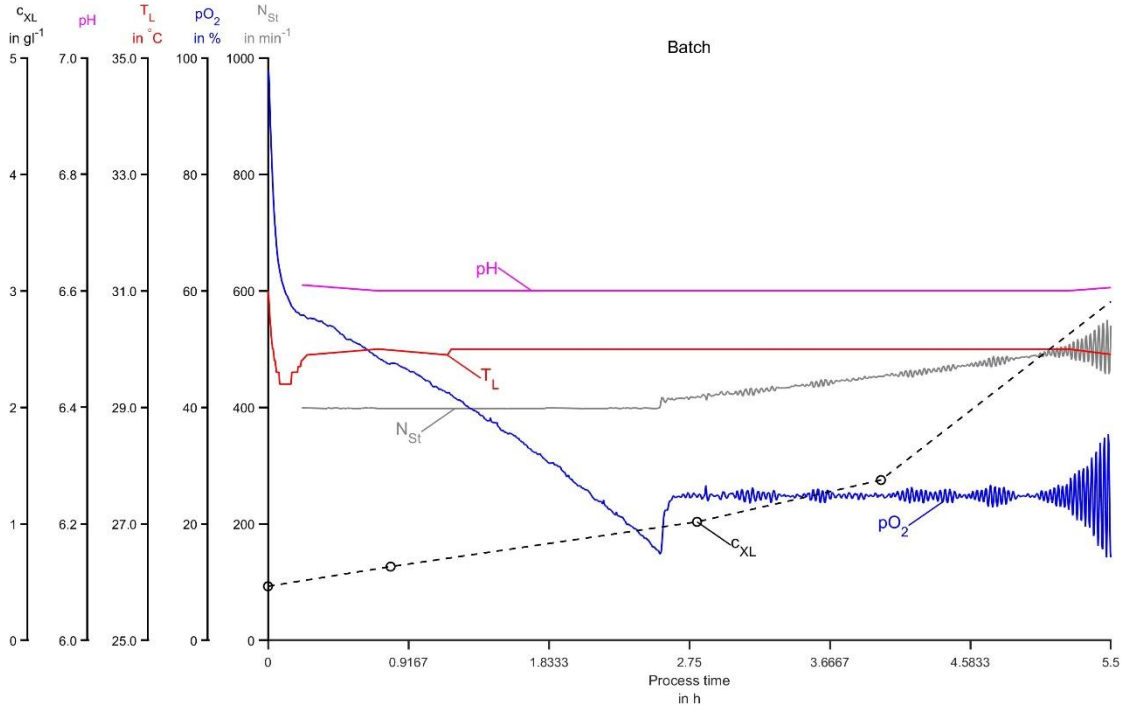

Figure 38: Batch phase of JW_3625. This graph shows the variables: c_{XL}, pH, temperature, N_{St} und pO_2. The temperature and pH value are regulated constantly at their setpoint during the batch phase. The pO_2 reaches 25 % after 2.5 hours, which activates the pO_2 control. This regulates the pO_2 to 25 % and causes the stirring speed to increase. Both signals show significant noise at the end of the batch phase. Cell growth is confirmed by the signal of cell concentration.

Following the batch phase, the production phase was initiated. The pH continued to be regulated at 6.6, while the temperature was reduced to 22 °C and maintained at this setpoint for the remainder of the process. The substrate was switched to methanol (S2), and an initial pulse was applied to reach a methanol concentration of approximately 4.3 g/L.

During the production phase, methanol was gradually metabolized by the cells, resulting in a continuous decrease in concentration. The process was terminated once the methanol concentration approached 0 g/L. The pO_2 signal during this phase was intermittently noisy but showed an overall tendency to remain regulated at approximately 25 %. The stirrer speed also displayed fluctuations and increased slightly over most of the production phase, indicating ongoing cellular activity.

At a process time pf 17.5 h, a small transient peak in the pO_2 signal was observed, leading to a temporary decrease in stirrer speed. No clear cause for this behavior could be identified. Notably, the measured cell concentration increased sharply during the production phase. This behavior is atypical for a methanol-induced production and can be attributed to the incorrectly triggered batch end signal. As a consequence, glycerol (S1) was not completely consumed at the end of the batch phase, allowing the cells to continue growth during the production phase. This interpretation is further supported by the slow decrease in methanol concentration over approximately 15 h, indicating that glycerol was still used as the primary substrate for a substantial part of the production phase.

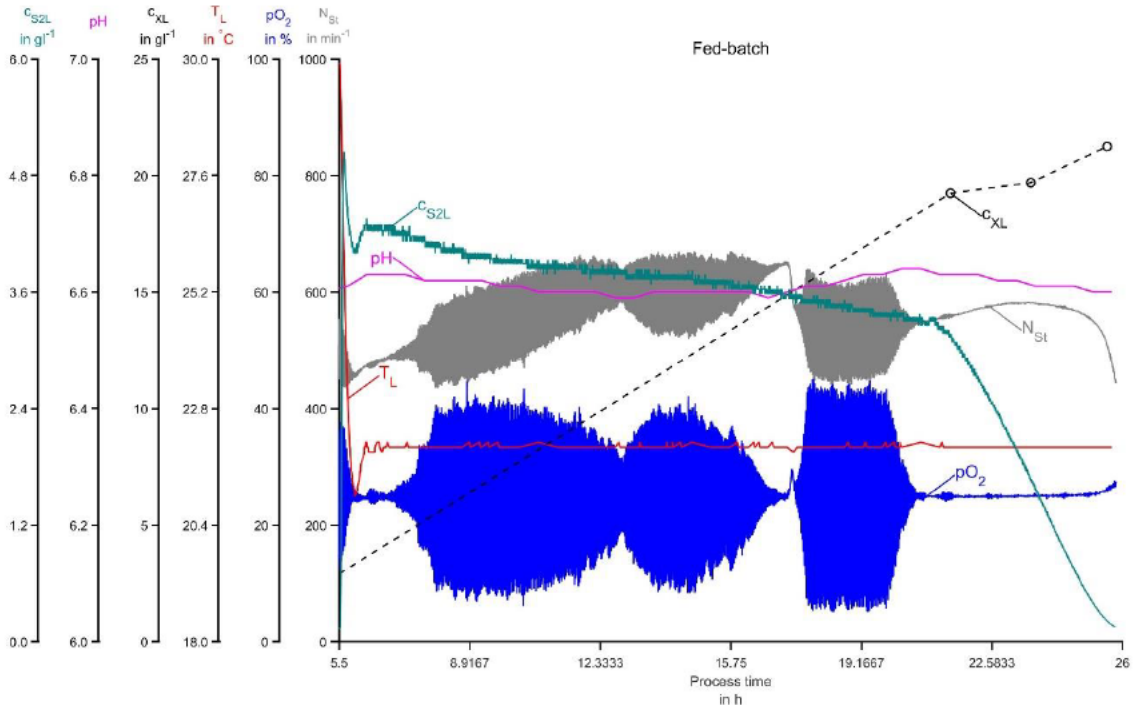

Figure 39: Production phase of JW_3625. Shown are the temporal courses of methanol concentration (c_{S2L}), cell concentration (c_{XL}), pH value, temperature (ϑ_L), stirrer speed (N_{St}) and dissolved oxygen (pO_2). The pH and temperature are controlled at their set value. pO_2 was regulated at 25 % by the increasing stirrer speed. Cell concentration shows growth during the production phase which was carried out until the methanol depletion.

A.6.3.1 SDS-PAGE

The SDS-PAGE analysis, shown in Figure 40, of the samples obtained from process JW_3625 show visible protein bands at approximately 64 kDa, which corresponds to the expected molecular weight of KlenTaq DNA polymerase. The target band is detectable in both the thermally purified culture supernatant and the only centrifuged culture supernatant (without thermal purification). Despite the low signal intensity, the presence of this band confirms successful expression of KlenTaq polymerase.

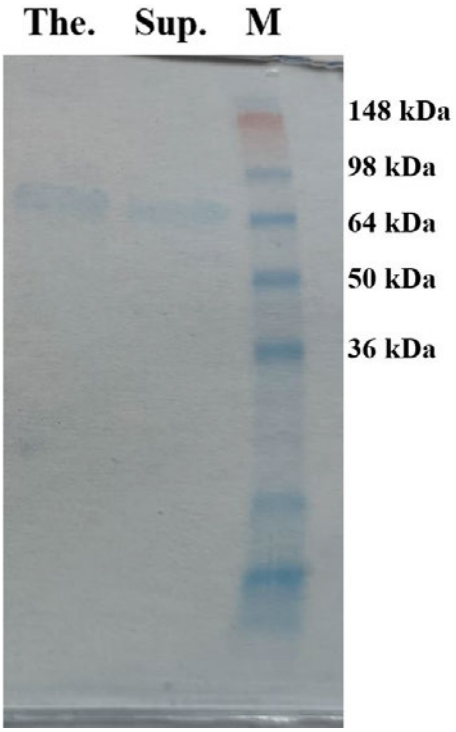

Figure 40: SDS-Gel of samples taken during the cultivation JW_3625. Samples: The.: Culture supernatant (thermally purified), Sup.: Purified culture supernatant (only cells removed), M: Marker.

A.6.4 Process JW_3825

The cultivation JW_3825 was initiated with an initial cell concentration of 0.76 g/L. A complete run was performed, consisting of batch, fed batch and production phases. Throughout the entire process, the pH was controlled at 6.5. During the production phase, the cultivation temperature was increased from 22 °C to 30 °C. The total process duration was 51 h, comprising a 6 h batch phase, a 20 h fed batch phase, and a production phase lasting approximately 25 h. An overview of the complete cultivation is shown in Figures 41-43.

Figure 41 illustrates the batch phase of cultivation JW_3825. During this phase, both pH and temperature remained highly stable at their respective setpoints of 6.5 and 30 °C. After approximately 1.2 h, the dissolved oxygen tension decreased to 25 %, at which its control was initiated. This regulation is reflected by a continuous increase of the stirrer speed over the course of the batch phase, allowing the pO_2 level to be maintained at the setpoint. With increasing process time, the pO_2 signal exhibited slightly increased noise, however, a clear batch end signal was still detectable after 6 h. The cell concentration showed exponential growth throughout the batch phase.

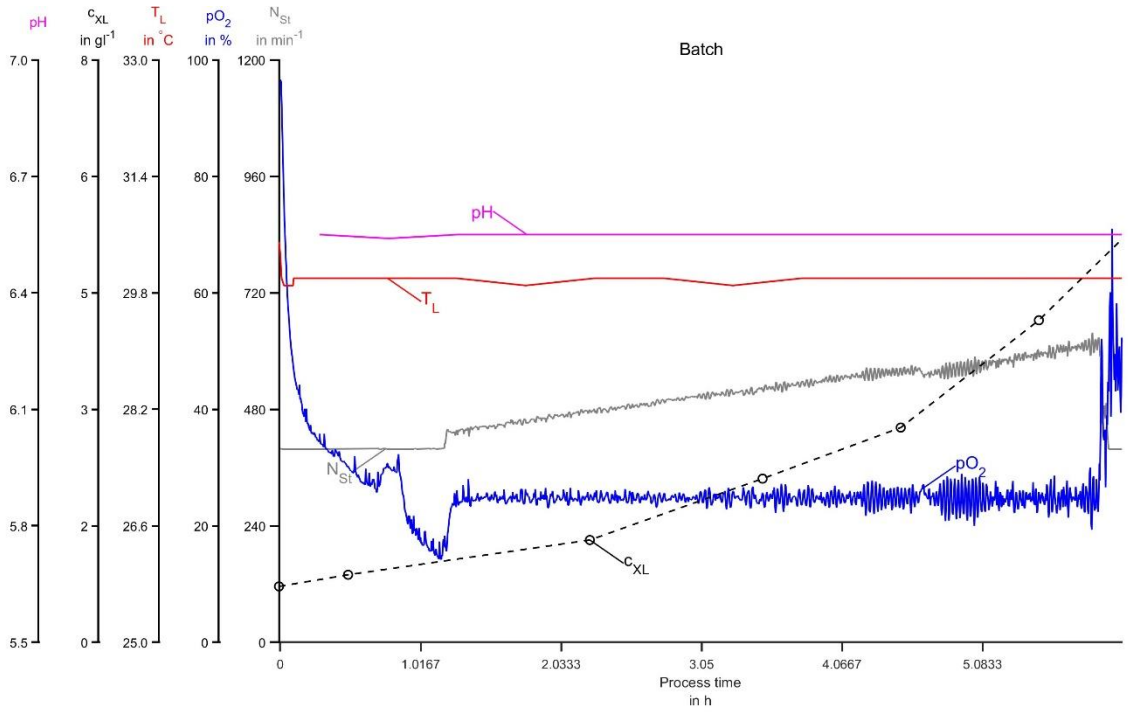

Figure 41: Batch phase of JW_3825. Shown are the temporal courses of cell concentration (c_{XL}), pH value, temperature (ϑ_L), stirrer speed (N_{St}) and dissolved oxygen (pO_2). The pH and temperature are controlled at their set value the entire batch phase. After reaching 25 %, the dissolved oxygen is regulated by adjusting the stirrer speed, which increases over the course of the batch phase. Cell concentration shows exponential growth.

During the fed batch phase (Figure 42), the pH and temperature remain constant. Q_{S1in} represents the feeding profile used for the addition of glycerol (S1) to the liquid phase. Glycerol is supplied to prevent substrate limitation during cell growth in the fed batch phase. At the beginning of the fed batch phase, the pO_2 signal and stirrer speed show instabilities, however, from approximately 12 h onward, the pO_2 remains relatively constant despite minor oscillations, while the stirrer speed increases slightly in an exponential manner. The measured cell concentration indicates growth throughout the fed batch phase.

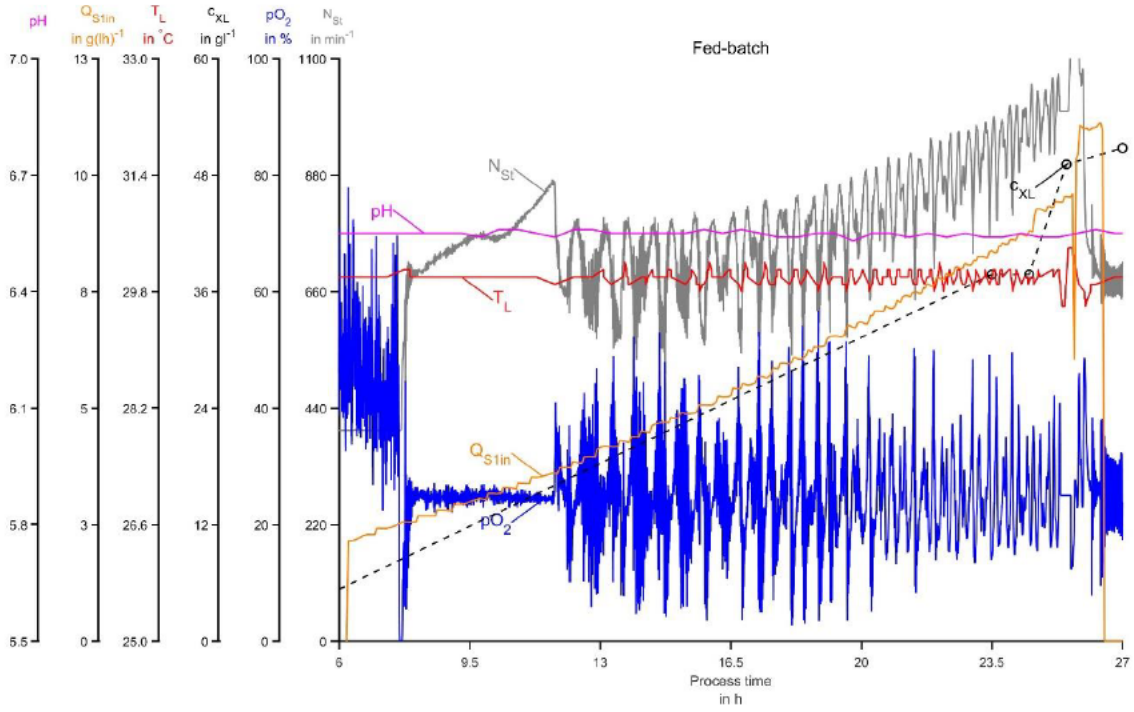

Figure 42: Fed-batch phase of JW_3825. Shown are the temporal courses of specific substrate supply rate (Q_{S1in}), cell concentration (c_{XL}), pH value, temperature (ϑ_L), stirrer speed (N_{St}) and dissolved oxygen (pO_2). The pH and temperature are controlled at their set value, while the temperature experiences minor oscilations. pO_2 was regulated at 25 % by the increasing stirrer speed. Specific substrate supply rate follows the feeding profile and cell concentration shows growth during the fed batch phase.

During the production phase, shown in Figure 43, the pH was continuously regulated at 6.5 and the temperature was maintained at 30 °C. At the beginning of the production phase, an initial methanol pulse was added to the liquid phase. This resulted in an apparent methanol concentration of approximately 42 g/L, however, this absolute value is incorrect due to an erroneous calibration of the methanol probe based on a temperature of 22 °C instead of the actual process temperature of 30 °C. Nevertheless, the relative decrease in methanol concentration over time remains interpretable. The methanol concentration continuously declined and approached depletion at approximately 37 h. which is reflected by an increase in the pO_2 signal observed between 37 h and 47 h. This increase indicates reduced oxygen consumption due to substrate depletion. At 47 h, methanol was added again, leading to a decrease in the pO_2 signal as the cells restarted metabolic activity upon new substrate addition. The stirrer speed decreased until 37 h and remained constant at 400 rpm thereafter, as the pO_2 did not fall below the control setpoint 25 %. No further increase in cell concentration was observed during the production phase.

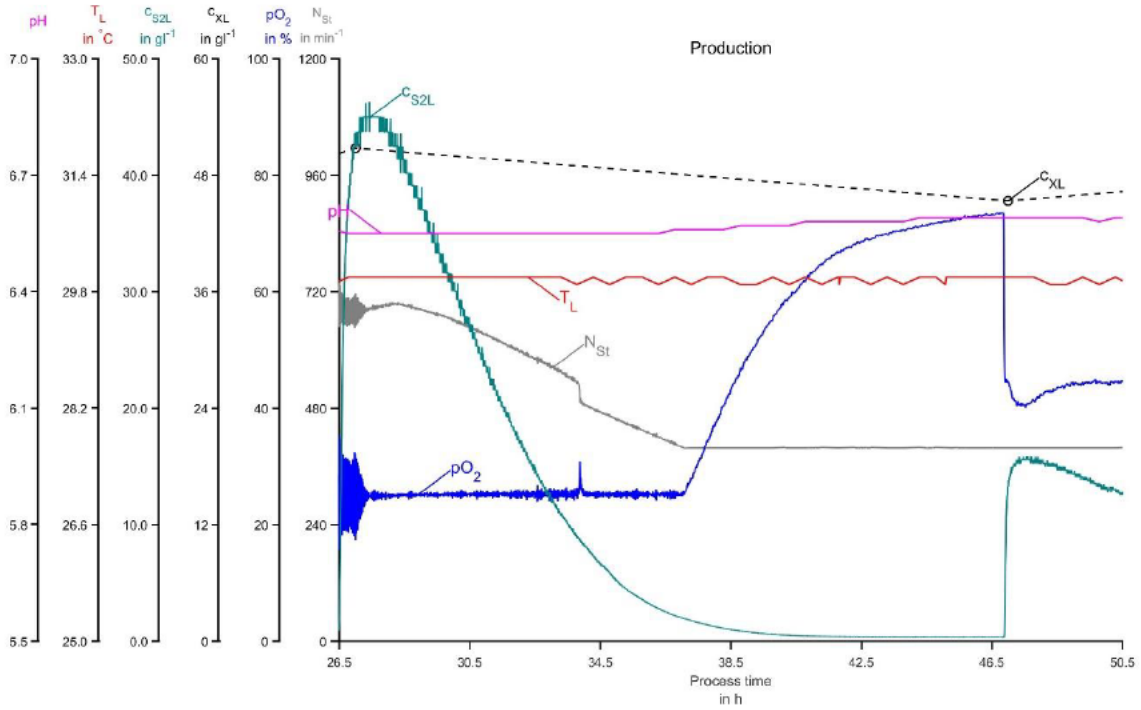

Figure 43: Production phase of JW_3825. Shown are the temporal courses of methanol concentration (c_{S2L}), cell concentration (c_{XL}), pH value, temperature (ϑ_L), stirrer speed (N_{St}) and dissolved oxygen (pO_2). pH and temperature are maintained at the set values during the production phase. As the methanol concentration reaches zero, the pO_2 signal experiences an increase until new addition of methanol. Resulting in a decrease in pO_2 signal, but not reaching the setpoint 25 %, as the stirrer speed reaches its lower limit at 400 rpm from 37 h. The cell concentration does not indicate any increase.

A.6.5 Process JW_4025

Cultivation JW_4025, was started with an initial cell concentration of 0.31 g/L and was designed to resemble protein expression conditions in the Erlenmeyer flask experiments as closely as possible. Therefore, the process consisted only of a batch and a production phase, the pH was not regulated, and the temperature was controlled at 30 °C throughout the whole process. The entire cultivation lasted 47 h, the batch phase lasted 14.2 h and the production phase 32.8 h accordingly. The cultivation plots are shown in Figures 44-45.

Figure 44 illustrates the batch phase of the cultivation JW_4025. The temperature was successfully controlled at 30 °C in this phase. The pH remained stable at 6.6 for the first 5 h without regulation or addition of corrective agents. Subsequently the pH gradually decreased and, with increasing cell concentration, dropped more rapidly to a value of approximately 6.2. The dissolved oxygen declined continuously and reached the control setpoint of 25 % after approximately 11 h. From this point onward, the pO_2 was regulated at 25 % by increasing the stirrer speed, which rose sharply to 800 rpm. At the end of the batch phase after 14.2 h, a clear batch end signal was observed, characterized by a rapid increase in the pO_2 signal and a corresponding decrease in stirrer speed. The measured cell concentration exhibited clear exponential growth throughout the batch phase.

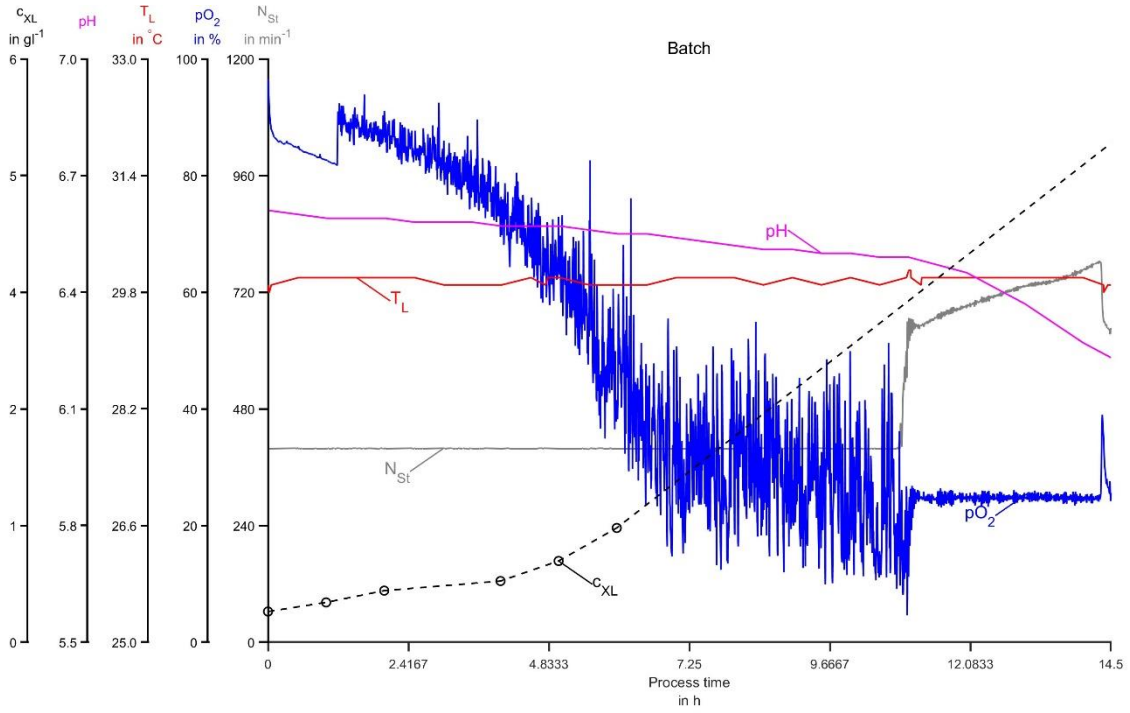

Figure 44: Batch phase of JW_4025. Shown are the temporal courses of cell concentration (c_{XL}), pH value, temperature (ϑ_L), stirrer speed (N_{St}) and dissolved oxygen (pO_2).

During the production phase, the pH increased to approximately 6.4 at the transition from the batch end and remained stable at this value throughout the remainder of the production phase without regulation. The temperature was continuously controlled and maintained at 30 °C. Methanol was used as the sole substrate in the production phase and was added to the liquid phase via an initial pulse at the beginning of this phase. This pulse resulted in a methanol concentration of approximately 6.5 g/L which was subsequently consumed by the cells over the course of the production phase. The stirrer speed decreased to 400 rpm at process time 25.5 h. Lower stirring speeds are avoided to prevent potential measurement artifacts affecting the pO_2 measurement. Following this adjustment, the dissolved oxygen signal increased continuously and reached 80 % by the end of cultivation, indicating reduced oxygen demand. No significant increase in cell concentration was observed during the production phase.

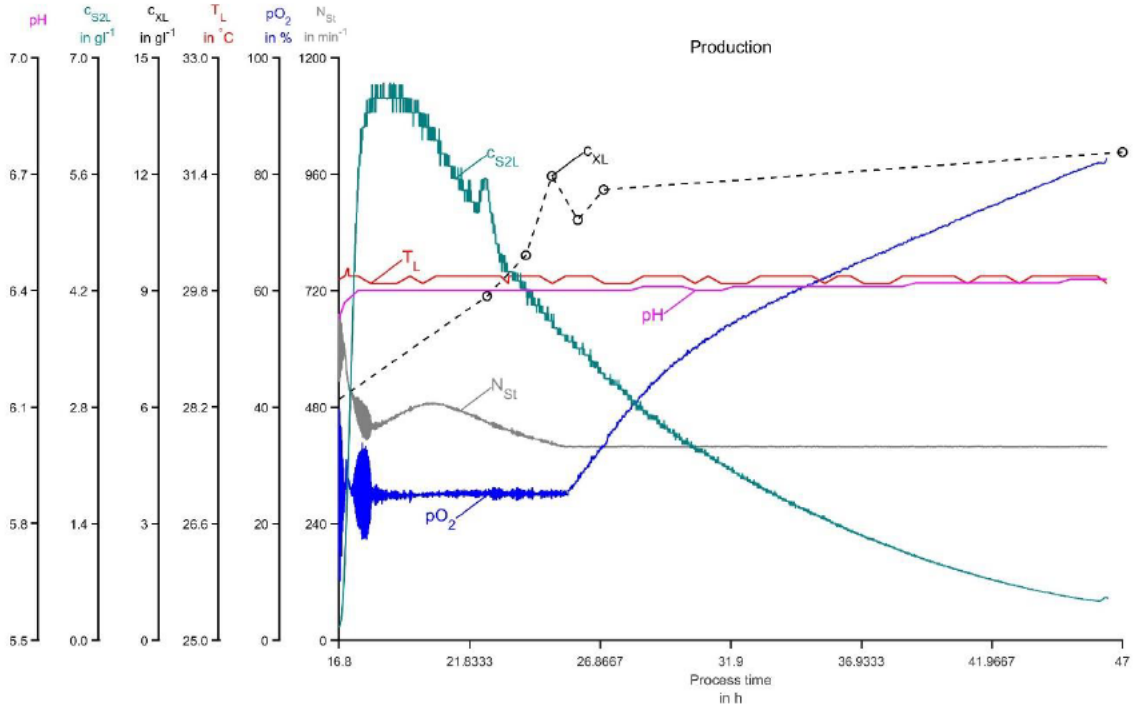

Figure 45: Production phase of JW_4025. Shown are the temporal courses of methanol concentration (c_{S2L}), cell concentration (c_{XL}), pH value, temperature (ϑ_L), stirrer speed (N_{St}) and dissolved oxygen (pO_2).

A.7 SDS-PAGE analysis of processes

Figure 46 shows an SDS-PAGE analysis of thermally purified supernatant and diafiltrated samples from cultivations JW_2825 and JW_3125. In the thermally purified samples both processes (lanes 2 and 4), a distinct protein band at approximately 63-65 kDa is visible, corresponding to the expected molecular weight of KlenTaq DNA polymerase.

For cultivation JW_2825, the diafiltrated sample (lane 1) shows a more intense and better-defined band compared to the thermally purified supernatant (lane 2), indicting an increase relative protein concentration after diafiltration.

In contrast, the diafiltrated sample of JW_3125 (lane 3) appears strongly smeared, which prevents a clear identification of a distinct band. While the presence of KlenTaq may be assumed based on the overall signal, no reliable conclusion can be drawn from this alone.

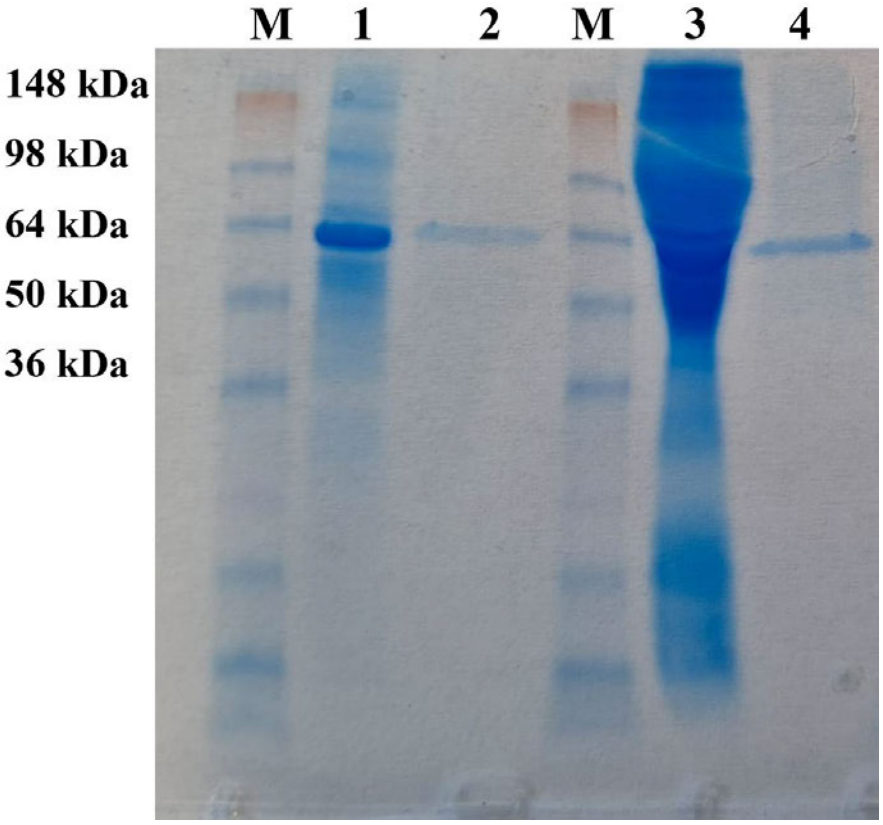

Figure 46: SDS-PAGE gel of samples from the cultivation JW_2825 and JW_3125. M: Marker, 1: JW_2825 Diafiltration, 2: JW_2825 Bioreactor supernatant (thermally purified), 3: JW_3125 Diafiltration, 4: JW_3125 Bioreactor supernatant (thermally purified).

Figure 47 shows an SDS-PAGE analysis of samples from cultivations JW_3825 and JW_3625. In the thermally purified samples both processes (lanes 2 and 6), a protein band at approximately 63-65 kDa is visible, corresponding to the expected molecular weight of KlenTaq DNA polymerase, the band of the process JW_3825 is more intense. The diafiltrated samples of both processes (lane 1 and 5) show a smeared appearance. Nevertheless, in both lanes a protein band can be discerned in the molecular weight range expected for KlenTaq DNA polymerase, allowing its presence to be assumed despite the reduced lane resolution.

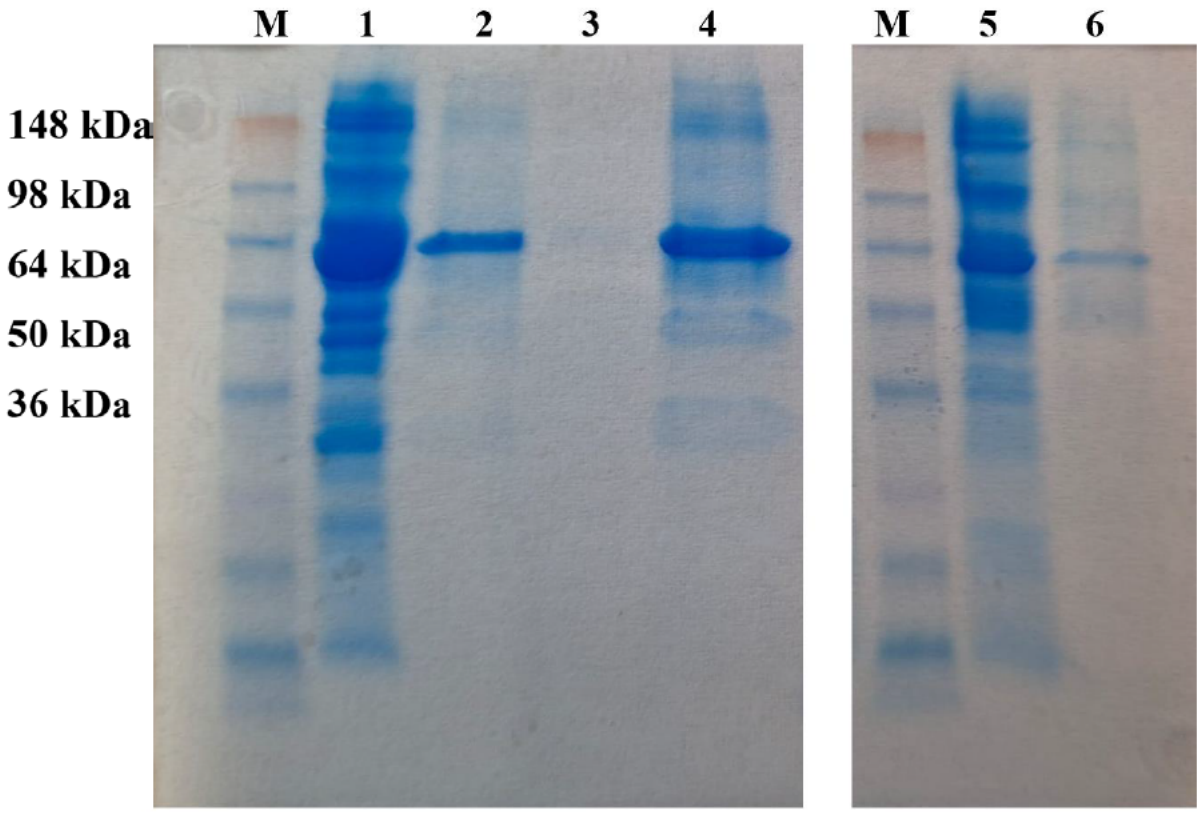

Figure 47: SDS-PAGE gel of samples from the cultivation JW_3825 and JW_3625. M: Marker, 1: JW_3825 Diafiltration, 2: JW_3825 Bioreactor supernatant (thermally purified), 3: JW_3825 IMAC (small tubes), 4: JW_3825 Precipitation, 5: JW_3625 Diafiltration, 6: JW_3625 Bioreactor supernatant (thermally purified)

Figure 48 shows the SDS-PAGE analysis of samples from cultivation JW_4025. Lane M contains the molecular weight marker, while lanes 1–3 represent diafiltrated, ultrafiltrated and thermally purified bioreactor supernatant, respectively.

A protein band at approximately 64 kDa, corresponding to KlenTaq DNA polymerase, is detectable in all three samples. Lanes 1 and 2 exhibit smeared band patterns, most likely caused by sample concentration during filtration. Nevertheless, the presence of the target band is still visible. In the thermally purified sample (lane 3), the band appears more defined, confirming successful expression of KlenTaq DNA polymerase.

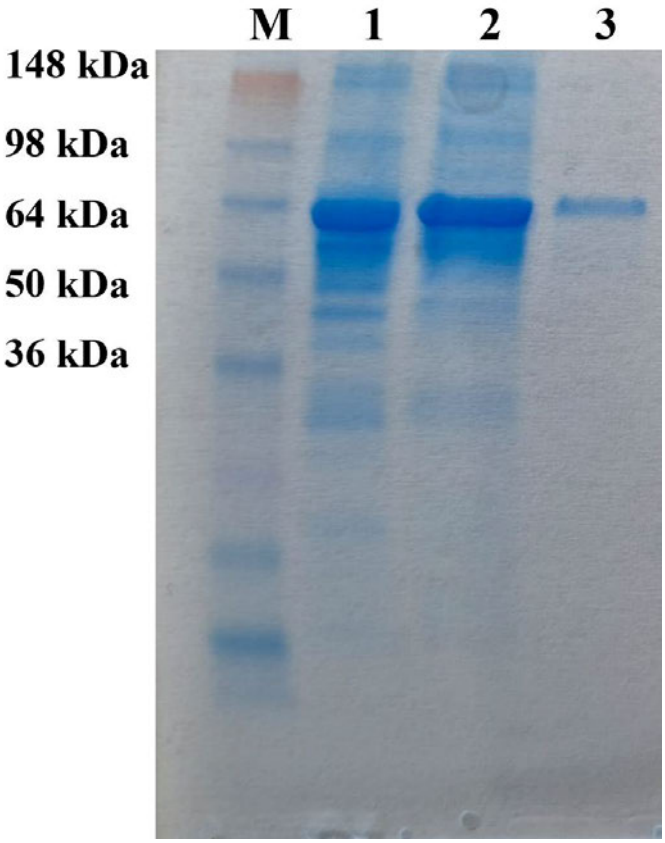

Figure 48: SDS-PAGE gel of samples from the cultivation JW_4025. M: Marker, 1: Diafiltration, 2: Ultrafiltration, 3: Bioreactor supernatant (thermally purified)

A.8 PCR analysis

PCR analysis demonstrated that the presence of bioreactor supernatant influenced the apparent polymerase activity. While the negative control showed no amplification, mixing enzymatically active Erlenmeyer flask samples with increasing amounts of bioreactor supernatant resulted in a reduced band intensity. This effect was most pronounced when not diafiltrated bioreactor supernatant was added, indicating the presence of inhibitory components in the cultivation broth. The corresponding PCR gel is shown in Figure 49.

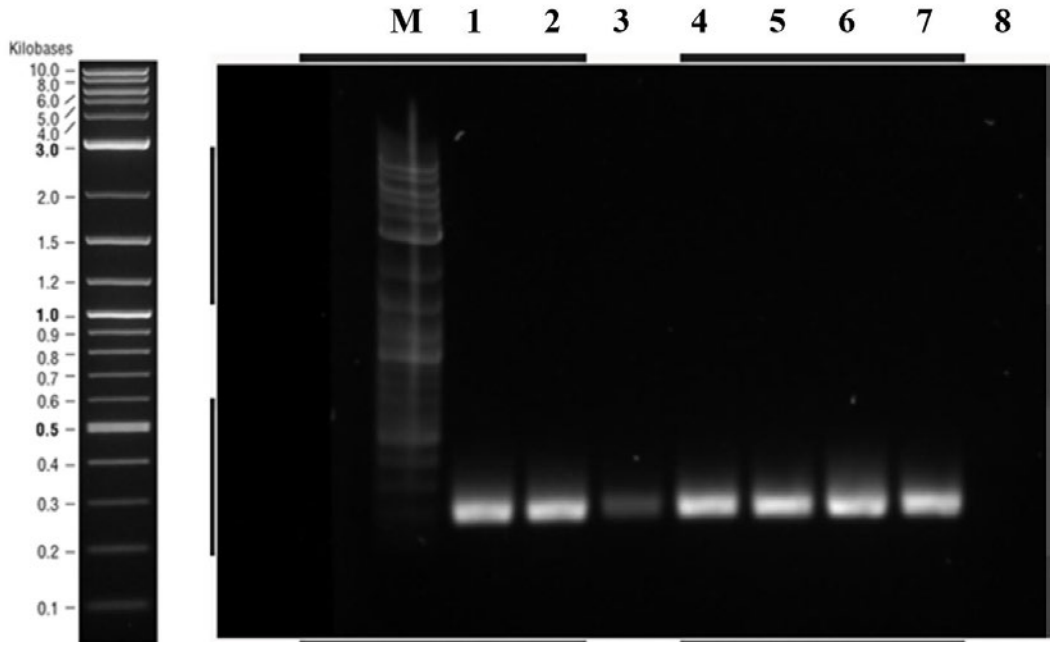

Figure 49: PCR of Erlenmeyer flask and JW_4025 process samples. M: Marker, 1: Erlenmeyer Flask, 2: 1 µL Erlenmeyer Flask + 1 µL Water, 3: 1 µL Erlenmeyer Flask + 1 µL JW4025 Bioreactor supernatant, 4: 1.5 µL Erlenmeyer Flask + 0.5 µL JW4025 Bioreactor supernatant, 5: JW4025 Diafiltration, 6: JW4025 Diafiltration, 7: JW4025 Diafiltration, 8: negative control. Conducted by Iris Ziehm

PCR assays of diafiltrated samples from different bioreactor processes revealed that polymerase activity was detectable only when sufficient diafiltration (~ 40 buffer exchange) could be achieved. No amplification was observed for samples JW_2825 and JW_3925, which was attributed to incomplete diafiltration caused by repeated membrane clogging during processing. All remaining samples showed detectable PCR products, confirming that effective buffer exchange is essential for obtaining functional enzymes. The corresponding PCR gel is provided in Figure 50.

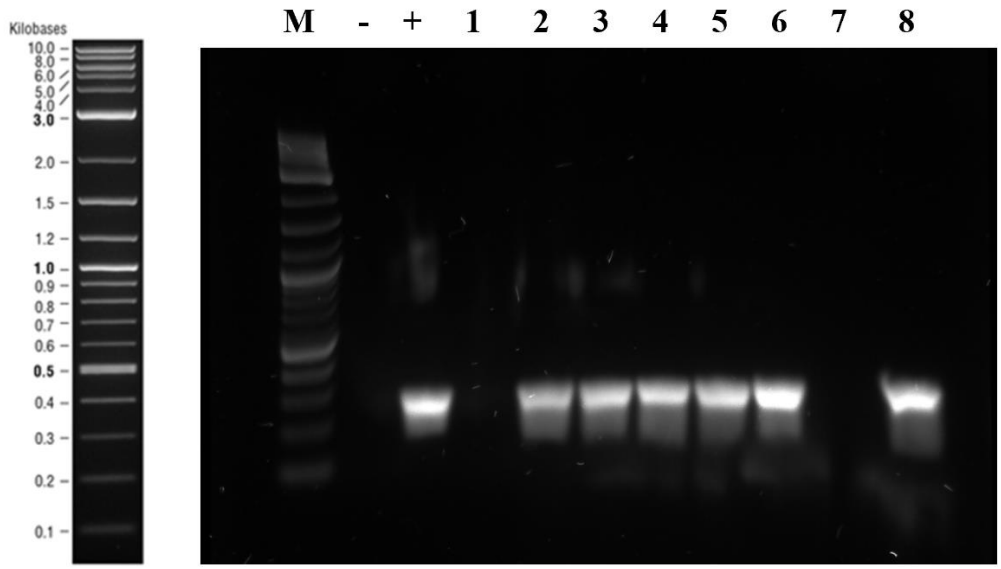

Figure 50: PCR of 40-fold buffer exchanged samples. M: Marker, -: negative control, +: positive control, 1: JW2825 Diafiltration, 2: JW3125 Diafiltration, 3: JW3425 Diafiltration, 4: JW3525 Diafiltration, 5: JW3625 Diafiltration, 6: JW3825 Diafiltration, 7: JW3925 Diafiltration 8: JW4025 Diafiltration.

Further PCR experiments demonstrated a clear dependence of polymerase activity on the extent of buffer exchange during diafiltration. Samples subjected to a 40-fold buffer exchange showed clear amplification products, whereas samples with only a 20-fold buffer exchange did not exhibit detectable activity. These results confirm that insufficient removal of inhibitory substances can impair enzymatic functionality. The corresponding PCR gel is shown in Figure 51.

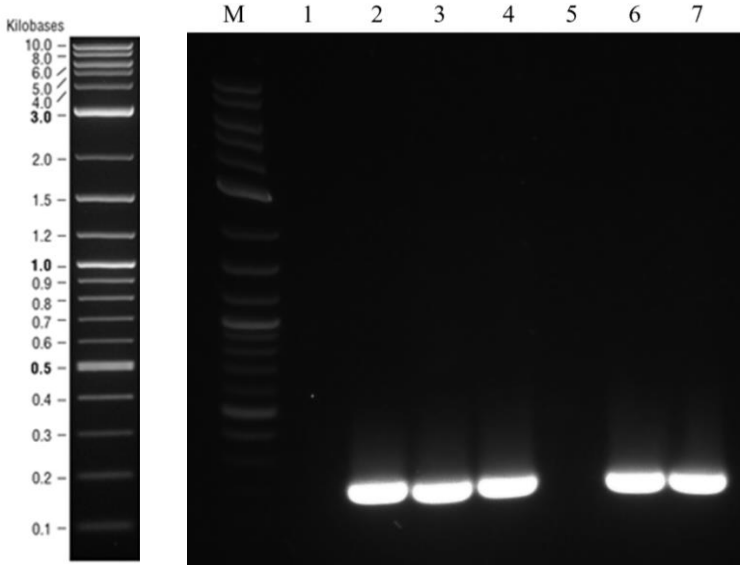

Figure 51: PCR of JW_4025 and JW_3825 samples (different diafiltration volumes). 1: negative control, 2: positive control, 3: JW_4025 1x Diafiltration (concentration falcon tube), 4: JW_ 3825 1x Diafiltration (concentration falcon tube), 5: JW_4025 TFUF Diafiltration (20x buffer exchange), 6: JW_3825 TFUF Diafiltration (40x buffer exchange), 7: Erlenmeyer flask

The PCR analysis revealed distinct differences in polymerase activity depending on the applied downstream processing strategy and sample matrix (Figure 52). Clear amplification products were obtained for the Erlenmeyer flask sample (lane 1), the diafiltrated sample from process JW_4025 (lane 6), as well as for the commercial Hemo KlenTaq polymerase used as positive control (lanes 15 and 16).

In contrast, samples obtained after ultrafiltration, IMAC purification or precipitation from process JW_4025 did not show detectable amplification products, indicating a loss or inhibition of enzymatic activity. These results demonstrate that diafiltration was a critical step for restoring polymerase activity, presumably by removing inhibitory low-molecular-weight compounds present in the culture supernatant.

This assumption is further supported by the mixing experiments. While dilution of the Erlenmeyer flask sample with water (lanes 8–10) did not affect PCR performance, mixing the same sample with bioreactor supernatant from process JW_3825 (lanes 11–13) completely suppressed amplification. This clearly indicates the presence of PCR-inhibitory components in the bioreactor supernatant, which can inactivate an otherwise functional polymerase.

Overall, these results confirm that the absence of enzymatic activity observed in several bioreactor-derived samples was not caused by insufficient expression of KlenTaq DNA polymerase, but rather by inhibitory effects of the process matrix, which could be effectively mitigated by extensive diafiltration.

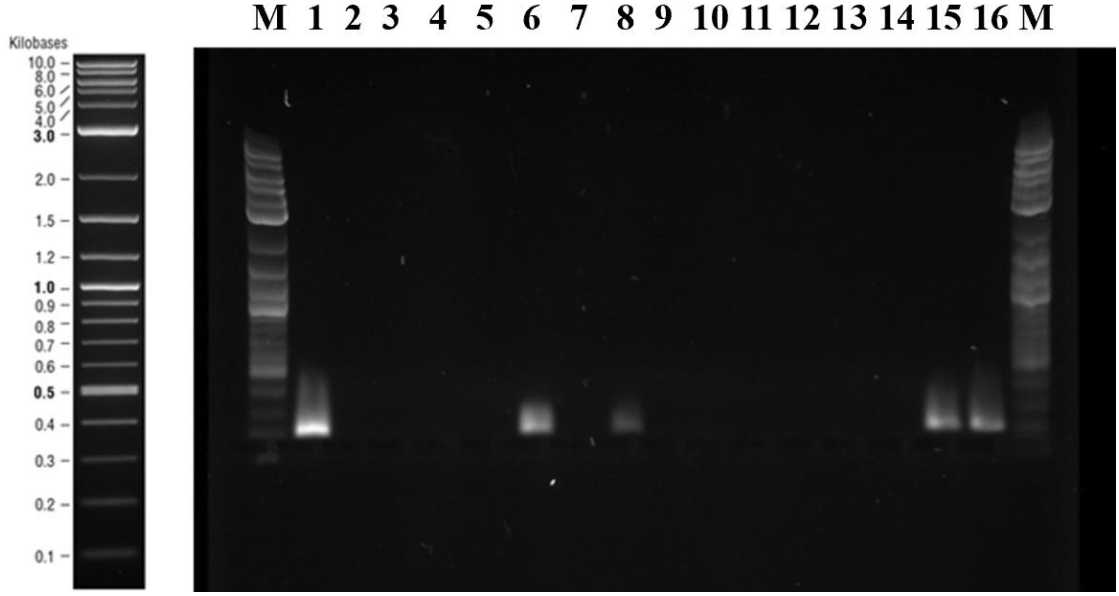

Figure 52: PCR of investigation supernatants influence on active polymerase. M: Marker, 1: Erlenmeyer Flask, 2: JW3825 Bioreactor supernatant, 3: JW3825 Precipitation, 4: JW4025 Ultrafiltration, 5: JW4025 IMAC, 6: JW4025 Diafiltration, 7: JW4025 Precipitation, 8: Erlenmeyer Flask 1:2 mixture with water, 9: Erlenmeyer Flask 1:3 mixture with water, 10: Erlenmeyer Flask 1:5 mixture with water, 11: Erlenmeyer Flask 1:2 mixture with JW3825 Bioreactor supernatant, 12: Erlenmeyer Flask 1:3 mixture with JW3825 Bioreactor supernatant, 13: Erlenmeyer Flask 1:5 mixture with JW3825 Bioreactor supernatant, 14: Negative control, 15: Hemo KlenTaq NEB, 16: Hemo KlenTaq NEB 1:5 mixture with water. Conducted by Iris Ziehm.

A.9 Evaluation of process productivity using x_{CO_2}

To evaluate whether process productivity could already be assessed during cultivation, the off-gas carbon dioxide mole fraction (x_{CO_2}) was analyzed and compared for all investigated processes. x_{CO_2} is commonly used as an indicator of overall metabolic activity and can, under defined conditions, provide indirect information on cellular respiration and substrate utilization. The corresponding x_{CO_2} profiles for the individual processes are shown in Figure 53, furthermore, Table 17 shows the process times for each production phase.

However, a clear distinction between more and less productive processes based solely on x_{CO_2} was not possible. The x_{CO_2} signals differed substantially between processes, which can be attributed to the varying cultivation strategies, media compositions, induction times, and production phase designs. In addition, several processes were affected by feed pump irregularities, which further influenced metabolic activity and off-gas composition. Therefore, the x_{CO_2} signal does not solely reflect product formation but also ongoing growth, residual substrate consumption, and transient process disturbances.

Therefore, x_{CO_2} alone proved to be insufficient as a reliable real-time indicator for comparing productivity across processes under the applied experimental conditions. A meaningful evaluation of process performance was only possible after completion of the cultivations using quantitative yield and productivity parameters, as summarized in the results tables.

Table 17: Process and their production times.

Process	Production time, h
JW_2825	53.2 - 135
JW_3125	23.2 – 51
JW_3625	5.5 - 26
JW_3825	26 – 51
JW_4025	17 – 46.5
JW_4725	32 – 62

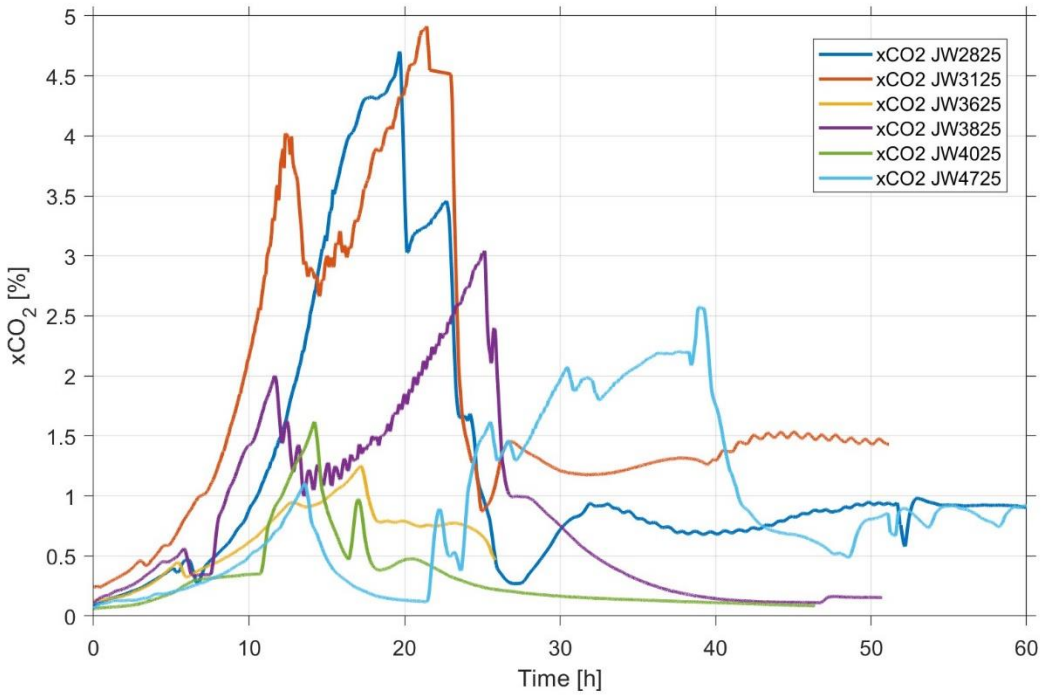

Figure 53: The x_{CO_2} values recorded for the respective processes are shown. The time axis was displayed up to 60 hours; the only process that lasted significantly longer than 60 hours was JW_2825, whereby the x_{CO_2} value remained constant from 60 hours until the end.